

MIT Joint Program on the Science and Policy of Global Change



Development of a Fast and Detailed Model of Urban-Scale Chemical and Physical Processing

Jason Cohen and Ronald Prinn

**Report No. 181
October 2009**

The MIT Joint Program on the Science and Policy of Global Change is an organization for research, independent policy analysis, and public education in global environmental change. It seeks to provide leadership in understanding scientific, economic, and ecological aspects of this difficult issue, and combining them into policy assessments that serve the needs of ongoing national and international discussions. To this end, the Program brings together an interdisciplinary group from two established research centers at MIT: the Center for Global Change Science (CGCS) and the Center for Energy and Environmental Policy Research (CEEPR). These two centers bridge many key areas of the needed intellectual work, and additional essential areas are covered by other MIT departments, by collaboration with the Ecosystems Center of the Marine Biology Laboratory (MBL) at Woods Hole, and by short- and long-term visitors to the Program. The Program involves sponsorship and active participation by industry, government, and non-profit organizations.

To inform processes of policy development and implementation, climate change research needs to focus on improving the prediction of those variables that are most relevant to economic, social, and environmental effects. In turn, the greenhouse gas and atmospheric aerosol assumptions underlying climate analysis need to be related to the economic, technological, and political forces that drive emissions, and to the results of international agreements and mitigation. Further, assessments of possible societal and ecosystem impacts, and analysis of mitigation strategies, need to be based on realistic evaluation of the uncertainties of climate science.

This report is one of a series intended to communicate research results and improve public understanding of climate issues, thereby contributing to informed debate about the climate issue, the uncertainties, and the economic and social implications of policy alternatives. Titles in the Report Series to date are listed on the inside back cover.


Henry D. Jacoby and Ronald G. Prinn,
Program Co-Directors

For more information, please contact the Joint Program Office

Postal Address: Joint Program on the Science and Policy of Global Change
77 Massachusetts Avenue
MIT E19-411
Cambridge MA 02139-4307 (USA)

Location: 400 Main Street, Cambridge
Building E19, Room 411
Massachusetts Institute of Technology

Access: Phone: +1(617) 253-7492
Fax: +1(617) 253-9845
E-mail: globalchange@mit.edu
Web site: <http://globalchange.mit.edu/>

 Printed on recycled paper

Development of a Fast and Detailed Model of Urban-Scale Chemical and Physical Processing

Jason Cohen* and Ronald Prinn

Abstract

A reduced form metamodel has been produced to simulate the effects of physical, chemical, and meteorological processing of highly reactive trace species in hypothetical urban areas, which is capable of efficiently simulating the urban concentration, surface deposition, and net mass flux of these species. A polynomial chaos expansion and the probabilistic collocation method have been used for the metamodel, and its coefficients were fit so as to be applicable under a broad range of present-day and future conditions. The inputs upon which this metamodel have been formed are based on a combination of physical properties (average temperature, diurnal temperature range, date, and latitude), anthropogenic properties (patterns and amounts of emissions), and the surrounding environment (background concentrations of certain species).

Probability Distribution Functions (PDFs) of the inputs were used to run a detailed parent chemical and physical model, the Comprehensive Air Quality Model with Extensions (CAMx), thousands of times. Outputs from these runs were used in turn to both determine the coefficients of and test the precision of the metamodel, as compared with the detailed parent model. The deviations between the metamodel and the parent model for many important species (O_3 , CO, NO_x , and BC) were found to have a weighted RMS error less than 10% in all cases, with many of the specific cases having a weighted RMS error less than 1%. Some of the other important species (VOCs, PAN, OC, and sulfate aerosol) usually have their weighted RMS error less than 10% as well, except for a small number of cases. These cases, in which the highly non-linear nature of the processing is too large for the third order metamodel to give an accurate fit, are explained in terms of the complexity and non-linearity of the physical, chemical, and meteorological processing. In addition, for those species in which good fits have not been obtained, the program has been designed in such a way that values which are not physically realistic are flagged.

Sensitivity tests have been performed, to observe the response of the 16 metamodels (4 different meteorologies and 4 different urban types) to a broad set of potential inputs. These results were compared with observations of ozone, CO, formaldehyde, BC, and PM_{10} from a few well observed urban areas, and in most of the cases, the output distributions were found to be within ranges of the observations.

Overall, a set of efficient and robust metamodels have been generated which are capable of simulating the effects of various physical, chemical, and meteorological processing, and capable of determining the urban concentrations, mole fractions, and fluxes of species, important to human health and the climate.

Contents

1. INTRODUCTION.....	2
1.1 Why Urban Area Metamodels are Needed	2
1.2 Prior Reduced Form Urban Process Models.....	4
2. BASIC COMPONENTS	6
2.1 Parent Urban Chemical Transport Model.....	6
2.2 Probabilistic Collocation Method	7
3. METHODOLOGY	9
3.1 Selected Inputs	9
3.2 Selected Outputs.....	19
3.3 Obtaining the Parameterizations.....	20
3.4 Differences Between This Work and Previous Work.....	21
4. RESULTS AND DISCUSSION	22
4.1 Concentrations, Mass Fluxes, and Deposition.....	22
4.2 Parameterization Tests.....	23
4.3 Sensitivity Tests	33
5. CONCLUSIONS.....	37

*Center for Global Change Science and Joint Program of the Science and Policy of Global Change Massachusetts Institute of Technology Cambridge MA, 02139. (email: jasonbc@mit.edu)

6. REFERENCES.....	38
APPENDIX.....	43

1. INTRODUCTION

1.1 Why Urban Area Metamodels are Needed

Urban regions have high concentrations of species which are harmful to human health, have a direct or indirect impact on the atmosphere’s radiative flux balance, and alter the land’s ability to uptake carbon. Furthermore, urban regions account for a large and increasing fraction of the Earth’s total population and anthropogenic emissions. However, modeling the effects of urban areas on the processing and export of anthropogenic emissions is not straightforward. Urban areas are not easily categorized in a simple or straight forward manner; they are located in regions of diverse geography and meteorology, they have non-constant emissions which are based on technological, economic, and political factors, and they exhibit strongly non-linear processing of primary anthropogenic pollutants. For these reasons, urban areas account for a large amount of the variability and uncertainty in the global atmospheric spatial and temporal distributions of primary and secondary anthropogenic pollutants.

Of the many substances emitted or processed in urban areas, only those having a large percentage of their global emissions, production, or destruction occurring in urban regions, those having a large impact on the global radiative balance, or those having concentrations in urban areas sufficient to affect human health, are the focus in this paper. These species are typically heterogeneously distributed over space and time within single urban regions, as well as between different urban regions, due to non-linear chemical and physical processing, differences in local and regional meteorology, and differences in local emissions. Thus, simulating their concentration and lifetime in urban atmospheres is already quite complex, and is made further complex since the net export of these species from the urban regions is required to obtain their global distribution, lifetime, and ultimately their impact on the climate. To address this level of complexity, properties of urban areas relating to geography, physics, chemistry, and people’s influence will have to be addressed at both the local and global scale.

Global chemistry and climate models, in general, use a spatial resolution which is much coarser than the spatial scales of real urban regions. This in turn requires that these models use, compute, or predict aggregated data or data on large spatial and temporal scales, and then use this data to parameterize, interpolate, or otherwise approximate the desired variables on the urban temporal and spatial scales. Therefore, physical variables which control the system, the concentrations of trace species, and human factors such as primary anthropogenic emissions pertaining to the urban system are averaged over, diluted into, or somehow statistically derived, for the entire urban area (a “dilution” approach). Because of this, many of the variables provided by global scale models and globally or regionally averaged data are approximations that are not valid or appropriate for use on urban spatial and temporal scales.

If one is to use such a parameterization in a global general circulation or chemical transport model, then it must be capable of computing the concentrations of important trace species within a given urban area, and the fluxes of these species to the coarser global scale grids from the urban scale grids and back again. In addition to these two things, the parameterization must be computationally feasible and yet still flexible enough to simulate the highly variable emissions, upwind conditions, geography, and relevant economic and human factors found in urban areas, both for the present and into the near future.

To keep it computationally reasonable, the parameterization will need to have its variables limited to those which are most important in accounting for the non-linear processing of the most important trace species and processes. Some of the specific variables to consider include: the emissions of critical chemical species, the specific temporal and spatial distributions of the emissions, the time of the year, the geographic location, the surface conditions, the elevation, the amounts of rainfall and cloudiness, the horizontal and vertical circulation, the local temperature, the upwind concentrations of the species interacting within the urban area, the amount of sunlight, the relative humidity, and the atmospheric liquid water content. At a minimum, such variables must be known both in the urban area and at its boundaries, as a function of the time of day. In addition to this, since export from one urban area can greatly impact a neighboring urban area's properties, it is important to know where urban areas are located in relation to each other.

The parameterization must be capable of capturing the non-linear chemical and physical processes which actually occur within the urban area, because these processes can cause results which are lower than, higher than, or differently distributed in the horizontal, vertical, or temporal, compared with the large-scale averaging or dilution approach. Urban scale processing causes certain species to have a net positive production (chemical production minus chemical, physical, and depositional loss) due to the inclusion of urban-scale processing, such as CO (where production from VOC oxidation far outweighs loss due to reaction with OH), NO₂ (from photochemical processing), and certain lower molecular weight VOCs (from the oxidation of certain larger molecular weight VOCs). Other species are formed nearly exclusively in urban areas as secondary products, which are greatly affected due to non-linear processing, such as peroxyacetyl nitrate (PAN), secondary organic carbon aerosol (OC), nitrate aerosol (NO₃⁻), and sulfate aerosol (SO₄⁻). For all of these species, the dilution approach will not accurately simulate their concentration in the urban area and their flux from the urban area to the global system. Other species have a net negative production due to processing in urban areas, such as some large VOCs (oxidized to smaller VOCs), NO, SO₂ (oxidized to NO₂ and SO₄⁻), highly water soluble species (adsorbed into the aqueous phase), and primary aerosols (removed through coagulation, rain, and deposition). For these species the simple dilution approach will also erroneously calculate their concentrations in the urban area and their flux from the urban area to the global system. A third subset of species can have either a net positive or negative production, such as: O₃, OH, some VOCs, and the optically important aerosols formed in the urban region. This subset of species has behavior that depends on many factors, such as the concentrations of other species in the urban area, whether it is raining or dry, the strength of vertical advection and

mixing, and the time of the day. In the case of these species, the simple dilution approach can potentially either underestimate or overestimate the concentration in the urban area and the flux from the urban area to the global system. Furthermore, the simple dilution approach does not capture the vertical, horizontal, and temporal characteristics of the urban concentrations or the fluxes from the urban region. One case in point is that modeling the processing occurring due to a small region of strong uplift, subsidence, or rainfall, over a heterogeneously distributed concentration field, can yield substantially different results than predicted by the simple averaging approach (which includes averaging the effects of the vertical air motion and/or the rainfall). This short-coming has been demonstrated in a study using ozone as an example, in which incremental improvements in the spatial resolution of the model's emissions, chemistry and physics made the results compare more closely with measurements (Wild and Prather 2006). However, even such efforts have only looked on horizontal spatial scales on the order of a degree, which are still far too coarse to precisely model processes occurring on the urban scale.

It is for these reasons that producing a metamodel (or a model of a model) is one way to integrate urban scale processing into global scale models. Such a metamodel should be computationally fast and capable of interacting as a component in a larger scale modeling system. The most important things to consider are how well the metamodel simulates physical and chemical processes, and how accurately it simulates urban concentrations and deposition, and mass fluxes to the global scale, under typical present day and potential future conditions.

1.2 Prior Reduced Form Urban Process Models

An early attempt at forming a parameterization of urban scale processing was made by (Calbo *et al.*, 1998). They used the California Institute of Technology urban model, driven by idealized (non-divergent, single directional, non-evolving) meteorology, and a simplified version of fast NO_x and VOC photochemistry which in turn drove ozone production for their gas-phase chemistry driver. The model was run using five layers in the vertical, with initial conditions being zero for many species outside the bottom two layers. For their model inputs, they used 14 different uncertain input variables including: date, latitude, average surface temperature, fractional cloud cover, mixed layer height, residence time of an air parcel, emissions of SO₂, emissions of CO, differential emissions between CO and VOCs, differential emissions between CO and NO_x, AQINO_x [air quality index for NO_x], AQIOZONE [air quality index for ozone], AQISO₂ [air quality index for SO₂], and AQIVOC [air quality index for VOCs]. The air quality indices are a means by which the initial concentrations of certain species were approximated.

Many assumptions were made with respect to the variables chosen. The latitudes for which this reduced form model was valid included the regions from 60°S to 60°N latitude. The average surface temperature and mixed layer height were scaled by a pre-defined function over time of the day. The fractional cloud cover was constant in both space and time. The residence time of an air parcel in the urban area determined the wind speed across the urban box model, and was constant over time. All emissions were assumed to occur within fixed geographical regions of the urban box model (near the center) and always at the same fixed ratios, and as a fixed function

of distance from the center of the urban area, with no emissions occurring near the edge of the urban area. Although the emissions of VOC and NO_x were given as separate inputs, these inputs were defined in such a way as to be partially correlated with the emissions of CO, in turn not allowing for conditions in which there was a strong reduction in one or two of these species, rather than all three simultaneously. Furthermore, the PDFs of the emissions of the input species were defined by beta distributions, and therefore had zero chance of being outside of the defined upper and lower boundaries. Finally, the initial conditions and boundary conditions were given using the Air Quality Indexes, which are defined based upon generally clean upwind conditions.

The authors produced their parameterization by using the probabilistic collocation method (PCM; Tatang *et al.*, 1997), which is a method by which their model's response space was approximated by a set of orthonormal "chaos" polynomials, which had their polynomial coefficients computed based on the PDFs of the input variables. All of their input parameters were fit using second order polynomials for each of the 14 input variables, which included all first order, second order, and cross combinations of the input variables. Using this method, they showed that there was a reasonable fit (the parameterized model being within 40% of the modeled variable) between the metamodel and the parent model for the mass fluxes of gas-phase species from the urban area, with the major exception being ozone.

A second attempt at an urban process PCM-based parameterization was made by Mayer *et al.* (2000), using the same parent model, chemical routines, and approach to idealized meteorology, as in Calbo *et al.* (1998). Some of the differences between this newer parameterization and the older one were related to the parent model setup. All five layers in the vertical were initialized with non-zero initial conditions, the urban area was 200km x 200km, the emissions only occurred in a core area of about 1.5° x 1.5°, and the air entering was assumed to be clean, exclusively matching values found in remote locations. Further differences arose from the use of slightly different input variables, which in this case used 13 of the same variables and 2 additional variables (an AQI for NO and another AQI for NO₂) to represent the initial single variable used for the AQI of NO_x. A third set of differences came from the variation of emissions as a function of time, with no diurnal variation assumed for SO₂ emissions, but an identical diurnal variation assumed for all other species.

The most significant differences, however, came from how the uncertainties were treated. The emission PDFs were based on fits to a normal function, and therefore they had a non-zero probability of being any finite value. Furthermore, the emission PDFs were formed independently of each other, allowing for higher or lower values of each emitted species to be modeled, while the other emitted species were generally near their median value. This change allowed for more regions of the parameter space to be explored by the reduced form model. Finally, the probabilistic collocation method employed in this case used some third order terms in addition to the complete set of second order terms in their polynomial chaos expansion. These additional terms were added specifically to look at higher order effects on the net flux of ozone from the urban region. In general, the results from this effort showed a more reasonable fit for all

mass fluxes of gas species of interest from the urban area, including ozone, compared to the previous work of Calbo *et al.* (1998).

2. BASIC COMPONENTS

2.1 Parent Urban Chemical Transport Model

Regional scale models of atmospheric chemistry and physics can effectively simulate the processing of emissions on spatial and temporal time scales resembling those on the urban scale, allowing for both the time varying concentrations within and the time varying export from a specific urban area to be computed. The model chosen to perform these calculations is the Comprehensive Air Quality Model with extensions (CAMx) (Environ, 2008), which is an eulerian model that solves the terrain following continuity equation, for the concentrations and fluxes of trace species. CAMx accounts for the emissions, vertical and horizontal transport and diffusion, gas and aerosol phase chemistry, and the wet and dry deposition of trace species. Additionally, CAMx takes into consideration how the properties of the Earth's surface, the given atmospheric conditions, and the amount of incident solar radiation as a function of space and time, further effect the concentrations and distributions of trace species. Much of the recent peer-reviewed literature relating to urban and regional air quality has relied on CAMx (see, e.g., (McDonald-Buller *et al.*, 2001; Nobel *et al.*, 2001; Andreani-Aksoyoglu *et al.*, 2004; Eben *et al.*, 2005; Junquera *et al.*, 2005; Mauzerall *et al.*, 2005; Morris *et al.*, 2005; Russell and Allen 2005; Chang and Allen 2006(a); Chang and Allen 2006(b); Jackson *et al.*, 2006; Morris *et al.*, 2006; Perez-Roa *et al.*, 2006; Riccio *et al.*, 2006; Tesche *et al.*, 2006; Zunckel *et al.*, 2006; Amiridis *et al.*, 2007; Byun *et al.*, 2007; de Foy *et al.*, 2007; Feldman *et al.*, 2007; Lei *et al.*, 2007; Liu *et al.*, 2007; Pirovano *et al.*, 2007; Zanis *et al.*, 2007; Andreani-Aksoyoglu *et al.*, 2008; Keller *et al.*, 2008; Russell 2008; and Song *et al.*, 2008)).

The specific way in which CAMx accounts for these processes is by solving for each of the terms separately in the equation:

$$\frac{\partial c}{\partial t} = -\nabla \cdot (c\mathbf{v}) + \frac{\partial(c\eta)}{\partial z} - c \frac{\partial}{\partial z} \left(\frac{\partial h}{\partial t} \right) + \nabla \cdot (\rho K_v \nabla (c/\rho)) + \frac{dc}{dt}_{\text{chemistry}} + \frac{dc}{dt}_{\text{emissions}} - \frac{dc}{dt}_{\text{deposition}} - \frac{dc}{dt}_{\text{removal}} \quad (1)$$

This equation is the continuity equation for a trace species in the atmosphere, in which the following variables are used: c is the concentration (moles or mass per unit volume) of a given species, \mathbf{v} is the horizontal wind velocity, η is the vertical wind velocity, h is the vertical layer height, ρ is the atmospheric density, and K_v is the turbulent exchange diffusion coefficient. The equation states that the net change in the concentration of a given species is the sum of: the convergence of the advective flux in the horizontal and vertical, and the diffusive flux; the chemical production and destruction, emissions, wet and dry deposition at the surface, and other physical removal processes (such as capture by cloud particles).

However, solving this equation is neither straight forward nor simple, requiring many assumptions. Firstly, all processes are treated as though they are uniformly distributed through each Eulerian grid box in which they occur; therefore emissions are diluted through the grids adjacent to the surface, physical and meteorological variables are assumed to have a single

average value over a grid box, and tracers are considered to have a constant concentration throughout a grid box. The advection routine is solved in mass-conserving flux form, driven by realistic assimilated meteorology from the 1995 OTAG campaign at four different sites, all using data from the same 2-day period of data collection (Corporation 1997). The amount of liquid water in the form of rain, the amount of cloud cover, and the mass flux of air (integrated over all four sides and the top of the urban area) through the boundaries of the urban area, are given in **Table 1**.

Table 1. Physical Descriptions of the Four Meteorological Scenarios used in this work.

Meteorology Case	Rainfall (mg/m³)	Cloudiness (%)	Air Flux (10⁹ kg/s)
R241-C63-W46	241.	62.8	4.56
R000-F00-W44	0.00	0.00	4.38
R002-F02-W16	1.72	1.75	1.61
R021-F19-W57	21.5	19.3	5.70

The vertical velocity is computed by integrating the density conservation equation. Wet removal occurs through Henry’s Law processes, physical mixing, aqueous phase chemistry, and impaction by falling precipitation. Dry removal occurs through first order surface resistance removal schemes for gases and aerosols, and gravitational settling for aerosols. Gas phase chemistry is based on the Carbon Bond 4 approach (Gery *et al.*, 1989; Yarwood 2005), with a newer and more detailed representation of terpenes, low volatility organic species, and improved night time nitrogen chemistry. Aerosol phase chemistry includes explicit inorganic aqueous phase chemistry, inorganic thermodynamics, and formation of secondary organic and inorganic aerosol. This is performed over a size-based sectional scheme, using fixed values for the edges of the size bins. The photolysis scheme uses a lookup table based on the TUV model, and accounts for reducing fluxes of incoming solar radiation as a function of overhead cloud thickness and reflection, and for surface reflection. And finally, the precipitation processes include rain, snow, and ice (all of which are internally computed, based on the temperature and the strength of the vertical convection in the region).

2.2 Probabilistic Collocation Method

The computational expense of running a detailed urban model, such as CAMx, is very large. Thus, using such a modeling platform directly to model the effects of hundreds or thousands of different urban areas, each day, over an even relatively short time horizon in the context of a global climate model is not computationally feasible. In addition to these direct computational expenses, there are further computational costs, such as two way interactions between the global model and the urban model relating to the physical and chemical variables which drive the temperature, rainfall, horizontal wind and its divergence, and chemical concentrations at the boundaries between the two models. Furthermore, to drive the urban process model, one is required to have data at highly refined spatial and temporal scales, which global scale models cannot provide directly. Therefore, there is a need to devise a computationally efficient

parameterization of the processes contained in a detailed urban model, that can be applied to a global model.

To form this parameterization, the probabilistic collocation method was used (Tatang *et al.*, 1997). This method is one of several mathematical techniques which can be used for creating a metamodel. Specifically, given a set of k input parameters x_j used to drive a model, $\{x_1, x_2, \dots, x_k\}$, there are M output responses y_j predicted by the model that are functions of the x_j values; $\{y_1, y_2, \dots, y_M\} = f(\{x_1, x_2, \dots, x_k\})$. In this case the y_j are the physical concentrations, mass fluxes, and deposition fluxes of species that we are interested in approximating. And since there is a range of possible values which each input parameter can take, it is important to treat the input variables as being independent of each other with their statistics defined by their PDF over this range. However, since all of the input variables are considered random, then the output variables also are considered random variables. It is this response surface which is being fitted to produce the metamodel.

The response surface is being fitted specifically by a set of orthonormal polynomials (P_k^i) where i ($= 1$ or m below) is the order of the polynomial, g is the PDF of the random input variable x_j , and δ_{lm} is the kronecker delta:

$$P_k^{-1} = 0 \quad (2a)$$

$$P_k^0 = 1 \quad (2b)$$

$$\int g(x_j) P_k^l(x_j) P_k^m(x_j) dx = \delta_{lm} \quad (2c)$$

Through these polynomials, the independent random variables can be written as $x_j = x_j^0 + x_j^1 * P_k^1$, and the dependent variable y_j can be approximated by the polynomial chaos expansion:

$$y_j = y_j^0 + \sum_{i=1, N} y_j^i P_k^i \quad (3)$$

where y_j^i is a coefficient to be fit based on the parent model's predicted value for y_j at the given set of inputs $\{x_j\}$, and N is the order of the order of the polynomial fit.

In addition to forming the basis for the polynomial chaos expansion, the orthonormal polynomials are also used to help select the set of parameter values which are used to initialize the parent model. This set of input values, called collocation points, are solved for by finding the $N+1$ roots of the $N+1$ order polynomial corresponding to each input parameter x_j . These roots are from the high probability regions of each input parameter, and therefore the approximation of y_j is particularly good within the most probable range of values of the input parameters. In addition to this, a set of test points are generated from the solution of the $N+2$ roots of the $N+2$ order polynomial corresponding to each input parameter x_j . This second set of points form an excellent test in that they take into account what the next higher order of estimation would yield as a better set of points for sampling the probability space spanned by the input parameters. Thus, it is these approximations for each output parameter which are referenced herein as being the metamodel approximations.

3. METHODOLOGY

3.1 Selected Inputs

The smallest possible set of input variables capturing the effects of urban chemical and physical processing must be derived in order to form a reduced form model which is as compact as possible. This set of inputs needs to be flexible enough to be applicable to the many variations of the properties of urban areas found throughout the world both presently and in the future out to 2100. Specifically, the variables need to span the differences in geography, location, time of the year, atmospheric temperature, cloudiness, amount and type of precipitation, vertical motion, time tendency of emissions, spatial tendency of emissions, the amount of each type of emitted species, and the upwind concentrations of species of interest, as a function of space and time. Specifically, there are 18 uncertain input variables which are used to derive the model, each of which has its uncertainty based on a wide range of both present day conditions and those conditions expected out to 2100 [derived through the running of a set of climate policy and no climate policy economic scenarios using the MIT Joint Program's EPPA model (Paltsev *et al.*, 2005)]. These input variable PDFs are defined and described in **Table 2** using the following formuli:

$$\text{Uniform (} a \leq x \leq b \text{): } f(x) = 1/(b-a) \quad (4a)$$

$$\text{Beta (} a \leq x \leq b; p, q > 0 \text{): } f(x) = [(x-a)^{p-1}(b-x)^{q-1}] / [(\int_0^1 t^{p-1}(1-t)^{q-1} dt)(b-a)^{p+q-1}] \quad (4b)$$

$$\text{Lognormal (} x, m, \sigma > 0 \text{): } f(x) = \exp(-(\ln(x/m))^2 / (2\sigma^2)) / (x\sigma\sqrt{2\pi}) \quad (4c)$$

$$\text{Fixed: } f(x) = xS \quad (4d)$$

where a, b, p, q, m, σ , and S are the parameters, and x is the input value, which in the case of the fixed equation, is the emissions of the appropriate parent species (either CO or BC).

Table 2. Descriptions of the input variable PDFs used to drive the CAMx model. See equations 4(a) - 4(d) for PDF formuli and parameters.

Input Variable	Type of PDF	China	India	Developed	Developing
Day of the Year [Days]	Uniform (a,b)	1.000 365.0	1.000 365.0	1.000 365.0	1.000 365.0
Geographic Latitude of Urban Area [$^{\circ}+90$]	Beta (p,q,a,b)	3.663 3.897 112.7 134.3	1.736 1.694 99.70 121.4	5.802 9.842 124.7 141.3	3.309 2.625 65.70 143.3
Temporal Weight	Uniform (a,b)	0.000 1.000	0.000 1.000	0.000 1.000	0.000 1.000
Spatial Distance [km]	Uniform (a,b)	21.6 93.2	21.6 93.2	21.6 93.2	21.6 93.2
Daily Average: Surface Temperature [K]	Beta (p,q,a,b)	3.924 1.583 251.9 303.3	8.483 2.810 267.4 309.4	7.827 3.446 261.7 310.7	2.637 2.006 263.2 301.8
Diurnal Temperature [K]	Beta (p,q,a,b)	3.841 4.125 3.061 15.06	1.741 1.976 5.318 18.76	4.114 3.368 2.073 16.45	2.532 3.438 4.037 21.24

Emission Values:	Lognormal	3162.	2398.	7171.	5713.
CO [ton/day]	(m, σ)	1.908	1.563	2.651	1.995
VOC [ton/day]	Fixed (S)	.0814	.2194	.2180	.1891
NO _x [ton/day]	Fixed (S)	.3558	.2462	.2815	.1721
BC [ton/day]	Lognormal	88.56	39.88	75.45	68.15
	(m, σ)	2.133	1.761	2.387	2.459
SO ₂ [ton/day]	Fixed (S)	.7646	.3526	1.966	1.481
NH ₃ [ton/day]	Fixed (S)	1.104	3.468	.9779	.6038
OC [ton/day]	Fixed (S)	1.615	1.586	2.587	3.890
Boundary Values:	Lognormal	55.15	64.86	47.72	57.52
Ozone [ppb]	(m, σ)	1.321	1.184	1.320	1.317
CO [ppb]	Lognormal	163.8	234.3	119.0	194.3
	(m, σ)	1.776	1.625	1.558	1.753
NO _x [ppt]	Lognormal	18.63	18.63	12.73	24.59
	(m, σ)	1.601	1.601	1.337	1.486
SO ₂ [ppt]	Lognormal	562.0	619.8	515.7	475.6
	(m, σ)	1.634	1.699	1.545	2.057
Isoprene [ppt]	Lognormal	373.2	373.2	373.2	373.2
	(m, σ)	2.293	2.293	2.293	2.293

The first set of input variables in Table 2 are for the time, location, emission spatial distribution, and temperatures as discussed later. The second set of input variables are fluxes for those species that are directly emitted in the urban area. The directly emitted species are CO, NO_x (95% emitted as NO and 5% emitted as NO₂), VOCs, SO₂, BC (primary black carbon aerosol), and OC (primary organic carbon aerosol). The CO and BC emissions have been fitted by lognormal probability distribution functions, see **Figures 1, 2**, based on the results of 250 policy and 250 no policy runs of the MIT EPPA Model (Cossa 2004, Paltsev *et al.*, 2005).

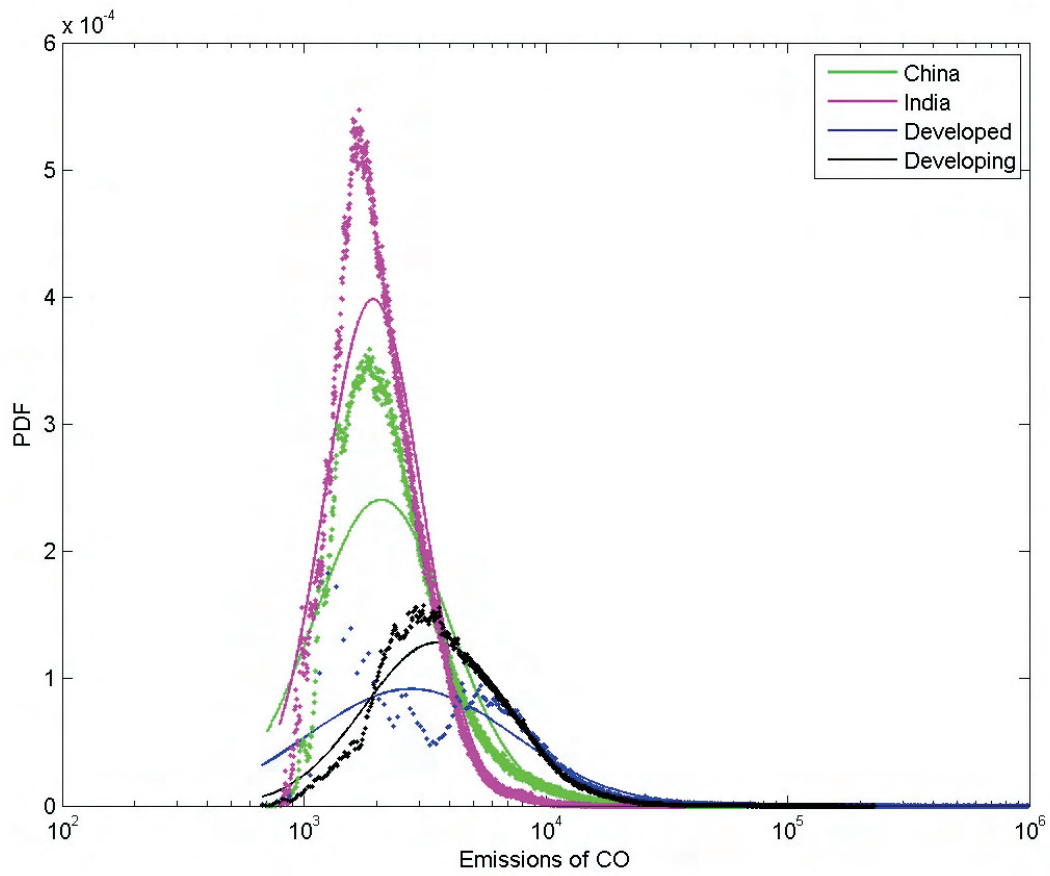


Figure 1. PDFs of CO emissions for each metamodel type, where the dots represent data points from the MIT EPPA Model and the lines represent the best lognormal fits of the data.

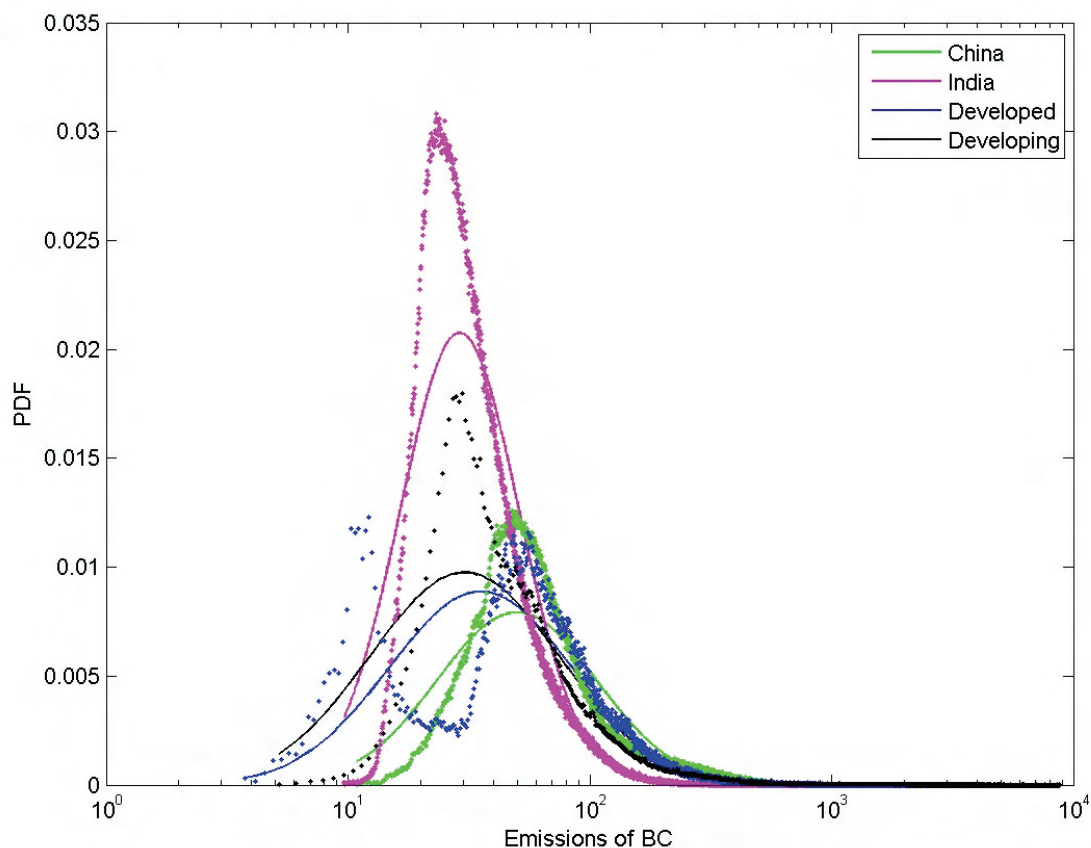


Figure 2. PDFs of BC emissions for each metamodel type, where the dots represent data points from the MIT EPPA Model and the lines represent the best lognormal fits of the data.

The remaining primary emitted species are chosen so that they linearly scale with the emissions of either CO or BC (these linear coefficients are listed in Table 2). The reason for doing this is two-fold. Firstly, the sources of the gas-phase species CO, NO_x, and VOCs tend to be similar and those of the aerosol phase species and their precursors BC, OC, SO₂, and NH₃ also tend to be similar. Secondly, since the probabilistic collocation method tends to sample the space best in regions which are of high probability, and since there is correlation between these species' emissions, a better sampling of the probability space and hence more reliable results are obtained using this method. The best fit linear relations between the emissions of these species are given in **Table 3** using the following formula:

$$X = \beta P + \alpha \tag{5}$$

Here P is the emissions of the parent species in g/day, X is the emissions of the subordinate species in g/day, and β and α are the best fit coefficients for the slope and intercept respectively.

Table 3. Best fit emissions correlation statistics.

Emitted Species, X/P	Model Location	Best Fit Slope, β	Best Fit Intercept, α
VOC / CO	China	0.0814	0.0426
VOC / CO	India	0.2194	-0.0190
VOC / CO	Developed	0.2180	0.3250
VOC / CO	Developing	0.1891	0.0571
NO _x / CO	China	0.3558	-0.0933
NO _x / CO	India	0.2462	-0.0711
NO _x / CO	Developed	0.2815	0.4149
NO _x / CO	Developing	0.1721	-0.0928
OC / BC	China	1.6145	0.0063
OC / BC	India	1.5864	0.0149
OC / BC	Developed	2.5874	0.0044
OC / BC	Developing	3.8897	-0.0179
SO ₂ / BC	China	0.7646	0.1138
SO ₂ / BC	India	1.3526	-0.0366
SO ₂ / BC	Developed	1.9656	0.1718
SO ₂ / BC	Developing	1.4809	0.1310
NH ₃ / BC	China	1.1041	0.0441
NH ₃ / BC	India	3.4816	0.0414
NH ₃ / BC	Developed	0.9779	0.0457
NH ₃ / BC	Developing	0.6038	0.0712

This technique employing E(CO) and E(BC) has been further shown to be superior to a previous effort which attempted to repeat this same procedure, but with all 7 primary emitted species being treated as independent. This previous effort showed that the results were not realistic when all of the emissions correlated with each other at high values.

The third set of input variables in Table 2 are the mole fractions of trace species along the boundaries (the four sides and the top) of the urban area that impact the chemical and physical processing inside the urban area. The trace species that will be considered in this analysis are CO, NO_x, O₃, VOCs (represented by isoprene), and SO₂. The mole fractions of these species have been taken from the aggregation of their values in the corresponding latitude bands from the aforementioned IGSM set of 250 policy and no-policy runs, except for isoprene, which was taken from measured data (Houweling 1998; Yokouchi 1994). These aggregated sets of concentration data were then fitted by lognormal probability distribution functions, as given in **Figure 3**.

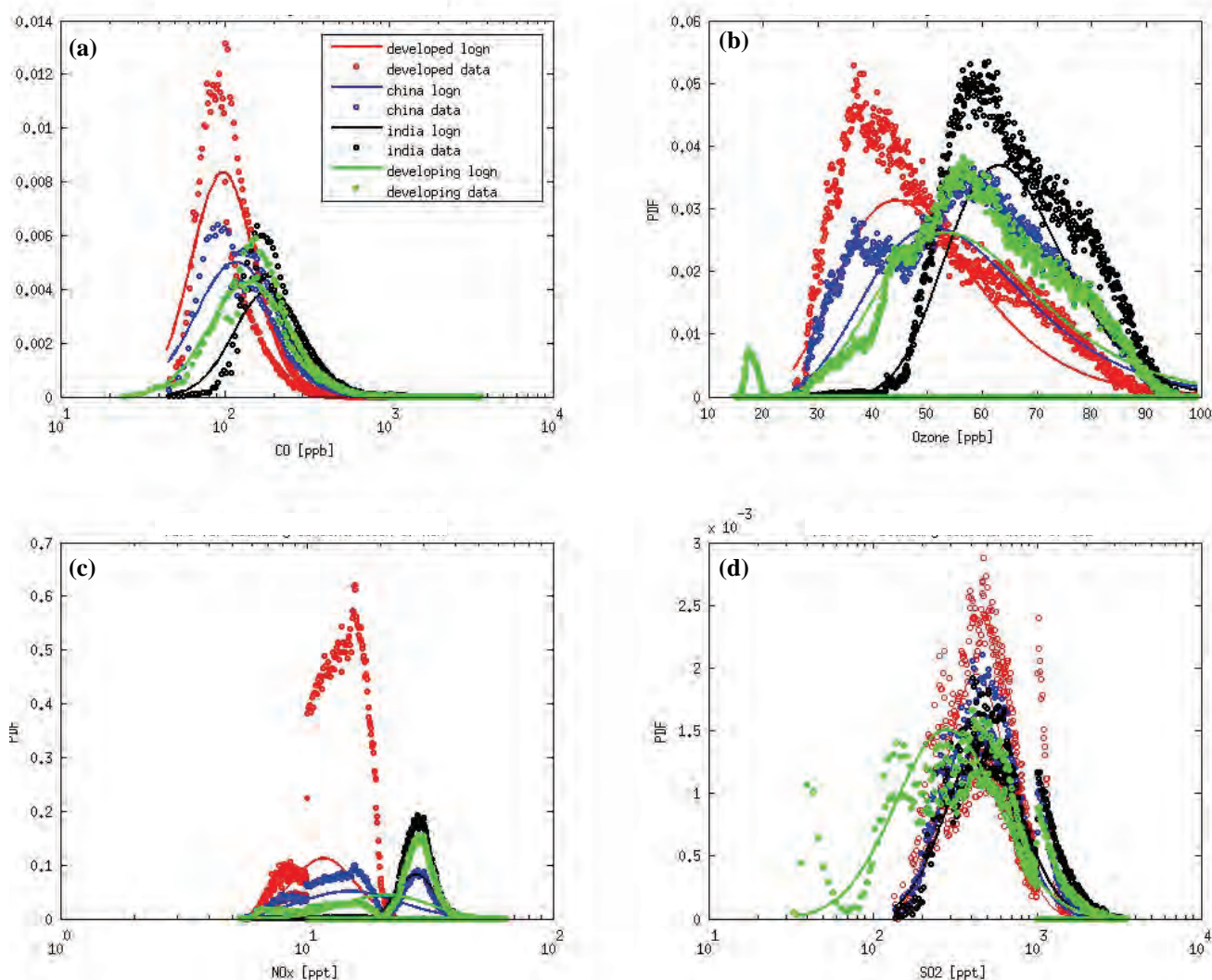


Figure 3. PDFs of boundary mole fractions of important species: **(a)** CO, **(b)** ozone, **(c)** NO_x, and **(d)** SO₂, where the dots are the underlying data points and the lines represent the best lognormal fits to the data.

The main problems with using the results from multiple runs of the IGSM to produce these various PDFs are that the IGSM does not produce results that provide a full probabilistic sampling of polluted upwind air and the MIT IGSM does not predict certain species which could be important, such as specific VOC species. However, using the IGSM gives a better indication of how these species will change over time, and since all are fit with lognormal PDFs, values which are considerably larger are more likely sampled. One way to improve this upon this IGSM data source would be to consider incorporating boundary conditions of anthropogenic and natural aerosols, such as BC, OC, SO₄, NO₃, mineral dust, and sea salt. Note that species which have a significant flux from urban regions and a negligible flux into urban regions, such as PAN, are also not considered as input variables, since their input fluxes have very little impact on their urban concentration or processing.

As noted earlier, the first set of input variables in Table 2 describe the physical properties of the urban area. The first two of these variables are the day of the year and the latitude of the urban region. These are both needed for computing the ultraviolet radiative flux. A uniform variable has been assigned, from 1 to 365 for the day of the year. A beta fit of the distribution of latitudes of each urban area has been made for each region, making the assumption that each urban area is of equal importance. The latitudinal PDF for each region is given in **Figure 4**.

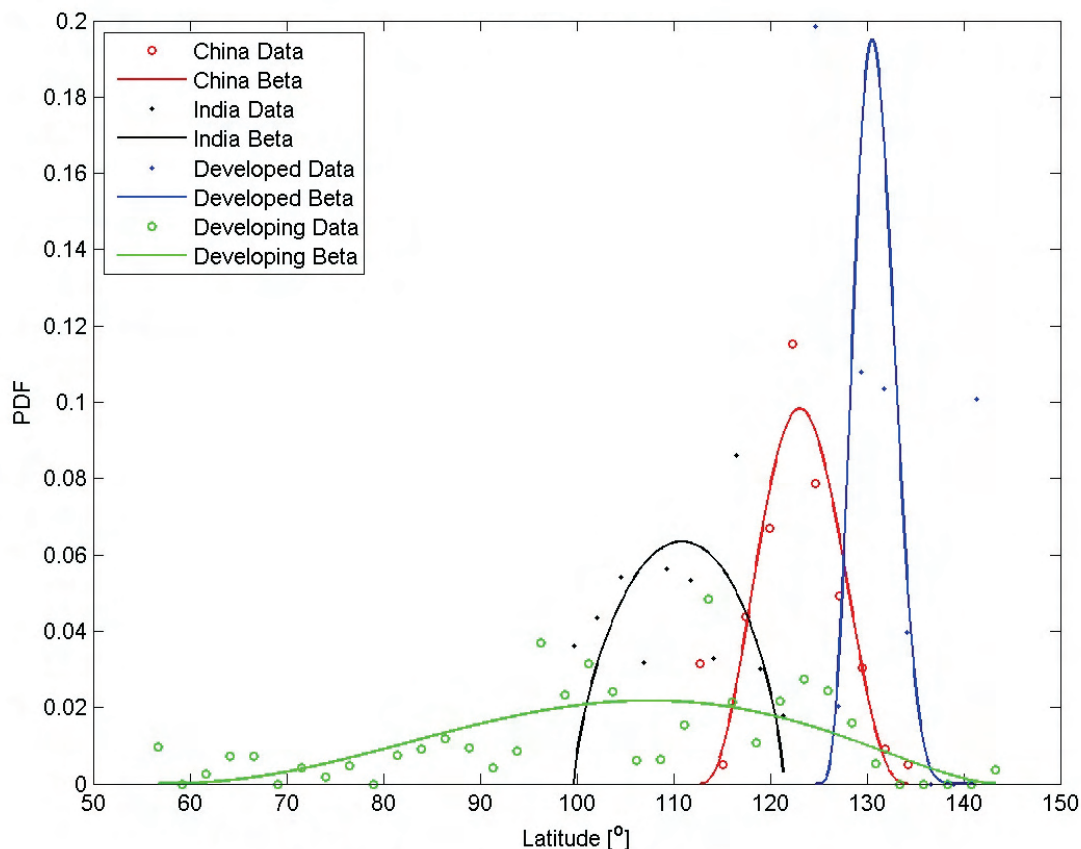


Figure 4. PDFs of the number of degrees latitude North, from the South Pole, for the urban areas, where the dots are the fraction of urban areas in each latitude bin (urban area location data are from (Center, 2000)) and the lines represent the best beta function fits to the data.

Another two inputs are the daily average temperature and the daily diurnal temperature, at the surface of the urban area. The atmospheric temperature in the urban area and its range are important variables for determining the rates of many chemical reactions, Henry’s Law partitioning, gas/aerosol phase partitioning, the state of water in the urban atmosphere, and the state and amount of precipitation. For the purposes of determining their global distribution, historical temperature data (Jones *et al.*, 1999) has been weighted by the beta PDF of latitude (Figure 4) for each urban area, and the resulting data fitted by a beta function. The average

temperature of each vertical layer above the surface is computed assuming a linear decline with height with standard linear lapse rate of 6.5K/km. The spatial and temporal deviations from these layer averages in the temperature of each grid box of the urban domain are taken from the meteorology chosen for that particular urban region. The average daily surface temperature and average daily diurnal surface temperature are given in **Figures 5 and 6**.

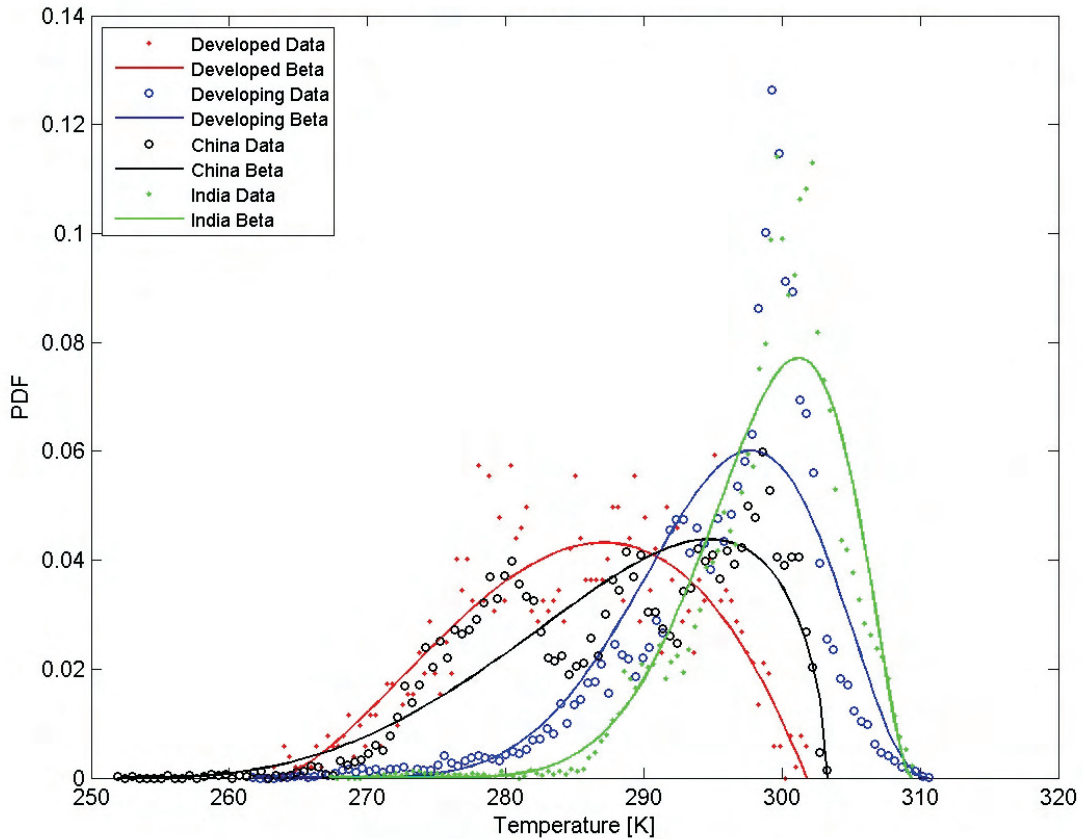


Figure 5. PDFs of the average daily surface temperature for each urban area, where the dots are the data for the monthly averaged daily average surface temperature, and the lines represent the best beta function fits to the data.

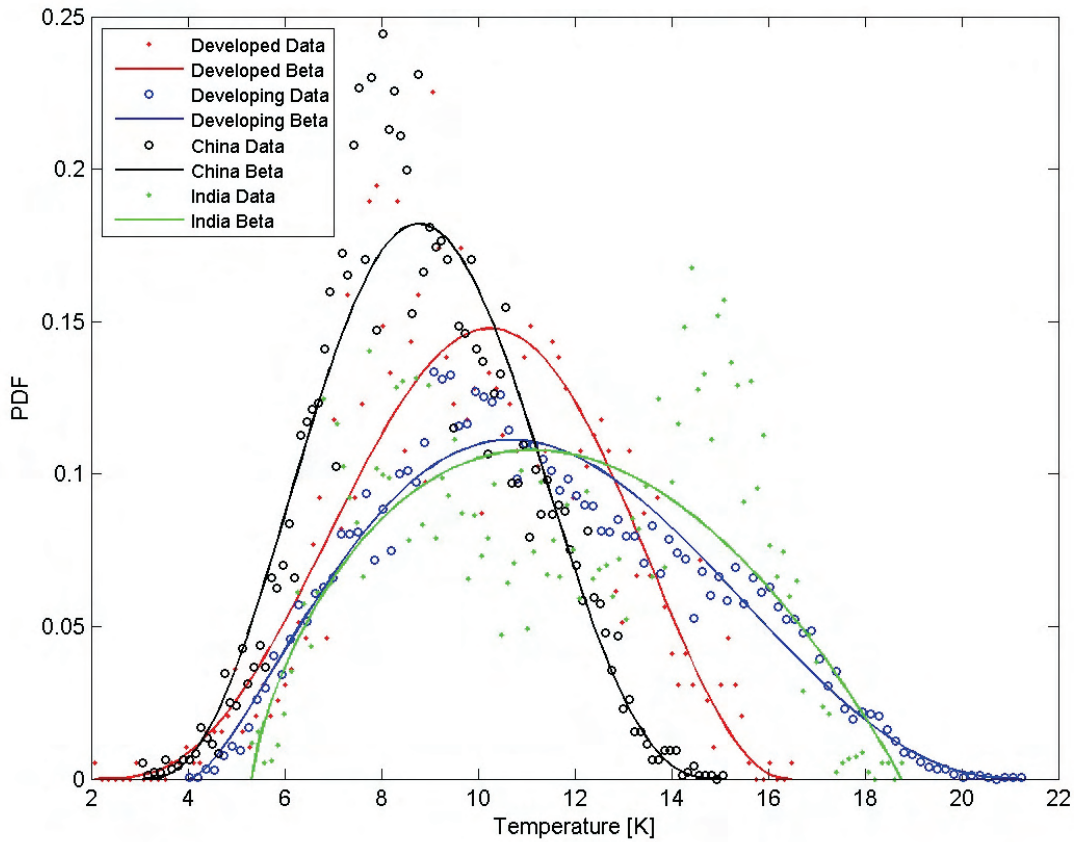


Figure 6. PDFs of the average daily diurnal temperature variation (daily high minus daily low) for each urban area, where the dots are the data for the monthly averaged daily diurnal surface temperature range, and the lines represent the best beta function fit to the data.

The final physical input to consider is rainfall (and the associated cloudiness), which impacts the radiative fluxes, the uptake of soluble gases, and the removal rate of aerosols. After extensive testing, it has been found that treating these inputs as separate variables using the PCM approach does not yield reasonable results, due to the extremely non-linear impact these variables have on the system. Therefore, separate metamodells were formed for each of the four meteorological conditions.

Another set of driving variables are designed to simulate the transportation and habitation choices people make that have an impact on the processing of species in urban regions. The first variable represents the temporal distribution of emissions. It is commonly found that emissions in urban areas have a time profile which is doubly peaked, with the peaks occurring around the times of the morning and evening rush hours. Furthermore, the middle of the day is found to have a plateau with a considerably higher amount of emissions than the nighttime plateau, as shown in **Figure 7**.

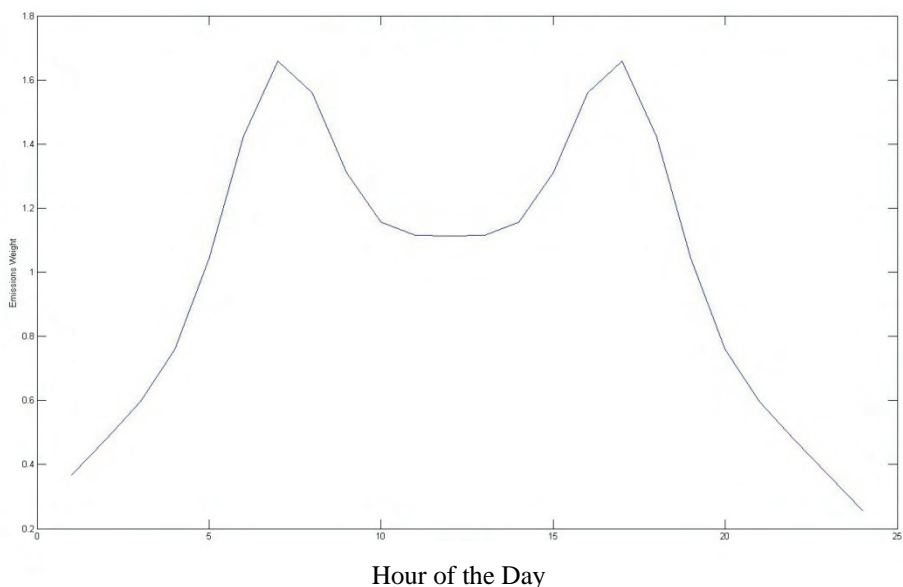


Figure 7. The temporal weight of emissions (normalized to unity), as a function of time, for an urban area. Specifically, this is the emission time distribution obtained if the input variable $wt = 1.0$.

To account for this, an input variable (wt) is defined that is uniformly distributed from 0 to 1, and is the weight given to this double peak temporal emissions spectrum when it is linearly added to a time invariant emissions profile. Therefore, for any given value of wt the weights assigned to the double-peaked distribution is wt and the weight assigned to the time invariant emissions distribution is $1-wt$ (Yang *et al.*, 2005). A second input variable relates to the spatial distribution of emissions in the urban region. Such a distribution must consider that urban areas vary greatly in terms of their density of people, activity, and thus emissions. For example, some urban areas, such as Shenzhen, China are very dense, while others, such as the New York City Metro Area, USA are much more diffuse. In general, different emitted species come from different sources, which themselves may be distributed independently from one another in many cases. However, since most emissions are related to the population in the urban centers, the emissions of both CO and BC are considered to be spatially correlated. These spatial distributions are fitted by a 2-dimensional Gaussian function whose standard diameter has a uniform distribution ranging from the assumed minimum size of a present world megacity of 21.6km (Shenzhen, China) to the assumed maximum size of a present world megacity of 93.2km (New York Metro Area, USA). Two examples are given in **Figure 8**, in which the color, an indication of the spatial weighting of emissions, clearly shows how strong of a change this variable makes on the distribution of emissions.

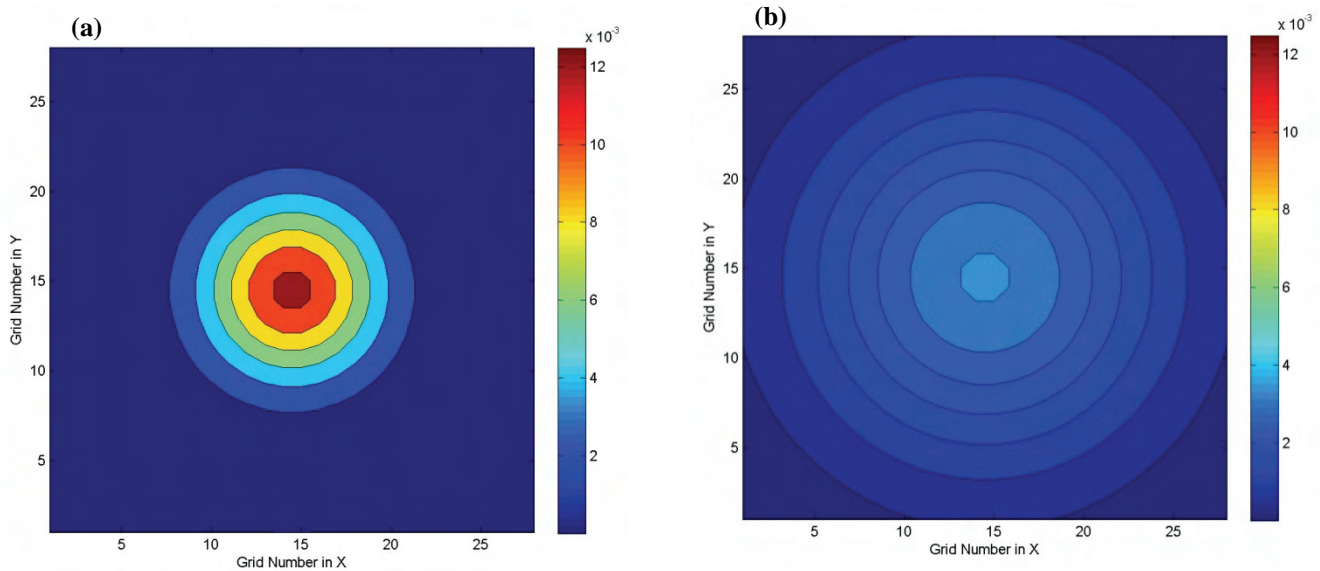


Figure 8. Example of how the geospatial normalized emissions weight changes for two example cases, where the color scale is identical for both plots. Frame **(a)** corresponds to a gaussian standard diameter of 40km and frame **(b)** to a gaussian standard diameter of 80km.

Another input is required to simulate whether VOC emissions consist of a larger fraction of light hydrocarbons, corresponding to a more developed economy, or whether they have a larger fraction of heavier hydrocarbons, corresponding to a developing economy. This final decision is made based on whichever region the urban area is in, with the Developed world using the IPCC Third Assessment Report guidelines for Developed Nations emissions speciation of VOCs and the rest of the world using the IPCC Third Assessment Report guidelines for Developing Nations emissions speciation of VOCs (Prather *et al.*, 2001). Since this final decision determines whether there are zero or non-zero values of many VOCs, the credibility of the output of these VOC species will not be the same for the developed urban nation metamodel as it will for the other three.

As previously mentioned, the impacts of the circulation, water content, and temperature on the processing in urban areas must be considered in detail. To address this issue, four different realistic sets of meteorology have been used to drive the urban modeling system. The point of employing these widely different cases is to numerically analyze the impact of adopting different types of realistic meteorology. This also allows for the feedback of rainfall in the global scale parent model to influence the processing at the urban scale.

3.2 Selected Outputs

The specific outputs from CAMx which were fit include chemical mole fractions / concentrations of trace species in the urban area [ppm (gases) and $\mu\text{g}/\text{m}^3$ (aerosols)], the net mass flux of trace species through the boundaries of the urban area [kg/day], the mass flux of trace species deposited to the surface [kg/day], and the concentrations of 7 specific trace species, of

interest to human health and policy, over the bottom three vertical layers of the urban area (under 100m) [ppm (gases) and $\mu\text{g}/\text{m}^3$ (aerosols)]. The 19 simulated trace gases and 32 simulated aerosol categories which were fit were further aggregated over space and time to produce 24 hour averaged values of 17 output trace gases and 8 output aerosol species. The exception to 24-hour averaging is for those species specific to specific human health input calculations, which have been averaged over the appropriate time span for each given species. The specific species simulated by the reduced form models are given in **Table 4** for both the climate and human health related outputs.

Table 4. Species simulated by the urban metamodels.

All Modeled Species (daily average unless otherwise stated)		
Ozone	Xylene	Black Carbon Mass
CO	C ₂ H ₄	Organic Carbon Mass
NO	C ₂ H ₆	Nitrate Mass
NO ₂	Peroxyacetyl Nitrate	Surface PM10
N _x O _y	H ₂ O ₂	Surface PM2.5
HNO ₃	NH ₃	Surface 8-Hour Ozone
SO ₂	Sulfate Number	Surface 6-Hour Ozone
H ₂ SO ₄	Black Carbon Number	Surface Ozone
HCHO	Organic Carbon Number	Surface NO _x
CH ₃ CHO	Nitrate Number	Surface SO ₂
Toluene	Sulfate Mass	

3.3 Obtaining the Parameterizations

The parameterizations formed in this work are based on a full third order polynomial chaos expansion, which includes all 3rd order cross terms, all degenerate 2nd order terms and cross terms, and all degenerate 1st order terms, for all 18 input variables. The fits were performed using the probabilistic collocation technique.

The chemical species modeled were selected either because the components have a direct or indirect impact on the radiative balance of the atmosphere at scales beyond the urban region from which they are emitted, or because they have consequences for human health. Furthermore, the majority of these species have non-linear gas-phase, liquid phase, or heterogeneous chemical or physical processing, causing their concentrations on the urban scale to not be accurately predictable using typical global scale grid sizes. These non-linear processes make prediction using a simple dilution or averaging approach in coarse resolution grids imprecise. One of the reasons for this is that these species have loss, production, and transformation lifetimes shorter than or similar to the timescales of large scale advection, mixing, and chemical processes found in typical global scale models.

The consideration of urban processing requires that the spatial and temporal resolution in the urban model be sufficiently fine so as to resolve these non-linear effects. To achieve this, the urban area was modeled using an Eulerian framework, with a uniform horizontal grid spacing of 4km x 4km in the North/South and East/West directions, over a total region of 108km x 108km.

In the vertical, 13 layers were chosen with pressure coordinates, from the surface up to the free troposphere, as given in **Table 5**.

Table 5. Average pressure at the top of each vertical layer of the urban modeling domain.

Vertical Layer	Pressure [hPa]	Vertical Layer	Pressure [hPa]
1	986	8	909
2	970	9	889
3	966	10	860
4	962	11	826
5	955	12	783
6	942	13	713
7	926		

The time step was allowed to vary between 3 minutes and 1 minute, so that the numerical solution of the equations would always remain stable. Finally, to make sure that any initialization assumptions were not affecting the results, the urban model was integrated for 96 hours, with the initial 72 hours being treated as a spin up and the final 24 hours being the result used.

3.4 Differences Between This Work and Previous Work

A significant difference between our new approach and prior efforts is inclusion of the impacts of liquid water, and its associated chemical and physical processes which do not occur under the dry conditions in prior efforts. One such impact involves aqueous chemistry. A second impact involves a large uptake of soluble gases from the gas to the aerosol phase, including a very large uptake of sulfuric acid and other sulfuric acid forming precursors. A third impact of including liquid water is that rainfall removes many gases and aerosols from the urban atmosphere and deposits these species to the surface, simultaneously lowering their atmospheric concentrations inside the urban area and suppressing the flux of these species from the urban area.

Another significant difference is inclusion of regions of strong vertical advection. These regions allow for efficient transport of trace species through the boundary layer, thereby altering their rates of chemical and physical transformation, and surface deposition, and hence their lifetimes within the urban area. These effects can be especially important if they occur during certain times of the day for photolysis reactions, at times when there is a considerable temperature gradient for temperature dependent reactions, or when there are strong liquid water or aerosol gradients for species having strong liquid water or aerosol uptake potential. These effects can substantially increase or decrease the amount of a species ultimately exported from an urban area.

A third significant difference comes from the consideration of variability in both atmospheric properties and surface emissions. For example, large changes in the height of the boundary layer affect the net transfer in the vertical of trace species, and whether these species are shielded from or exposed to sunlight. Furthermore, emissions occurring at different times of the day lead directly to a difference in the local concentrations near the surface. When these effects are

combined, it can lead to considerable changes in fluxes of mass, and to non-linear chemical feedbacks.

By specifically addressing these processes, this present modeling effort is an improvement over previous modeling efforts, which used non-varying winds, imposed uniformly and non-divergently with flow only from West to East. A further improvement is the use of multiple cases of meteorology. This enables studies of the effects of differences in rain, cloudiness, and wind fields within and at the boundaries of the regions that can affect the concentrations in the region and mass fluxes from the region.

There are some effects, however, which could not be included but could be important to address in the future. The inclusion of meteorology for regions which have complex topography, such as for Mexico City, Mexico or Chongqing, China would provide a more realistic treatment of these types of urban region. The inclusion of meteorology for urban regions which are in the equatorial latitudes, such as Singapore, would further provide a more realistic treatment in these urban regions. Furthermore, inclusion of realistic meteorology as a function of different seasons of the year would also provide a more realistic treatment of urban processing with respect to annual cycles. Other improvements could include consideration of urban scale “topography” (buildings and other built structures), and online calculation of absorption and scattering, fluid dynamics, and hydrological processes.

The Probabilistic Collocation Method using third order fits is a significant improvement when compared with previous efforts, which only used second order fits. In particular the following species have had their prediction capability improved, or were not modeled in previous efforts: primary aerosols, secondary aerosols, aerosol precursors, aerosol size distributions, ozone, PAN, and certain VOCs. Since using a higher order polynomial fit requires that more specific points be sampled from each input PDF, the metamodel is more precise for more extreme values of the input. It allows for the polynomial fit to be more reliable near the center of the input PDFs. A third order fit can also simulate up to two changes in the direction of the response based on the input variables, because it has two inflection points, compared with just a single change in the case of a 2nd order fit, which has only one inflection point.

The metamodel was finally tested, using the input variables that would be used to build a full 4th order polynomial approximation. Besides testing the metamodel performance, this exercise showed that a third order fit is sufficient for most of the species being modeled. There are however a few exceptions, where high degrees of non-linearity result in a better fit being obtained using a higher order polynomial. However, the improvement is generally not large, and would consume a large amount of resources to produce.

4. RESULTS AND DISCUSSION

4.1 Concentrations, Mass Fluxes, and Deposition

For the parent CAMx model runs, we have examined the results for the urban concentrations, mass fluxes from the urban area, and mass fluxes deposited to the surface in the urban area, for each trace species. When looking at the results of the concentrations in mole fraction form,

regions of higher mole fractions must have a larger net chemical production (production minus loss) of the species. Conversely, regions with lower mole fractions must have more a smaller or negative net chemical production of the species. Also, if the mole fraction remains constant across different regions, then this means that there is negligible net chemical production. By looking at these and other results, we have determined that the parent model's behavior makes physical sense.

When looking at the metamodel results for the mass fluxes, emissions, chemical production or loss, and the deposition, it is straightforward to determine whether the urban area is a net importer or exporter of the species of interest. For a species to have a mass flux which is not equal to its emissions, there must be a net amount of chemical processing, deposition, or convergence or divergence in the continuity equation (see Equation 1). A convenient metric is the ratio of the export flux to the emissions:

$$\text{Flux/Emiss} = (\text{Emiss} + \text{Chem} - \text{Dep})/\text{Emiss} = 1 + \text{Chem/Emiss} - \text{Dep/Emiss} \quad (6)$$

Here the Flux is the net mass flux [g/day] through the 5 boundaries of the urban region, Emiss is the emissions [g/day] into the urban area, Chem is the net chemical production [g/day] within the urban region, and Dep is the deposition [g/day] to the surface of the urban region. Using this metric, if the mass flux is positive and larger than the emissions, then the in-situ chemical net production must be larger than the in-situ depositional losses. Conversely, if a species has a mass flux which is positive but smaller than its emissions, its losses due to deposition must be greater than its net chemical production. Furthermore, for a species to have a mass flux which is negative (a net flux into the region), the in-situ net chemical loss must be so large as to consume not only all of the emissions, but also some of the species mass transported through the boundaries into the urban area. This mass flux / emissions ratio therefore provides two ways to test the validity of the model results. Firstly, any species which has a clean (zero) upwind boundary condition must have a mass flux larger than or equal to zero. Secondly, a species which has no atmospheric chemical production sources in the urban area, such as Black Carbon, must have a mass flux smaller than or equal to its emissions.

4.2 Parameterization Tests

The essential test of the reliability of the reduced form model's precision and accuracy is to see how its outputs compare with the parent model. This was determined by analyzing the concentrations, mass fluxes, and surface deposition computed from running the parent model and the metamodels at all of the 3rd and 4th order collocation points. This test does not of course determine the accuracy and precision of the underlying CAMx model, but this task has been carried out by many others (see Section 2.1). Scatter plots of these results, the ideal fit line (parent model = metamodel), and the associated RMS error, are given for a subset of output species (ozone, CO, formaldehyde, BC, OC, and sulfate aerosol) in **Appendices A1-A4** for each of the four meteorology scenarios associated with the China metamodel, and respectively, **Appendices A5-A8** for the India metamodel, **Appendices A9-A12** for the Developed metamodel, and **Appendices A13-A16** for the Developing metamodel.

To quantify the goodness of the fits we use a simple statistical method. The RMS and normalized RMS errors are computed. If X_i is the value computed by the metamodel, X_i^* is the value computed by the CAMx model, and n is the number of points analyzed in each grouping (in the case of the non-weighted RMS error, only the numerator is used), we have:

$$\text{normalized RMS} = \sqrt{(\sum_{i=1,n}(X_i^*-X_i)^2/n)} / \sqrt{(\sum_{i=1,n}X_i^2/n)} \quad (7a)$$

$$\text{RMS} = \sqrt{(\sum_{i=1,n}(X_i^*-X_i)^2/n)} \quad (7b)$$

The RMS error gives a measure of the absolute magnitude of the error. These statistics are calculated for the results of the metamodel based on the set of 3rd order input collocation points, and the results of the metamodel based on the aggregated sets of 3rd and 4th order input collocation points. The error associated with the 3rd order data points is representative of how well the metamodel corresponds to the data that was used to fit it. The error associated with the aggregated set of 3rd and 4th order data points is representative of how well the metamodel performs when used under realistic modeling conditions, at which the inputs are constrained only to be in the range given by the input PDFs used to construct the metamodel, but otherwise are random. The results are given in **Tables 6-17** for the aggregated set of 3rd and 4th order data points.

Two conclusions are readily drawn from Tables 6-17 and Figures A1-A16. The first is that the parent and metamodel outputs from the 3rd order input points fit almost perfectly, and secondly that under certain conditions, there are a small number of far-outliers for the outputs from the 4th order input points, under some model and meteorological conditions, which contribute to almost all of the RMS differences from the ideal fit. The very small number of points which are not physically possible (negative deposition or negative concentration), which are occasionally found only in these 4th order points (less than 1% of the points in all cases) are identified in our metamodel coded and are discarded with a note to that effect in the output. All of these physically impossible points, as well as the far outliers, in all cases, are due to inputs which are outside of the space spanned by the 3rd order collocation points.

Table 6. Normalized fractional RMS errors for species mole fractions/concentrations using the China metamodel.

Species	R241-F63-W46	R000-F00-W44	R021-F19-W57	R002-F02-W16
Ozone	9.73E-05	1.23E-04	9.29E-05	3.90E-04
CO	1.06E-04	1.00E-04	1.15E-04	1.55E-04
NO	2.35E-03	1.85E-03	3.04E-03	3.41E-03
NO ₂	9.20E-03	6.49E-03	1.04E-02	6.94E-03
N _x O _y	1.49E-03	1.09E+00	3.20E+00	2.36E-01
HNO ₃	1.76E-03	4.70E-02	4.95E-03	1.01E-01
SO ₂	8.99E-03	7.39E-03	1.71E-03	1.83E-02
H ₂ SO ₄	6.69E-01	1.01E-01	1.02E-01	1.47E-01
HCHO	3.77E-03	3.44E-03	2.95E-03	9.69E-03
CH ₃ CHO	1.60E-03	2.22E-03	2.26E-03	8.75E-03
Toluene	1.84E-04	1.44E-04	1.34E-04	4.81E-03
Xylene	1.81E-04	1.35E-04	1.37E-04	3.71E-03
C ₂ H ₄	1.22E-04	1.52E-04	2.51E-04	5.12E-03
C ₂ H ₆	1.37E-04	1.30E-04	1.40E-04	5.29E-03
PAN	1.85E-02	1.20E-02	1.39E-02	2.12E-02
H ₂ O ₂	7.17E-03	8.55E-03	8.03E-03	7.87E-03
NH ₃	3.93E-03	1.87E-03	4.19E-04	8.71E-03
Sulfate num	8.83E-03	3.09E-03	3.63E-03	7.51E-03
BC num	6.17E-04	2.13E-04	7.50E-04	2.95E-04
OC num	6.10E-04	2.19E-04	7.59E-04	3.29E-04
Nitrate num	1.65E-02	1.56E-02	6.44E-03	8.41E-03
Sulfate mass	5.23E-03	1.16E-03	1.43E-03	1.27E-02
BC mass	1.05E-02	1.31E-02	1.43E-02	3.05E-03
OC mass	1.05E-02	1.31E-02	1.43E-02	3.08E-03
Nitrate mass	5.85E-03	6.15E-03	9.27E-03	1.42E-02

Table 7. Normalized fractional RMS errors for species mass fluxes using the China metamodel.

Species	R241-F63-W46	R000-F00-W44	R021-F19-W57	R002-F02-W16
Ozone	7.38E-03	5.53E-03	5.95E-03	4.91E-03
CO	1.63E-04	1.69E-04	1.69E-04	1.94E-04
NO	2.61E-03	1.93E-03	2.74E-03	3.79E-03
NO ₂	8.87E-03	5.83E-03	8.46E-03	6.39E-03
N _x O _y	1.14E-02	1.28E-01	1.68E-02	1.04E-01
HNO ₃	5.25E-03	4.33E-02	1.02E-02	5.05E-02
SO ₂	3.75E-02	1.19E-02	5.23E-02	4.06E-03
H ₂ SO ₄	7.07E-01	1.41E-01	6.79E-02	1.04E-01
HCHO	5.78E-03	3.60E-03	5.23E-03	9.42E-03
CH ₃ CHO	3.29E-03	3.87E-03	4.16E-03	9.07E-03
Toluene	2.25E-04	1.60E-04	1.47E-04	4.74E-03
Xylene	2.35E-04	1.95E-04	1.42E-04	3.61E-03
C ₂ H ₄	1.25E-04	1.91E-04	2.32E-04	5.19E-03
C ₂ H ₆	1.59E-04	1.59E-04	1.58E-04	5.62E-03
PAN	2.09E-02	1.27E-02	1.73E-02	2.07E-02
H ₂ O ₂	1.73E-02	1.98E-02	2.02E-02	1.78E-02
NH ₃	6.44E-03	2.63E-03	2.83E-03	1.12E-02
Sulfate num	3.95E-03	9.26E-03	1.44E-03	1.11E-02
BC num	1.86E-02	5.64E-03	1.86E-02	2.69E-03
OC num	1.86E-02	5.60E-03	1.86E-02	2.72E-03

Nitrate num	1.29E-02	1.77E-02	9.93E-03	1.29E-02
Sulfate mass	7.01E-03	3.80E-03	1.59E-03	4.72E-03
BC mass	1.03E-03	5.82E-04	4.34E-04	6.36E-04
OC mass	1.02E-03	6.16E-04	4.53E-04	6.80E-04
Nitrate mass	1.35E-02	1.69E-02	1.04E-02	4.06E-02

Table 8. Normalized fractional RMS errors for species deposition using the China metamodel.

Species	R241-F63-W46	R000-F00-W44	R021-F19-W57	R002-F02-W16
Ozone	8.32E-04	1.33E-03	1.22E-03	4.17E-03
CO	0.00E+00	0.00E+00	0.00E+00	0.00E+00
NO	2.54E-03	2.61E-03	2.68E-03	3.14E-03
NO ₂	1.70E-02	1.41E-02	1.50E-02	8.91E-03
N _x O _y	1.27E-02	1.01E+00	3.22E+00	9.82E-02
HNO ₃	2.85E-03	1.55E-01	1.12E-02	1.63E-01
SO ₂	4.93E-03	3.13E-03	2.52E-03	2.53E-02
H ₂ SO ₄	6.99E-01	1.75E-01	1.35E-01	1.57E-01
HCHO	5.38E-03	3.11E-03	4.48E-03	9.29E-03
CH ₃ CHO	2.52E-03	2.50E-03	2.89E-03	8.04E-03
Toluene	2.49E-04	2.88E-04	2.64E-04	5.36E-03
Xylene	2.37E-04	2.46E-04	2.46E-04	4.49E-03
C ₂ H ₄	1.38E-04	2.05E-04	1.99E-04	5.43E-03
C ₂ H ₆	1.88E-04	1.98E-04	2.32E-04	5.61E-03
PAN	2.96E-02	8.80E-03	1.73E-02	1.96E-02
H ₂ O ₂	8.32E-03	8.22E-03	8.08E-03	7.19E-03
NH ₃	1.84E-03	1.16E-03	9.57E-04	1.04E-02
Sulfate num	8.79E-03	3.01E-03	6.29E-03	3.65E-03
BC num	2.03E-03	9.12E-03	9.06E-03	4.36E-03
OC num	2.04E-03	9.13E-03	9.06E-03	4.36E-03
Nitrate num	1.08E-02	2.49E-02	7.15E-03	5.82E-03
Sulfate mass	1.18E-02	1.47E-02	7.82E-03	3.53E-02
BC mass	1.92E-04	2.23E-02	1.71E-03	6.15E-03
OC mass	1.91E-04	2.23E-02	1.71E-03	6.15E-03
Nitrate mass	2.29E-02	3.62E-03	7.26E-03	2.10E-02

Table 9. Normalized fractional RMS errors for species mole fractions/concentrations using the India metamodel.

Species	R241-F63-W46	R000-F00-W44	R021-F19-W57	R002-F02-W16
Ozone	1.73E-04	1.42E-04	1.69E-04	3.40E-04
CO	4.49E-05	4.41E-05	4.81E-05	6.53E-05
NO	2.53E-04	2.91E-04	3.30E-04	4.40E-04
NO ₂	3.77E-04	3.47E-04	4.86E-04	5.10E-04
N _x O _y	0.00E+00	2.55E-01	3.14E-02	2.01E-02
HNO ₃	1.05E-03	9.42E-04	5.34E-04	1.41E-02
SO ₂	3.00E-03	8.61E-04	1.20E-03	6.58E-04
H ₂ SO ₄	0.00E+00	2.36E-01	1.39E-01	6.03E-02
HCHO	1.91E-03	1.44E-03	1.11E-03	4.18E-04
CH ₃ CHO	8.34E-04	1.09E-03	7.46E-04	4.75E-04
Toluene	8.95E-05	9.60E-05	9.15E-05	1.00E-04
Xylene	9.77E-05	1.25E-04	1.06E-04	2.19E-04
C ₂ H ₄	9.54E-05	1.05E-04	9.58E-05	1.53E-04
C ₂ H ₆	8.24E-05	7.79E-05	8.22E-05	8.15E-05

PAN	9.14E-03	3.92E-03	4.36E-03	1.07E-03
H2O2	2.68E-03	3.07E-03	2.88E-03	2.71E-03
NH3	6.16E-04	2.65E-04	4.28E-04	6.66E-04
Sulfate num	1.54E-03	3.70E-04	2.14E-04	8.43E-04
BC num	1.23E-04	2.03E-04	1.44E-04	1.69E-04
OC num	1.09E-04	1.43E-04	1.00E-04	1.11E-04
Nitrate num	4.80E-03	1.42E-03	2.70E-03	4.26E-03
Sulfate mass	1.88E-03	6.74E-04	3.32E-03	2.66E-03
BC mass	1.24E-03	4.65E-03	7.42E-03	8.46E-03
OC mass	1.20E-03	4.69E-03	7.42E-03	7.98E-03
Nitrate mass	4.83E-03	2.95E-03	6.21E-03	2.08E-03

Table 10. Normalized fractional RMS errors for species mass fluxes using the India metamodel.

Species	R241-F63-W46	R000-F00-W44	R021-F19-W57	R002-F02-W16
Ozone	1.19E-03	1.11E-03	1.03E-03	1.07E-03
CO	1.15E-04	1.17E-04	1.22E-04	1.10E-04
NO	3.40E-04	5.88E-04	4.02E-04	8.00E-04
NO ₂	4.47E-04	5.53E-04	4.38E-04	7.21E-04
N _x O _y	2.03E-02	1.16E-02	2.83E-02	7.63E-03
HNO ₃	2.01E-03	7.37E-03	3.62E-03	9.38E-03
SO ₂	6.52E-04	2.87E-03	8.35E-04	1.87E-02
H ₂ SO ₄	3.48E-05	1.98E-01	5.67E-01	8.07E-02
HCHO	2.77E-03	1.24E-03	2.09E-03	6.13E-04
CH ₃ CHO	1.66E-03	1.86E-03	2.05E-03	1.08E-03
Toluene	1.11E-04	1.11E-04	1.03E-04	1.29E-04
Xylene	1.23E-04	1.44E-04	1.25E-04	3.05E-04
C ₂ H ₄	1.10E-04	1.20E-04	1.11E-04	2.00E-04
C ₂ H ₆	9.63E-05	9.72E-05	9.61E-05	9.60E-05
PAN	1.06E-02	3.02E-03	5.87E-03	1.34E-03
H ₂ O ₂	1.14E-02	1.37E-02	1.38E-02	1.18E-02
NH ₃	5.03E-04	7.76E-04	4.14E-04	1.54E-03
Sulfate num	8.14E-04	5.30E-04	1.63E-03	5.80E-03
BC num	2.83E-03	4.99E-03	7.33E-03	2.79E-03
OC num	2.76E-03	5.05E-03	7.31E-03	2.44E-03
Nitrate num	6.95E-03	5.60E-03	1.04E-02	7.55E-03
Sulfate mass	5.61E-04	4.33E-04	3.41E-04	2.49E-04
BC mass	1.52E-04	1.82E-04	1.90E-04	1.60E-04
OC mass	1.40E-04	1.15E-04	1.30E-04	1.38E-04
Nitrate mass	5.71E-03	3.76E-03	6.24E-03	3.65E-03

Table 11. Normalized fractional RMS errors for species deposition using the India metamodel.

Species	R241-F63-W46	R000-F00-W44	R021-F19-W57	R002-F02-W16
Ozone	4.64E-04	4.00E-04	4.30E-04	4.92E-04
CO	0.00E+00	0.00E+00	0.00E+00	0.00E+00
NO	1.03E-04	1.13E-04	1.29E-04	1.31E-04
NO ₂	4.48E-04	4.59E-04	2.79E-04	3.06E-04
N _x O _y	2.05E-03	7.61E-03	8.80E-03	1.21E-02
HNO ₃	9.92E-04	1.47E-03	8.21E-04	1.91E-02
SO ₂	1.98E-03	3.66E-04	1.50E-03	4.50E-03
H ₂ SO ₄	1.03E-05	2.59E-01	9.76E-02	8.92E-02

HCHO	2.75E-03	2.54E-04	1.99E-03	5.82E-04
CH3CHO	1.50E-03	1.19E-04	8.85E-04	4.84E-04
Toluene	8.19E-05	1.89E-04	1.09E-04	1.04E-04
Xylene	8.55E-05	2.05E-04	1.36E-04	2.44E-04
C2H4	8.44E-05	1.02E-04	1.07E-04	1.01E-04
C2H6	7.57E-05	7.94E-05	9.25E-05	7.81E-05
PAN	1.33E-02	1.92E-03	5.85E-03	3.05E-03
H2O2	2.91E-03	2.66E-03	3.04E-03	2.58E-03
NH3	4.39E-04	2.14E-04	3.90E-04	6.92E-04
Sulfate num	2.24E-03	7.67E-04	1.04E-03	1.67E-03
BC num	2.50E-04	2.79E-03	6.29E-03	4.25E-03
OC num	2.54E-04	2.79E-03	6.29E-03	4.24E-03
Nitrate num	7.08E-03	5.72E-03	1.04E-02	1.65E-03
Sulfate mass	2.23E-03	1.29E-03	1.47E-03	2.70E-03
BC mass	1.40E-04	1.89E-03	1.50E-04	4.83E-04
OC mass	1.42E-04	1.89E-03	1.50E-04	4.83E-04
Nitrate mass	6.10E-03	2.31E-03	4.98E-03	4.04E-03

Table 12. Normalized fractional RMS errors for species mole fractions/concentrations using the Developed metamodel.

Species	R241-F63-W46	R000-F00-W44	R021-F19-W57	R002-F02-W16
Ozone	6.32E-04	7.09E-04	1.99E-03	1.03E-03
CO	5.86E-04	6.41E-04	1.28E-03	4.52E-04
NO	1.41E-02	1.62E-02	8.62E-02	1.74E-02
NO ₂	2.48E-02	2.06E-02	2.36E-02	1.53E-02
N _x O _y	1.33E-01	5.21E-03	8.37E-02	4.61E-03
HNO ₃	1.05E-01	1.09E-01	2.26E-02	1.08E-01
SO ₂	5.33E-03	7.20E-02	1.17E-01	5.44E-02
H ₂ SO ₄	2.23E-01	1.44E-01	3.48E-02	5.61E-02
HCHO	7.12E-02	4.12E-02	1.77E-02	1.64E-02
CH3CHO	8.31E-02	4.50E-02	3.49E-02	7.32E-03
Toluene	3.94E-03	1.89E-02	2.55E-01	3.74E-03
Xylene	8.31E-03	2.31E-02	2.69E-01	1.12E-02
C2H4	6.66E-01	9.16E-02	1.80E-01	3.75E-07
C2H6	3.31E-01	7.66E-02	1.55E-01	9.24E-08
PAN	9.08E-02	9.20E-02	4.31E-02	1.39E-02
H2O2	3.23E-03	2.36E-03	2.45E-03	2.31E-03
NH3	8.79E-03	2.19E-02	4.85E-02	1.36E-02
Sulfate num	1.51E-02	5.56E-02	1.07E-01	3.78E-02
BC num	7.42E-04	2.37E-04	2.47E-04	6.82E-04
OC num	5.55E-03	7.84E-02	1.32E-01	4.83E-03
Nitrate num	4.17E-02	2.80E-01	7.74E-02	2.77E-01
Sulfate mass	1.08E-02	5.27E-02	8.59E-02	2.94E-02
BC mass	2.79E-02	3.56E-03	2.00E-02	3.02E-03
OC mass	2.74E-02	9.10E-02	1.62E-01	2.93E-03
Nitrate mass	2.15E-02	3.69E-02	1.38E-01	1.47E-02

Table 13. Normalized fractional RMS errors for species mass fluxes using the Developed metamodel.

Species	R241-F63-W46	R000-F00-W44	R021-F19-W57	R002-F02-W16
Ozone	1.99E-02	1.22E-02	3.56E-02	1.16E-02
CO	7.05E-04	8.53E-04	1.57E-03	5.15E-04

NO	1.29E-02	1.55E-02	8.86E-02	1.72E-02
NO ₂	1.77E-02	1.16E-02	2.35E-02	1.21E-02
N _x O _y	4.98E+00	1.98E-01	6.52E+00	8.72E-02
HNO ₃	1.04E-01	8.59E-02	5.61E-02	1.06E-01
SO ₂	1.23E-02	4.31E-02	1.41E-01	6.23E-02
H ₂ SO ₄	1.10E+00	1.70E-01	2.49E-01	1.40E-01
HCHO	4.91E-02	3.90E-02	2.37E-01	1.45E-02
CH ₃ CHO	6.44E-02	3.93E-02	1.34E-01	1.59E-02
Toluene	4.42E-03	1.98E-02	2.53E-01	4.62E-03
Xylene	1.05E-02	2.72E-02	2.75E-01	1.39E-02
C ₂ H ₄	6.66E-01	2.85E-01	7.15E+00	7.68E-03
C ₂ H ₆	6.63E-01	2.77E-01	6.66E+00	7.27E-03
PAN	1.03E-01	9.26E-02	2.73E-01	1.83E-01
H ₂ O ₂	1.47E-02	1.46E-02	1.52E-02	1.47E-02
NH ₃	1.81E-02	7.40E-01	1.39E+00	1.09E-02
Sulfate num	1.14E-02	7.39E-02	6.99E-02	3.63E-02
BC num	3.40E-02	1.93E-02	4.24E-02	5.15E-03
OC num	3.30E-02	7.00E-02	1.94E-01	6.65E-03
Nitrate num	2.23E-01	1.16E-01	4.42E+00	1.07E-01
Sulfate mass	1.59E-02	8.20E-02	9.70E-02	2.20E-02
BC mass	1.47E-03	4.64E-04	2.38E-04	1.01E-03
OC mass	7.40E-03	7.47E-02	1.27E-01	6.26E-03
Nitrate mass	3.33E-01	2.80E-01	3.28E+00	2.80E-01

Table 14. Normalized fractional RMS errors for species deposition using the Developed metamodel.

Species	R241-F63-W46	R000-F00-W44	R021-F19-W57	R002-F02-W16
Ozone	3.00E-03	5.44E-03	9.77E-03	2.68E-03
CO	0.00E+00	0.00E+00	0.00E+00	0.00E+00
NO	1.38E-02	1.85E-02	7.58E-02	1.86E-02
NO ₂	3.31E-02	2.77E-02	2.43E-02	2.05E-02
N _x O _y	1.50E-01	5.47E-03	8.39E-02	5.48E-03
HNO ₃	1.05E-01	1.35E-01	1.88E-02	1.14E-01
SO ₂	3.25E-03	7.39E-02	1.27E-01	3.30E-02
H ₂ SO ₄	1.03E-01	1.73E-01	6.15E-02	6.13E-02
HCHO	6.95E-02	4.41E-02	4.95E-02	3.95E-02
CH ₃ CHO	8.39E-02	4.48E-02	1.76E-02	3.06E-02
Toluene	3.67E-03	1.69E-02	2.54E-01	1.93E-03
Xylene	6.67E-03	1.69E-02	2.70E-01	6.96E-03
C ₂ H ₄	6.68E-01	9.15E-02	1.77E-01	3.46E-04
C ₂ H ₆	6.28E-01	9.17E-02	1.66E-01	9.60E-06
PAN	1.04E-01	1.04E-01	4.14E-02	1.28E-01
H ₂ O ₂	2.34E-03	4.24E-03	3.05E-03	2.76E-03
NH ₃	3.57E-03	1.79E-02	4.05E-02	1.43E-02
Sulfate num	1.37E-02	2.72E-02	7.57E-02	1.28E-02
BC num	9.34E-03	6.62E-03	1.91E-02	2.08E-02
OC num	9.36E-03	8.94E-02	1.43E-01	2.08E-02
Nitrate num	8.86E-02	2.50E-02	1.21E-01	9.22E-03
Sulfate mass	1.85E-02	8.30E-02	8.31E-02	3.92E-02
BC mass	2.39E-04	2.57E-02	1.06E-03	6.83E-03
OC mass	2.86E-04	5.26E-02	1.50E-01	6.83E-03
Nitrate mass	9.16E-02	2.75E-01	6.75E-02	2.76E-01

Table 15. Normalized fractional RMS errors for species mole fractions/concentrations using the Developing metamodel.

Species	R241-F63-W46	R000-F00-W44	R021-F19-W57	R002-F02-W16
Ozone	1.87E-04	2.69E-04	2.51E-04	6.00E-04
CO	2.66E-04	2.90E-04	2.87E-04	3.74E-04
NO	1.58E-03	1.08E-03	1.89E-03	1.22E-03
NO ₂	5.17E-03	6.60E-04	3.66E-03	1.90E-03
N _x O _y	6.21E-02	2.39E-01	2.56E-01	1.42E-01
HNO ₃	5.32E-03	2.37E-02	2.72E-02	1.85E-02
SO ₂	8.12E-03	2.76E-02	2.91E-02	5.19E-02
H ₂ SO ₄	2.66E-02	1.54E-01	1.63E-01	1.53E-02
HCHO	1.36E-03	3.57E-03	3.16E-03	3.26E-03
CH ₃ CHO	1.30E-03	2.49E-03	2.13E-03	1.41E-03
Toluene	3.42E-04	3.68E-04	3.63E-04	2.02E-03
Xylene	3.53E-04	8.17E-04	8.67E-04	3.22E-03
C ₂ H ₄	3.14E-04	5.52E-04	7.48E-04	3.60E-03
C ₂ H ₆	3.32E-04	3.59E-04	3.34E-04	3.42E-04
PAN	3.34E-03	1.90E-03	1.68E-03	4.09E-03
H ₂ O ₂	4.60E-03	8.44E-03	7.27E-03	7.00E-03
NH ₃	1.17E-02	1.53E-02	2.78E-02	4.28E-02
Sulfate num	1.35E-02	2.51E-02	3.08E-02	4.80E-02
BC num	4.68E-04	3.36E-04	4.10E-04	1.19E-03
OC num	4.57E-04	3.33E-04	3.88E-04	1.10E-03
Nitrate num	1.00E-02	1.38E-02	1.74E-02	1.79E-02
Sulfate mass	1.45E-02	1.85E-02	3.17E-02	2.47E-02
BC mass	1.33E-02	5.21E-03	2.27E-02	1.43E-03
OC mass	1.32E-02	5.03E-03	2.26E-02	1.37E-03
Nitrate mass	6.77E-03	1.79E-02	1.32E-02	1.07E-02

Table 16. Normalized fractional RMS errors for species mass fluxes using the Developing metamodel.

Species	R241-F63-W46	R000-F00-W44	R021-F19-W57	R002-F02-W16
Ozone	7.98E-03	6.39E-03	6.18E-03	6.00E-03
CO	6.35E-04	6.32E-04	6.35E-04	6.37E-04
NO	8.74E-04	1.81E-03	1.08E-03	2.32E-03
NO ₂	1.37E-03	3.14E-03	1.53E-03	3.58E-03
N _x O _y	1.51E-01	3.52E-01	3.26E-01	1.27E-01
HNO ₃	8.11E-03	3.47E-02	1.57E-02	3.18E-02
SO ₂	1.40E-02	7.01E-03	2.41E-02	4.68E-02
H ₂ SO ₄	1.91E-01	6.20E-02	7.09E-02	4.57E-02
HCHO	1.06E-03	2.90E-03	1.82E-03	1.46E-03
CH ₃ CHO	1.35E-03	2.25E-03	1.63E-03	2.42E-03
Toluene	6.88E-04	6.79E-04	6.52E-04	1.99E-03
Xylene	7.05E-04	1.20E-03	8.24E-04	2.61E-03
C ₂ H ₄	6.48E-04	8.62E-04	7.46E-04	3.10E-03
C ₂ H ₆	6.35E-04	6.30E-04	6.35E-04	6.32E-04
PAN	3.35E-03	2.06E-03	2.60E-03	5.05E-03
H ₂ O ₂	4.08E-03	1.39E-02	1.19E-02	1.21E-02
NH ₃	1.12E-02	2.37E-02	2.11E-02	1.54E-02
Sulfate num	6.81E-03	1.89E-02	7.59E-03	9.50E-03
BC num	9.49E-03	1.26E-02	4.80E-02	6.77E-03
OC num	9.39E-03	1.25E-02	4.74E-02	6.59E-03

Nitrate num	9.20E-03	1.54E-02	2.81E-02	1.21E-02
Sulfate mass	6.64E-03	4.62E-03	9.83E-03	2.82E-02
BC mass	7.89E-04	7.50E-04	7.60E-04	1.40E-03
OC mass	7.78E-04	8.07E-04	8.02E-04	1.27E-03
Nitrate mass	1.28E-02	1.76E-02	1.63E-02	2.20E-02

Table 17. Normalized fractional RMS errors for species deposition using the Developing metamodel.

Species	R241-F63-W46	R000-F00-W44	R021-F19-W57	R002-F02-W16
Ozone	1.44E-03	2.13E-03	2.14E-03	2.43E-03
CO	0.00E+00	0.00E+00	0.00E+00	0.00E+00
NO	3.36E-03	3.40E-03	3.44E-03	4.38E-03
NO ₂	1.61E-02	1.09E-02	1.17E-02	5.36E-03
N _x O _y	2.67E-01	2.21E-01	1.44E-01	1.52E-01
HNO ₃	2.42E-03	6.31E-02	5.49E-02	1.90E-02
SO ₂	7.54E-03	1.50E-02	1.91E-02	3.70E-02
H ₂ SO ₄	1.30E-01	7.24E-03	6.15E-03	9.53E-03
HCHO	4.71E-03	3.32E-03	5.23E-03	5.07E-03
CH ₃ CHO	3.36E-03	1.99E-03	3.73E-03	1.51E-03
Toluene	5.41E-04	2.60E-04	6.22E-04	1.11E-03
Xylene	5.11E-04	3.18E-04	1.75E-03	2.57E-03
C ₂ H ₄	3.01E-04	9.25E-04	9.78E-04	3.61E-03
C ₂ H ₆	1.68E-04	1.41E-04	1.73E-04	1.57E-04
PAN	5.59E-03	4.45E-03	2.67E-03	1.61E-03
H ₂ O ₂	1.29E-02	7.34E-03	1.47E-02	7.47E-03
NH ₃	7.89E-03	1.88E-02	1.79E-02	7.32E-02
Sulfate num	2.30E-02	8.66E-03	3.61E-02	1.17E-03
BC num	1.84E-02	1.80E-02	1.09E-02	9.47E-03
OC num	1.84E-02	1.80E-02	1.09E-02	9.49E-03
Nitrate num	1.26E-02	3.16E-02	2.23E-02	8.13E-03
Sulfate mass	2.45E-02	5.67E-02	5.25E-02	3.95E-02
BC mass	4.42E-04	2.90E-02	1.89E-03	1.30E-02
OC mass	4.50E-04	2.90E-02	1.89E-03	1.30E-02
Nitrate mass	1.13E-02	2.98E-02	4.41E-02	1.71E-02

The results of the statistical analysis of the 3rd order collocation points (not shown in Tables 6-17) are nearly perfectly consistent for the concentrations, mass fluxes, and deposition fluxes of all species, under all of meteorological conditions, using all of the metamodels. The value of the normalized RMS error is always less than 1.8×10^{-5} for the China metamodel, 1.6×10^{-5} for the India metamodel, 1.6×10^{-4} for the developed metamodel, and 4.5×10^{-5} for the developing metamodel. This shows that the metamodels behave precisely and accurately, in relation to the parent model, at input values close to the 3rd order collocation points. And furthermore, since the input values are based on data which is significant to only 2 or 3 decimal places, the errors are smaller than the significance levels of the input parameters, which effectively shows that the results are perfect.

The results of the analysis of the concatenation of the 3rd and 4th order collocation points (Tables 6-17) are those which best represent the performance of the model over the ranges given by the input variable PDFs, because they best sample the accuracy of the reduced form model

over a wide range of reasonable input values. The normalized RMS error is always less than 10% under all meteorological conditions, for all metamodels, and for all quantities being modeled (concentration, flux, and deposition) for ozone, CO, NO, NO₂, H₂O₂, BC mass, and BC number.

Sulfur is not predicted as accurately as the above species. This is partially due to the non-linear processes for sulfate production; the major pathway usually involves liquid water, but under certain situations, the usually slow gas-phase production mechanisms can become important. This is shown by the fact that sulfur is predicted reasonably well, except in the case of the developed metamodel, which has a different VOC emissions profile, and hence a different OH concentration and a different oxidative capacity. Additionally, the meteorology case which is modeled the least well (R021F19W57) has the most extreme horizontal and temporal gradients of cloud cover and liquid water content. Specifically, the normalized RMS errors for SO₂, sulfate aerosol mass, and sulfate aerosol number, are always less than 10% under all meteorological conditions, for all metamodels, and for all quantities being modeled, except for the developed metamodel, meteorological scenario R021-F19-W57. In these exceptional cases, the normalized RMS error for SO₂ is always less than 15%, and the normalized RMS error for sulfate aerosol number is always less than 11%.

VOCs and OC (due to secondary production) are also less well predicted than the above species. Part of the reason is the same as in the case of sulfur. However, the different VOC emissions profile has a further impact, since some species have negligible emissions in the developed metamodel cases. The resulting concentrations are so small that the fits are not precise, but the species fits are also not too relevant in these cases. The normalized RMS errors for formaldehyde, acetaldehyde, toluene, xylene, ethene, ethane, OC mass and OC number are always less than 10% under all meteorological conditions, for all metamodels except for the developed metamodel, and for all quantities modeled. The normalized RMS errors for formaldehyde and acetaldehyde are always less than 10%, except for the deposition value in the R021-F19-W57 meteorological case, where they are less than 24% and 14% respectively. The normalized RMS errors for toluene and xylene are always less than 10%, except for all the modeled quantities in the meteorological case R021-F19-W57, where they are always less than 28%. The normalized RMS errors for ethene and ethane for the developed metamodel are unacceptably large except for meteorology cases R002-F02-W16 (errors always less than 10%) and R000-F00-W44 (errors always less than 29%). This is because these latter two exceptional cases have longer air residence times in the urban area, less variation in rain, and less variation in solar insolation, so there is more chance for the chemical processing to come to something closer to a pseudo-steady state, compared with the other meteorological cases. Finally, due to the fact that some of the OC production is based on secondary processing of heavy VOCs, the normalized RMS error for OC is not as good as that of BC for the developed metamodel. However, only in one meteorological scenario, R021-F19-W57 is the normalized RMS error greater than 10%, and even then it is always less than 20%. This is because in the high rain scenarios, the washout effects of rain are more acute, and in the low rain scenario, the chemical processing of the heavy VOCs is simulated more precisely.

Ammonia is well predicted, again except for the case of the developed metamodel. In the case of the developed metamodel, the deposition of ammonia is so imprecise, that it is not trustworthy to use at all. However, since deposition accounts for only a very small amount of the loss of ammonia from the urban environment, the concentration and mass fluxes are both always modeled with a normalized RMS error of less than 10%. The deposition of nitrate aerosols is also not very precise for two of the meteorological cases for the developed city metamodel.

Finally, PAN is reasonably well modeled except in the developed city metamodel. This species involves the chemistry of both the nitrogen cycle (NO_2) and the VOC cycle. Overall, the deposition of PAN is found to have a normalized RMS error of less than 28%, the mass flux is found to have a normalized RMS error of less than 13%, and the normalized RMS error of the concentration is always less than 10%.

The meteorology clearly plays a significant role for essentially all species. In rainy meteorological conditions, much of the chemistry is dominated by the aqueous phase and wet removal, and there is less photochemistry due to a lower level of incident UV. In dry meteorological conditions, the results are heavily influenced by greater UV, different amounts of vertical advection, less wet removal, and considerable dry aerosol processing. In addition, meteorological scenarios which are more variable tend to produce large spatial and temporal gradients, causing the system to behave less linearly. Finally, the time scale over which the species remain in the urban area is very important, with the processing likely to be more complete, and hence easier to predict, the longer the residence time of air in the urban area.

4.3 Sensitivity Tests

The sensitivity of the response of these metamodels to different input parameters has been investigated, to make sure that the metamodels are reliable under many different input conditions. The results from the polynomial fits should be robust under input conditions which are considered to be in the high probability region of their distribution, but these can vary considerably, both to represent different types of urban regions, and to account for changes which may happen over time to currently existing urban regions. Some of the issues to look into include the impact of variations in the spatial and temporal emissions profiles, impacts of variations of temperature, and impacts of extremely high levels of emissions, either separately or in some combination. Some of the more non-linear responses are likely to be seen in terms of ozone formation at very high levels of NO_x , secondary OC formation, sulfate aerosol formation, and VOC oxidation (for example, as reflected in the formaldehyde concentrations).

To accomplish this investigation, each metamodel was run using the same set of 50,000 independently and randomly sampled numbers. These were chosen by selecting a random number between 0.15 and 0.85 for each input variable, to be used in each of the 50,000 runs. This number was then used as the CDF (cumulative distribution function) value thus defining a choice for the input variable. PDFs of each of the input variables so generated, for each of the different metamodels, are given in **Appendix A17(a,b)**. This process enables testing of the metamodels at input values that evenly favor both the highly probable and less probable regions

of the input variables. The graphs of the results for the outputs are given in **Appendices A18-A21**.

It is important to compare the results of the output mole fractions and concentrations with those measured in actual urban areas. Although these are not exactly the same thing, since the measured values from urban areas are usually taken at a point near the surface and are not large spatial averages, the orders of magnitude should at least be comparable. For species with a large surface source, it is expected to have a modeled volume-averaged value lower than the actual measured values, and conversely in the case of species with high destruction near the surface.

Six of the species that are important both on the urban and global scale, and have measurements readily available in urban areas are ozone, CO, formaldehyde, OC, sulfate aerosol, and BC. The results for each of these species as shown in Appendices A18-A21 are compared with the minima, medians, means, and maxima for the measurements on the same plots where available. The medians of the metamodel outputs are also shown on the plots. In general, the results of this sensitivity analysis compare reasonably well with the actual measured mole fractions and concentrations of ozone, CO, formaldehyde and BC in each simulated area. Note that in the case of OC and sulfate aerosols, there are few actual measurements on a species by species basis, as compared with a total PM basis, and hence measured values of OC and sulfate are not available here for comparison.

The order of magnitude of ozone concentrations predicted by the metamodel is slightly higher than observed for the maximums, and reasonable for the medians, across all scenarios, with the ranges of the maximum and median concentrations, for each meteorological scenario, being respectively: 293ppb-1520ppb and 58.4ppb-84.3ppb for the Developed metamodel, 311ppb-436ppb and 118ppb-154ppb for the India metamodel, 381ppb-437ppb and 108ppb-129ppb for the Developing metamodel, and 326ppb-418ppb and 88.4ppb-113ppb for the China metamodel. These metamodel medians and maxima are larger than the observed mean monthly average value of 23ppb and maximum monthly average of 110ppb found in the Guadalajara, Mexico urban area (Sanchez *et al.*, 2009). As expected, the model results are higher than the measured values, because the model is giving the total vertically averaged ozone concentration in the urban area, which includes the upper regions which have no surface deposition, less titration by fresh NO emissions, and further time for the NO₂/NO ratio to increase.

The order of magnitude of the CO concentrations predicted by the metamodel is reasonable, with the ranges of the maximum and median concentrations, for each meteorological scenario, being respectively: 8.49ppm-27.9ppm and 0.522ppm-1.55ppm for the Developed metamodel, 1.12ppm-3.40ppm and 0.240ppm-0.620ppm for the India metamodel, 3.86ppm-12.8ppm and 0.452ppm-1.34ppm for the Developing metamodel, and 1.82ppm-5.64ppm and 0.265ppm-0.705ppm for the China metamodel. These results are somewhat lower than the average observed monthly average concentration of 1.942ppm and the observed maximum monthly average concentration of 9.166ppm found in the Guadalajara urban area (Sanchez *et al.*, 2009). As expected, the modeled values are slightly lower than the measured values, since the background CO concentration is usually lower than the surface CO concentration due to surface emissions.

The formaldehyde concentration predicted by the metamodel shows ranges of the maximum and median concentrations, for each meteorological scenario, to be respectively: 23.5ppb-250ppb and 0.746ppb-107ppb for the Developed metamodel, 9.40ppb-38.5ppb and 0.685ppb-5.53ppb for the India metamodel, 10.1ppb-129ppb and 0.968ppb-10.7ppb for the Developing metamodel, and 6.82ppb-18.1ppb and 0.332ppb-1.73ppb for the China metamodel. The metamodel results are low or comparable to the observed average monthly concentration of 4ppb-9ppb and observed maximum average monthly concentration of up to 35ppb in Mexico City (Lei *et al.*, 2009) and also compared to the observed mean daily values of 10ppb-19ppb and maximum daily value of up to 46ppb for Kolkata India (Dutta *et al.*, 2009). The modeled concentrations are expected to be lower than the surface measurements, both because the background formaldehyde in the parent model run is zero, and surface emissions enhance the surface concentrations.

The ranges of the maxima and medians of the BC mass concentration, as predicted by the metamodels for each meteorological scenario respectively are: 29.6ug/m³-229ug/m³ and 2.19ug/m³-16.3ug/m³ for the Developed metamodel, 8.97ug/m³-74.1ug/m³ and 1.24ug/m³-9.20ug/m³ for the India metamodel, 35.8ug/m³-258ug/m³ and 2.14ug/m³-17.5ug/m³ for the Developing metamodel, and 27.8ug/m³-208ug/m³ and 2.60ug/m³-20.1ug/m³ for the China metamodel. These values are generally lower than the August 2006 average BC concentration in Hyderabad, India of 12ug/m³ (Badarinath *et al.*, 2009); a March to May monthly average high and low concentration of BC in Hyderabad of 5ug/m³-35ug/m³ and in Delhi, India of 5ug/m³-45ug/m³ (Beegum *et al.*, 2009); a November 2006 to February 2007 monthly average BC concentration in Karachi, Pakistan of 10ug/m³, a June to September monthly average BC concentration of 2ug/m³, and a daily mean BC concentration in the range from 1ug/m³-15ug/m³ (Dutkiewicz *et al.*, 2009); a Lahore, Pakistan average Winter BC concentration of 21.7ug/m³, with the range over any given day from 5ug/m³-110ug/m³ (Husain *et al.*, 2007); and a Rio de Janeiro mean annual BC concentration of 1.4ug/m³-3.3ug/m³ (Godoy *et al.*, 2009). Since the background boundary concentration of BC in the model is assumed to be zero, and since the maximum concentrations are near the surface source, the average BC concentration in the model should be lower than the measured values.

The ranges of the maxima and medians of the OC mass concentration, as predicted by the metamodels for each meteorological scenario respectively are: 77.0ug/m³-4630ug/m³ and 5.75ug/m³-28.8ug/m³ for the Developed metamodel, 14.3ug/m³-113ug/m³ and 1.98ug/m³-16.0ug/m³ for the India metamodel, 140ug/m³-1010ug/m³ and 8.53ug/m³-73.6ug/m³ for the Developing metamodel, and 45.2ug/m³-337ug/m³ and 4.22ug/m³-32.8ug/m³ for the China metamodel. Finally, the ranges of the maxima and medians of the sulfate mass concentration, as predicted by the metamodel for each meteorological scenario respectively are: 27.6ug/m³-835ug/m³ and 3.53ug/m³-18.2ug/m³ for the Developed metamodel, 15.9ug/m³-798ug/m³ and 4.10ug/m³-28.0ug/m³ for the India metamodel, 80.7ug/m³-335ug/m³ and 4.40ug/m³-30.9ug/m³ for the Developing metamodel, and 89.3ug/m³-468ug/m³ and 3.17ug/m³-24.6ug/m³ for the China metamodel. These metamodel values are lower than the observed total PM₁₀ monthly average concentration of 50.9ug/m³ and a maximum monthly average concentration of 265.ug/m³ found

in the Guadalajara urban area (Sanchez *et al.*, 2009). The modeled concentrations are expected to be lower, given that PM10 includes dust, nitrate aerosol, and BC, in addition to OC and Sulfate.

Furthermore, the Flux/Emissions ratio for each of these species has been investigated and compared with the ratios expected to result from the chemical and physical processing of the species. The graphs of these ratios are given in **Appendices A22-A25** for CO, NO₂, formaldehyde, BC, OC, and sulfate aerosol. The median value of the ratio in the case of CO is close to 1.0 in all metamodel cases, indicating that the effects of deposition and chemistry are not significant when compared with emissions, over the 24 hour timescale of the urban metamodel run. This means that a significant fraction of the VOC may not be fully oxidized to CO by the time it has been exported from the urban area.

The Flux/Emissions ratio for formaldehyde can be used to investigate the extent of the VOC emissions oxidized before being exported from the urban area. In the case of formaldehyde there are a few competing factors. First, in cases of large rainfall or cloudiness, less formaldehyde is produced through photochemistry and more is removed through wet deposition. In these cases, the median value of the ratio is found to be small, often under 0.2, whereas in cases of small rainfall and small cloud cover, the median of the ratio, is up around 0.4. Second, in cases of low molecular weight VOC emissions typical in developed urban regions, the median value of the ratio can be as high as 0.8 depending on the meteorology.

The Flux/Emissions ratio for NO₂ is useful for determining what the expected ozone production will be downwind from the urban area. Since only 5% of the emissions of NO_x is in the form of NO₂, any ratio which is larger than 0.05 indicates an increase in the export of NO₂, with respect to the simple dilution approach. The results show that the median value of the ratio actually ranges from 0.1 to 0.4, depending on the meteorology scenario.

The Flux/Emissions ratio for BC should be and always is in the range from 0.0 to 1.0. It is also a very strong function of the amount of rainfall, with the median value being as low as 0.35 in the case of high rainfall and the median value being as high as 0.95 in the case of no rainfall. This further indicates that dry deposition is much less important than wet deposition in the case of BC.

The Flux/Emissions ratio for OC should always be the same as or larger than BC, since the sources of OC are both direct emissions like BC plus a small amount of secondary production due to oxidation of high molecular weight VOCs. This results in the median ratio of OC always being about equal to that of BC in the cases of high rainfall, and from 1% to 5% higher in the case of low rainfall.

Finally, the Flux/Emissions ratio for SO₂ should always be larger than or equal to 0.0, indicating how much of the gas is converted to sulfate aerosol as a result of urban processing. The ratio is a less strong function of the rainfall for SO₂ than for BC and OC. This results from the fact that an important production mechanism for sulfate aerosol requires the presence of liquid water (although the same removal mechanisms are at play for all three aerosol types). What is particularly interesting is that the median of the SO₂ ratio in the case of the India metamodel is from 0.05 to 0.10 larger than in the other three metamodel cases, for each of the

meteorological scenarios. This is caused at least in part by the higher average temperature in Indian cities increasing the oxidation efficiency of SO₂ in the gas and aqueous phases.

5. CONCLUSIONS

Reduced form metamodels have been produced to simulate the effects of chemical and physical processing of highly reactive trace species in urban areas. These metamodels are built to be able to simulate urban areas in diverse geographical regions, multiple realistic meteorological conditions, and a range of human-induced patterns and distributions of anthropogenic emissions. These reduced form metamodels are designed to efficiently simulate the urban concentration, surface deposition, and net mass flux of species important to human health and climate.

These metamodels have been designed to be fast enough, so that they can be implemented into a global scale model and thus better capture the concentrations and mass fluxes found in real urban areas, as compared with the “dilute and process” method that large-scale models currently use. Polynomial chaos expansions have been fitted based on a broad range of conditions, applicable both to the present and hypothetical future world, so that they will remain applicable both for current conditions and for studies which look at the chemistry of urban areas in the future.

The various outputs are based on a combination of 18 inputs. The inputs include physical properties, such as the local temperature, daily diurnal temperature range, the day of the year, and the geographic location. Others include the anthropogenic properties of urban areas, such as the temporal and spatial weighting of emissions, and the emissions magnitude of several relevant anthropogenic species. Other inputs include the upwind (or background) concentrations of trace species, both anthropogenic and natural in nature, which have an impact on the processing in the urban area. These inputs have been gathered from multiple sources, and used to generate a set of PDFs of their potential values in urban areas.

These PDFs were then used to determine inputs at a set of collocation points at which to run the detailed parent chemical and physical model, CAMx, thousands of times. Another set of test points were also generated from these input PDFs, which were also used to run the parent CAMx model. Finally, the parent model outputs were used to both fit the coefficients of a full third order polynomial chaos expansion, which in turn becomes the metamodel, and to test the precision of the metamodels in terms of the parent model.

The deviations between the metamodel and the parent model were computed in terms of a normalized RMS error. Many important species, such as ozone, CO, NO_x, and BC were found to have a normalized RMS error less than 10% for all of the metamodels, under all meteorological conditions, with many of the species having a normalized RMS error less than 1%. Some of the other important species, such as VOCs, PAN, OC, and sulfate aerosol are usually fit well, except for a few meteorological cases in a few of the metamodel regions, in which they are fit less well. This is due to the highly non-linear nature of these chemical species, and the geographic areas and meteorological scenarios of choice. The reason for the less good fit in each of these cases is largely explained in terms of the physical, chemical, and meteorological processing. For those

species in which good fits have not been obtained, the program has been designed in such a way that values which are not physically reasonable are flagged.

Finally, a set of sensitivity tests have been performed, to observe the response of the various metamodels to very broad set of potential inputs compared to those used to produce the fits. The point of this test was to determine if the metamodel could handle multiple inputs from low probability regions of the input PDFs, and this was generally determined to be the case. Furthermore, these results were compared with observations of ozone, CO, formaldehyde, BC, and PM₁₀ from a few urban areas where they were available. In most of the cases, the output distributions were found to be similar to the observations, especially given that the metamodel predicts average urban concentrations, and not point surface measurements for these species.

It appears that these metamodels can efficiently and robustly simulate the urban concentrations, mole fractions, and fluxes of species, important to human health and the global scale climate, by taking into consideration the effects of various physical, chemical, and meteorological processing.

Acknowledgments

The authors gratefully acknowledge the financial support for this work from grants from the Federal Agencies and industries that sponsor the MIT Joint Program on the Science and Policy of Global Change. We especially thank Marcus Sarofim and Noelle Selin for their critical comments during the course of this work that significantly improved the metamodel performance.

6. REFERENCES

- Amiridis, V., D. Melas, D. S. Balis, A. Papayannis, D. Founda, E. Katragkou, F. Giannakaki, R. E. Mamouri, E. Gerasopoulos, and C. Zerefos. (2007). "Aerosol lidar observations and model calculations of the planetary boundary layer evolution over Greece, during the March 2006 total solar eclipse." *Atmospheric Chemistry and Physics* 7(24): 6181-6189.
- Andreani-Aksoyoglu, S. J. Keller, A. S. H. Prevot, U. Baltensperger, and J. Flemming . (2008). "Secondary aerosols in Switzerland and northern Italy: Modeling and sensitivity studies for summer 2003." *Journal of Geophysical Research-Atmospheres* 113(D6).
- Andreani-Aksoyoglu, S., A. S. H. Prevot, U. Baltensperger, J. Keller, and J. Dommen. (2004). "Modeling of formation and distribution of secondary aerosols in the Milan area (Italy)." *Journal of Geophysical Research-Atmospheres* 109(D5).
- Badarinath, K. V. S., S. K. Kharol, R. R. Reddy, K. R. Gopal, K. Narasimhulu, L. S. S. Reddy, and K. R. Kumar. (2009). "Black carbon aerosol mass concentration variation in urban and rural environments of India - a case study." *Atmospheric Science Letters* 10(1): 29-33.
- Beegum, S. N., K. K. Moorthy, S. S. Babu, S. K. Satheesh, V. Vinoj, K. V. S. Badarinath, P. D. Safai, P. C. S. Devara, S. Singh, V. Vinod, U. C. Durnka, and P. Pantl. (2009). "Spatial distribution of aerosol black carbon over India during pre-monsoon season." *Atmospheric Environment* 43(5): 1071-1078.
- Byun, D. W., S. T. Kim, and S. B. Kim. (2007). "Evaluation of air quality models for the simulation of a high ozone episode in the Houston metropolitan area." *Atmospheric Environment* 41(4): 837-853.

- Calbo, J., W. W. Pan, M. Webster, R. G. Prinn, and G. J. McRae. (1998). "Parameterization of urban subgrid scale processes in global atmospheric chemistry models." *Journal of Geophysical Research-Atmospheres* 103(D3): 3437-3451.
- Center for International Earth Science Information Network (CIESIN), Columbia University; International Food Policy Research Institute (IFPRI); and World Resources Institute (WRI). 2000. Gridded Population of the World (GPW), Version 2. Palisades, NY: CIESIN, Columbia University. Available at: <http://sedac.ciesin.columbia.edu/plue/gpw>.
- Chang, S. Y. and D. T. Allen (2006a). "Atmospheric chlorine chemistry in southeast Texas: Impacts on ozone formation and control." *Environmental Science & Technology* 40(1): 251-262.
- Chang, S. Y. and D. T. Allen (2006b). "Chlorine chemistry in urban atmospheres: Aerosol formation associated with anthropogenic chlorine emissions in southeast Texas." *Atmospheric Environment* 40: S512-S523.
- Corporation, S. A. I. (1997). PAMS data analysis: An investigation of local meteorological effects on ozone during the OTAG 1995 episode and the weekday/weekend differences in the Northeast Corridor.
- Cossa, P. 2004: *Uncertainty analysis of the cost of climate policies*. Master of Science Thesis in Technology and Policy, Massachusetts Institute of Technology, June.
- de Foy, B., W. Lei, M. Zavala, R. Volkamer, J. Samuelsson, J. Mellqvist, B. Galle, A. P. Martinez, M. Grutter, A. Retama, and L. T. Molina. (2007). "Modelling constraints on the emission inventory and on vertical dispersion for CO and SO₂ in the Mexico City Metropolitan Area using Solar FTIR and zenith sky UV spectroscopy." *Atmospheric Chemistry and Physics* 7: 781-801.
- Dutkiewicz, V. A., S. Alvi, B. M. Ghauri, M. I. Choudhary, and L. Husain. (2009). "Black carbon aerosols in urban air in South Asia." *Atmospheric Environment* 43(10): 1737-1744.
- Dutta, C., D. Som, A. Chatterjee, A. K. Mukherjee, T. K. Jana, and S. Sen. (2009). "Mixing ratios of carbonyls and BTEX in ambient air of Kolkata, India and their associated health risk." *Environmental Monitoring and Assessment* 148(1-4): 97-107.
- Eben, K., P. Juras, J. Resler, M. Belda, E. Pelikan, B. C. Kruger, and J. Keder. (2005). "An ensemble Kalman filter for short-term forecasting of tropospheric ozone concentrations." *Quarterly Journal of the Royal Meteorological Society* 131(613): 3313-3322.
- Feldman, M. S., T. Howard, E. McDonald-Buller, G. Mullins, D. T. Allen, A. Webb, and Y. Kimura. (2007). "Applications of satellite remote sensing data for estimating dry deposition in eastern Texas." *Atmospheric Environment* 41(35): 7562-7576.
- Gery, M. W., G. Z. Whitten, J. P. Killus, and M. C. Dodge. (1989). "A photochemical kinetics mechanism for urban and regional scale computer modeling." *Journal of Geophysical Research-Atmospheres* 94(D10): 12925-12956.
- Godoy, M., J. M. Godoy, L. A. Roldao, D. S. Soluri, and R. A. Donagemma. (2009). "Coarse and fine aerosol source apportionment in Rio de Janeiro, Brazil." *Atmospheric Environment* 43(14): 2366-2374.
- Houweling, S., F. Dentener, and J. Lelieveld. (1998). "The impact of nonmethane hydrocarbon compounds on tropospheric photochemistry." *Journal of Geophysical Research-Atmospheres* 103(D9): 10673-10696.

- Husain, L., V. A. Dutkiewicz, A. J. Khan, and B. M. Ghauri. (2007). "Characterization of carbonaceous aerosols in urban air." *Atmospheric Environment* 41(32): 6872-6883.
- Jackson, B., D. Chau, K. Gurer, and A. Kaduwela. (2006). "Comparison of ozone simulations using MM5 and CALMET/MM5 hybrid meteorological COOS fields for the July/August 2000 episode." *Atmospheric Environment* 40(16): 2812-2822.
- Jones, P. D., M. New, D. E. Parker, S. Martin, I. G. Rigor. (1999). "Surface air temperature and its changes over the past 150 years." *Reviews of Geophysics* 37(2): 173-199.
- Junquera, V., M. M. Russell, W. Vizuete, Y. Kimura, and D. Allen. (2005). "Wildfires in eastern Texas in August and September 2000: Emissions, aircraft measurements, and impact on photochemistry." *Atmospheric Environment* 39(27): 4983-4996.
- Keller, J., S. Andreani-Aksoyoglu, M. Tinguely, J. Flemming, J. Heldstab, M. Keller, R. Zbinden, and A. S. H. Prevot. (2008). "The impact of reducing the maximum speed limit on motorways in Switzerland to 80 km h⁻¹ on emissions and peak ozone." *Environmental Modelling & Software* 23(3): 322-332.
- Lei, W., B. de Foy, M. Zavala, R. Volkamer, and L. T. Molina. (2007). "Characterizing ozone production in the Mexico City Metropolitan Area: a case study using a chemical transport model." *Atmospheric Chemistry and Physics* 7: 1347-1366.
- Lei, W., M. Zavala, B. de Foy, R. Volkamer, M. J. Molina, and L. T. Molina, LT. (2009). "Impact of primary formaldehyde on air pollution in the Mexico City Metropolitan Area." *Atmospheric Chemistry and Physics* 9(7): 2607-2618.
- Liu, L., S. Andreani-Aksoyoglu, J. Keller, C. Ordonez, W. Junkermann, C. Hak, G. O. Braathen, S. Reimann, C. Astorga-Llorens, M. Schultz, A. S. H. Prevot, and I. S. A. Isaksen. (2007). "A photochemical modeling study of ozone and formaldehyde generation and budget in the Po basin." *Journal of Geophysical Research-Atmospheres* 112(D22).
- Mauzerall, D. L., B. Sultan, N. Kim, and D. F. Bradford. (2005). "NO_x emissions from large point sources: variability in ozone production, resulting health damages and economic costs." *Atmospheric Environment* 39(16): 2851-2866.
- Mayer, M., C. Wang, M. Webster, and R. G. Prinn. (2000). "Linking local air pollution to global chemistry and climate." *Journal of Geophysical Research-Atmospheres* 105(D18): 22869-22896.
- McDonald-Buller, E., C. Wiedinmyer, Y. Kimura, and D. Allen. (2001). "Effects of land use data on dry deposition in a regional photochemical model for eastern Texas." *Journal of the Air & Waste Management Association* 51(8): 1211-1218.
- Morris, R., B. Koo, and G. Yarwood. (2005). "Evaluation of multisectional and two-section particulate matter photochemical grid models in the western United States." *Journal of the Air & Waste Management Association* 55(11): 1683-1693.
- Morris, R. E., B. Koo, A. Guenther, G. Yarwood, D. McNally, T. W. Tesche, G. Tonnesen, J. Boylan, and P. Brewer. (2006). "Model sensitivity evaluation for organic carbon using two multi-pollutant air quality models that simulate regional haze in the southeastern United States." *Atmospheric Environment* 40(26): 4960-4972.
- Nobel, C. E., E. C. McDonald-Buller, Y. Kimura, and D. T. Allen. (2001). "Accounting for spatial variation of ozone productivity in NO_x emission trading." *Environmental Science & Technology* 35(22): 4397-4407.

- Paltsev S., J. Reilly, H. Jacoby, R. Eckaus and J. McFarland and M. Babiker, 2005: The MIT Emissions Prediction and Policy Analysis (EPPA) Model: Version 4. MIT JPSPGC Report 125, August, 72 p. (http://mit.edu/globalchange/www/MITJPSPGC_Rpt125.pdf).
- Perez-Roa, R., J. Castro, H. Jorquera, J. R. Perez-Correa, and V. Vesovic. (2006). "Air-pollution modelling in an urban area: Correlating turbulent diffusion coefficients by means of an artificial neural network approach." *Atmospheric Environment* 40(1): 109-125.
- Pirovano, G., I. Coll, M. Bedogni, S. Alessandrini, M. P. Costa, V. Gabusi, F. Lasry, L. Menut, and R. Vautard. (2007). "On the influence of meteorological input on photochemical modelling of a severe episode over a coastal area." *Atmospheric Environment* 41(30): 6445-6464.
- Riccio, A., G. Barone, E. Chianese, and G. Giunta. (2006). "A hierarchical Bayesian approach to the spatio-temporal modeling of air quality data." *Atmospheric Environment* 40(3): 554-566.
- Prather, M., D. Ehhalt, F. Dentener, R. Derwent, E. Dlugokencky, E. Holland, I. Isaksen, J. Katima, V. Kirchhoff, P. Matson, P. Midglet, and M. Wang 2001: Atmospheric Chemistry and Greenhouse Gases. In: *Climate Change 2001: The Scientific Basis. Contribution of Working Group I to the Third Assessment Report of the Intergovernmental Panel on Climate Change*, Houghton, J.T., Y. Ding, D.J. Griggs, M. Noguer, P.J. van der Linden, X. Dai, K. Maskell, and C.A. Johnson (eds.), Cambridge University Press, Cambridge, United Kingdom and New York, NY, USA, Chapter 4, pp. 239-287.
- Russell, A. G. (2008). "EPA Supersites Program-related emissions-based particulate matter modeling: Initial applications and advances." *Journal of the Air & Waste Management Association* 58(2): 289-302.
- Russell, M. and D. T. Allen (2005). "Predicting secondary organic aerosol formation rates in southeast Texas." *Journal of Geophysical Research-Atmospheres* 110(D7).
- Sanchez, H. U. R., M. D. A. Garcia, R. Bejaran, M. E. G. Guadalupe, A. W. Vazquez, A. C. P. Toledano, and O. D. Villasenor. (2009). "The spatial-temporal distribution of the atmospheric polluting agents during the period 2000-2005 in the urban area of Guadalajara, Jalisco, Mexico." *Journal of Hazardous Materials* 165(1-3): 1128-1141.
- Song, J., W. Vizuete, S. Chang, D. Allen, Y. Kimura, S. Kemball-Cook, G. Yarwood, M. A. Kiournourtzoglou, E. Atlas, A. Hansel, A. Wisthaler, and E. McDonald-Buller. (2008). "Comparisons of modeled and observed isoprene concentrations in southeast Texas." *Atmospheric Environment* 42(8): 1922-1940.
- Tatang, M. A., W. W. Pan, R. G. Prinn, and G. J. McRae. (1997). "An efficient method for parametric uncertainty analysis of numerical geophysical models." *Journal of Geophysical Research-Atmospheres* 102(D18): 21925-21932.
- Tesche, T. W., R. Morris, G. Tonnesen, D. McNally, J. Boylan, and P. Brewer. (2006). "CMAQ/CAMx annual 2002 performance evaluation over the eastern US." *Atmospheric Environment* 40(26): 4906-4919.
- Wild, O. and M. J. Prather (2006). "Global tropospheric ozone modeling: Quantifying errors due to grid resolution." *Journal of Geophysical Research-Atmospheres* 111(D11): 14.
- Yang, K. L., C. C. Ting, J. L. Wang, O. W. Wingenter, and C. C. Chan. (2005). "Diurnal and seasonal cycles of ozone precursors observed from continuous measurement at an urban site in Taiwan." *Atmospheric Environment* 39(18): 3221-3230.

- Yarwood G., S. R., M. Yocke, G.Z. Whitten (2005). "Updates to the carbon bond chemical mechanism: CB05. Final report prepared for US EPA". Available at: http://www.camx.com/publ/pdfs/CB05_Final_Report_120805.pdf."
- Yokouchi, Y. (1994). "Seasonal and diurnal-variation of isoprene and its reaction-products in a semirural Area." *Atmospheric Environment* 28(16): 2651-2658.
- Zanis, P., E. Katragkou, M. Kanakidou, B. E. Psiloglou, S. Karathanasis, M. Vrekoussis, E. Gerasopoulos, I. Lisaridis, K. Markakis, A. Poupkou, V. Amiridis, D. Melas, N. Mihalopoulos, and C. Zerefos. (2007). "Effects on surface atmospheric photo-oxidants over Greece during the total solar eclipse event of 29 March 2006." *Atmospheric Chemistry and Physics* 7(23): 6061-6073.
- Zunckel, M., A. Koosailee, G. Maure, K. Venjonoka, A. M. van Tienhoven, and L. Otter. (2006). "Modelled surface ozone over southern Africa during the cross border air pollution impact assessment project." *Environmental Modelling & Software* 21(7): 911-924.

APPENDIX

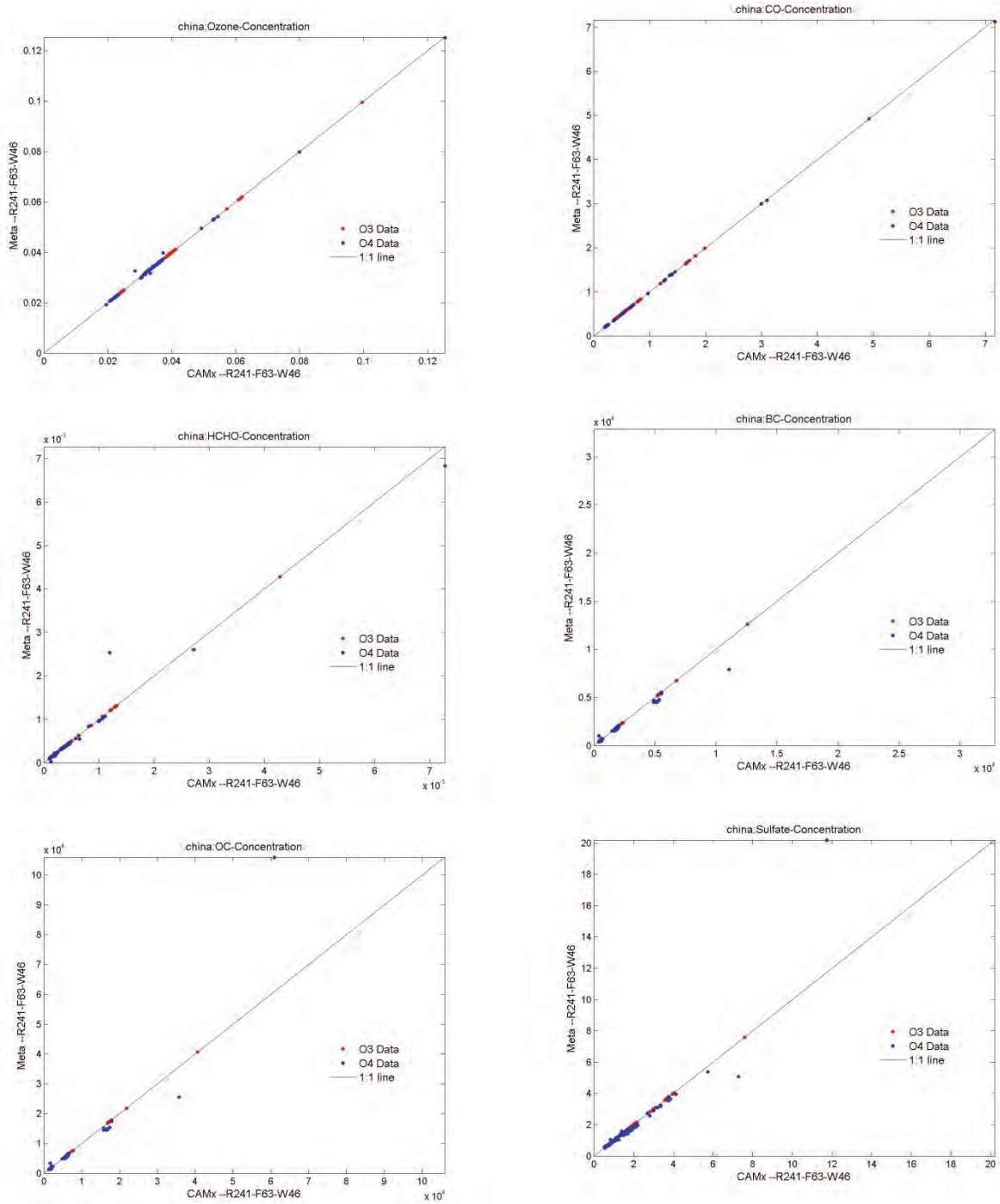


Figure A1. Results obtained for the urban concentrations of ozone, CO, formaldehyde, BC, OC, and sulfate based on runs of CAMx model (X-axis) compared with the China metamodel (Y-axis), for the R241-F63-W46 meteorology scenario.

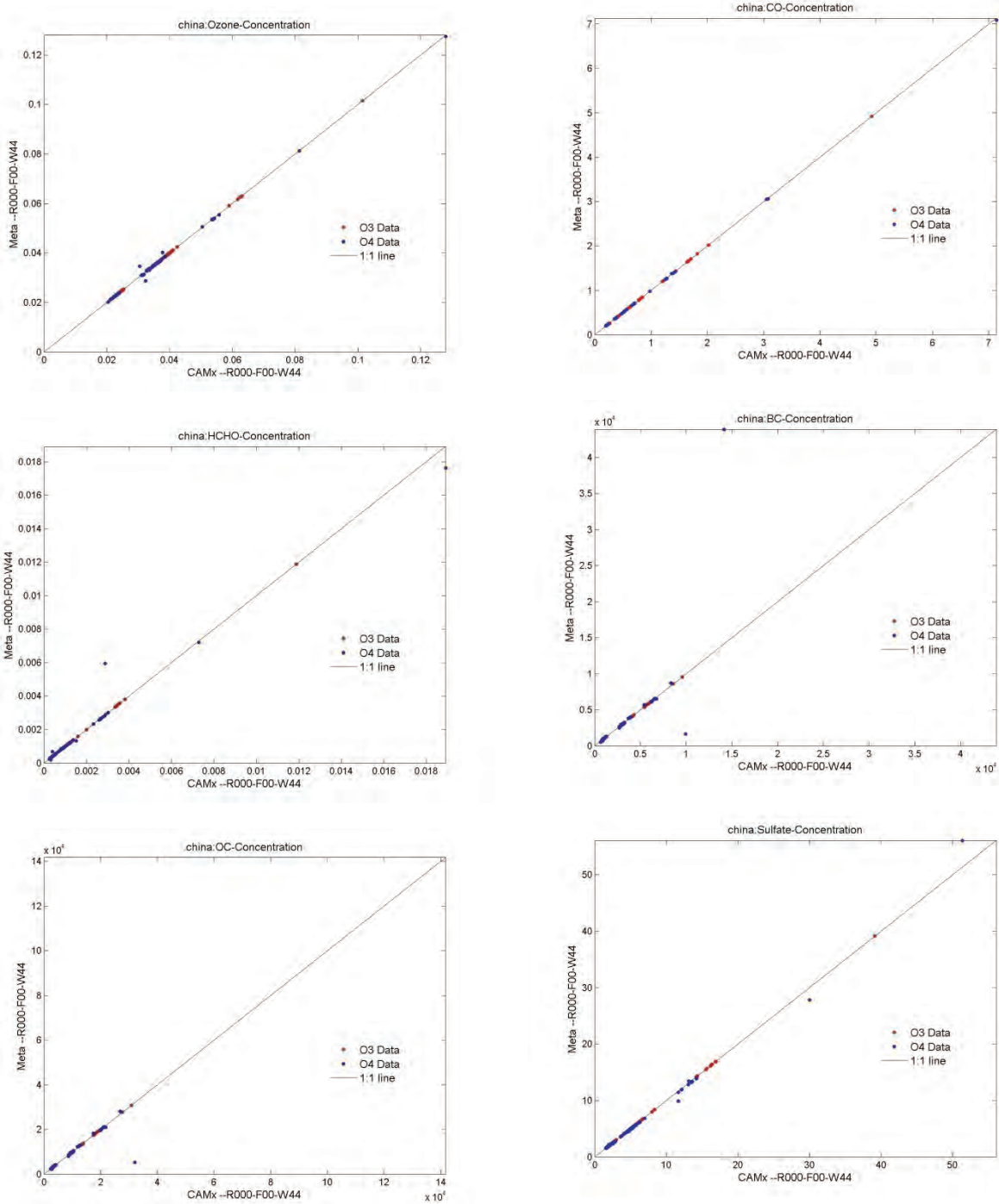


Figure A2. Results obtained for the urban concentrations of ozone, CO, formaldehyde, BC, OC, and sulfate based on runs of CAMx model (X-axis) compared with the China metamodel (Y-axis), for the R000-F00-W44 meteorology scenario.

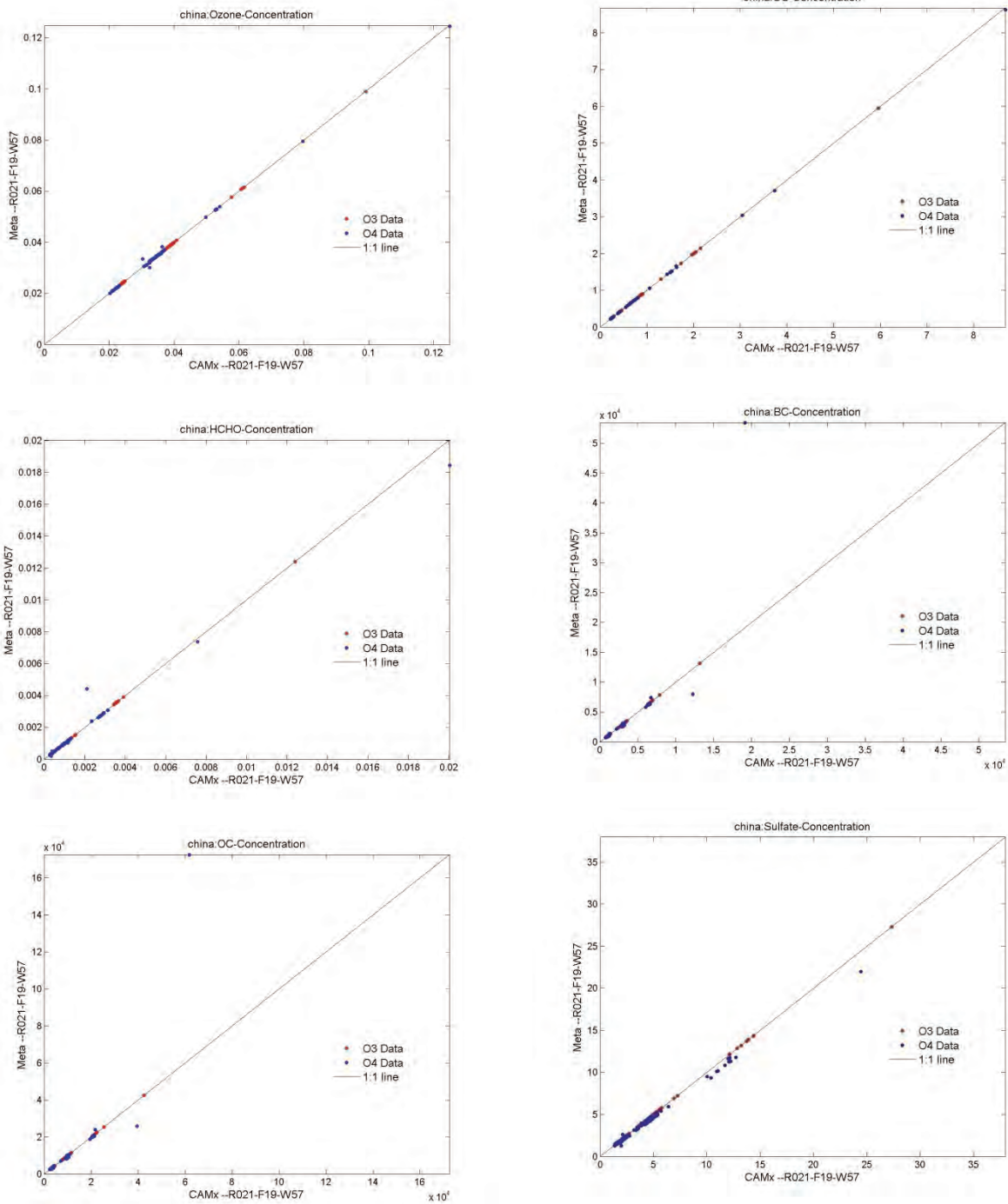


Figure A3. Results obtained for the urban concentrations of ozone, CO, formaldehyde, BC, OC, and sulfate based on runs of CAMx model (X-axis) compared with the China metamodel (Y-axis), for the R002-F02-W16 meteorology scenario.

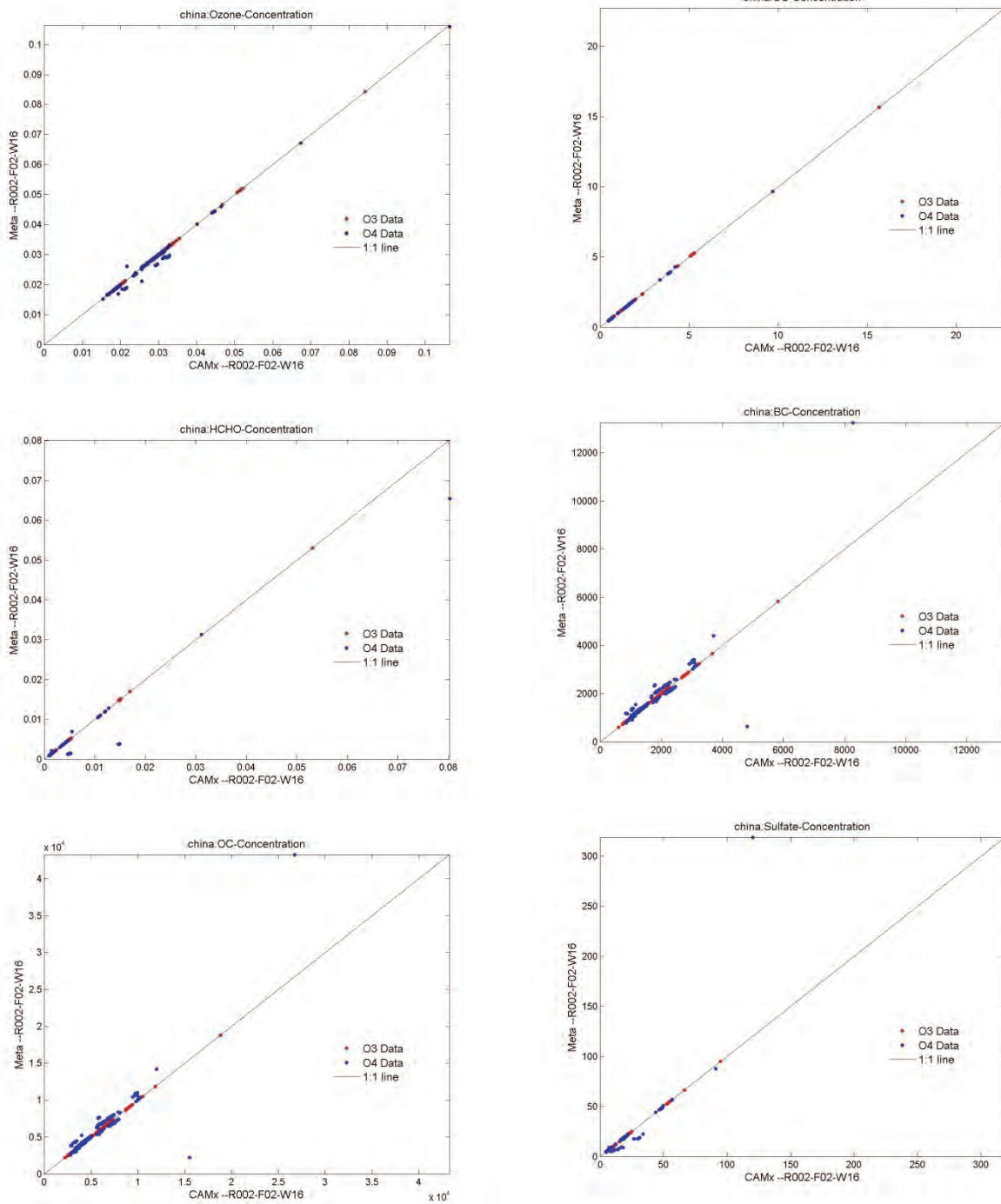


Figure A4. Results obtained for the urban concentrations of ozone, CO, formaldehyde, BC, OC, and sulfate based on runs of CAMx model (X-axis) compared with the China metamodel (Y-axis), for the R021-F19-W57 meteorology scenario.

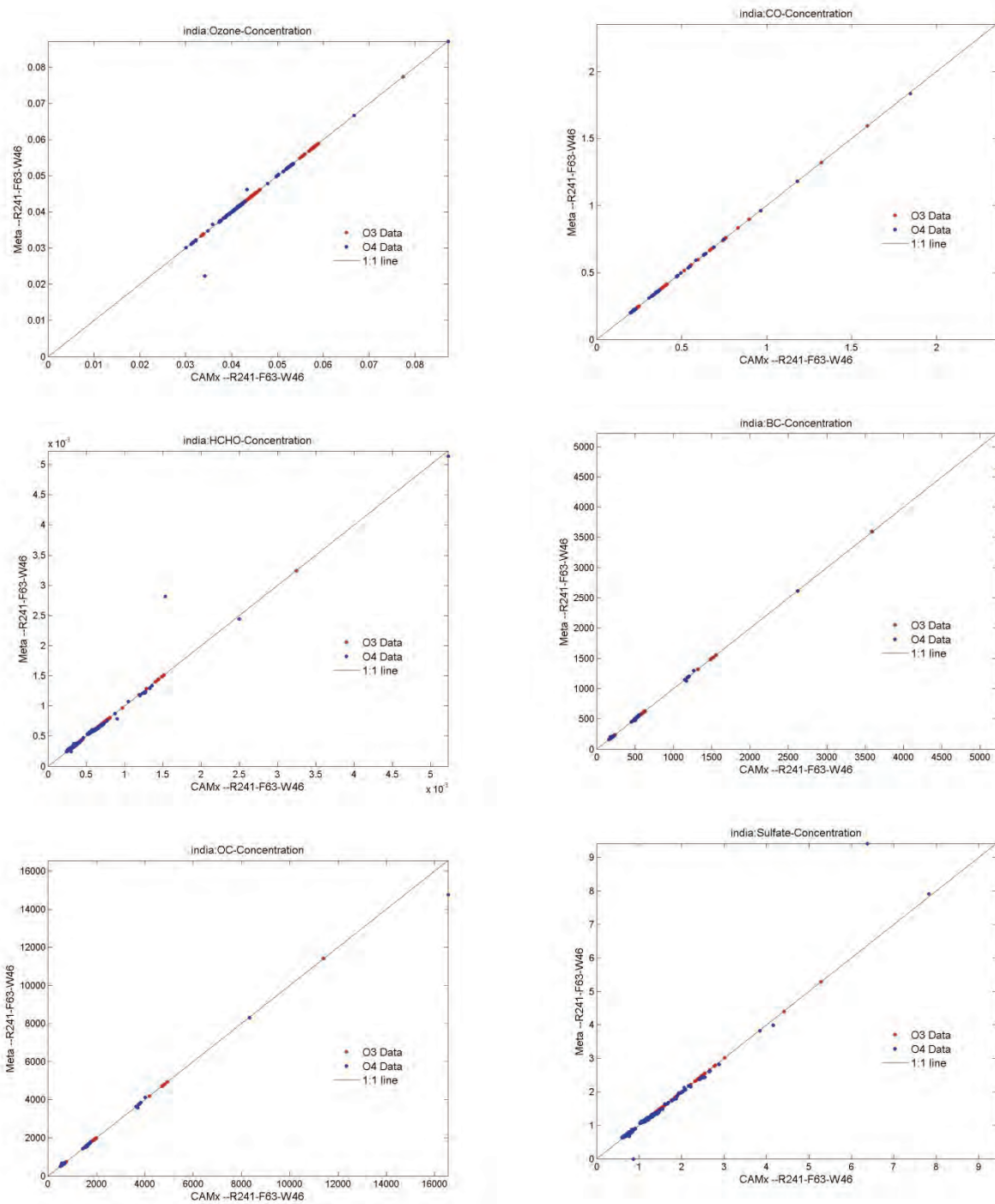


Figure A5. Results obtained for the urban concentrations of ozone, CO, formaldehyde, BC, OC, and sulfate based on runs of CAMx model (X-axis) compared with the India metamodel (Y-axis), for the R241-F63-W46 meteorology scenario.

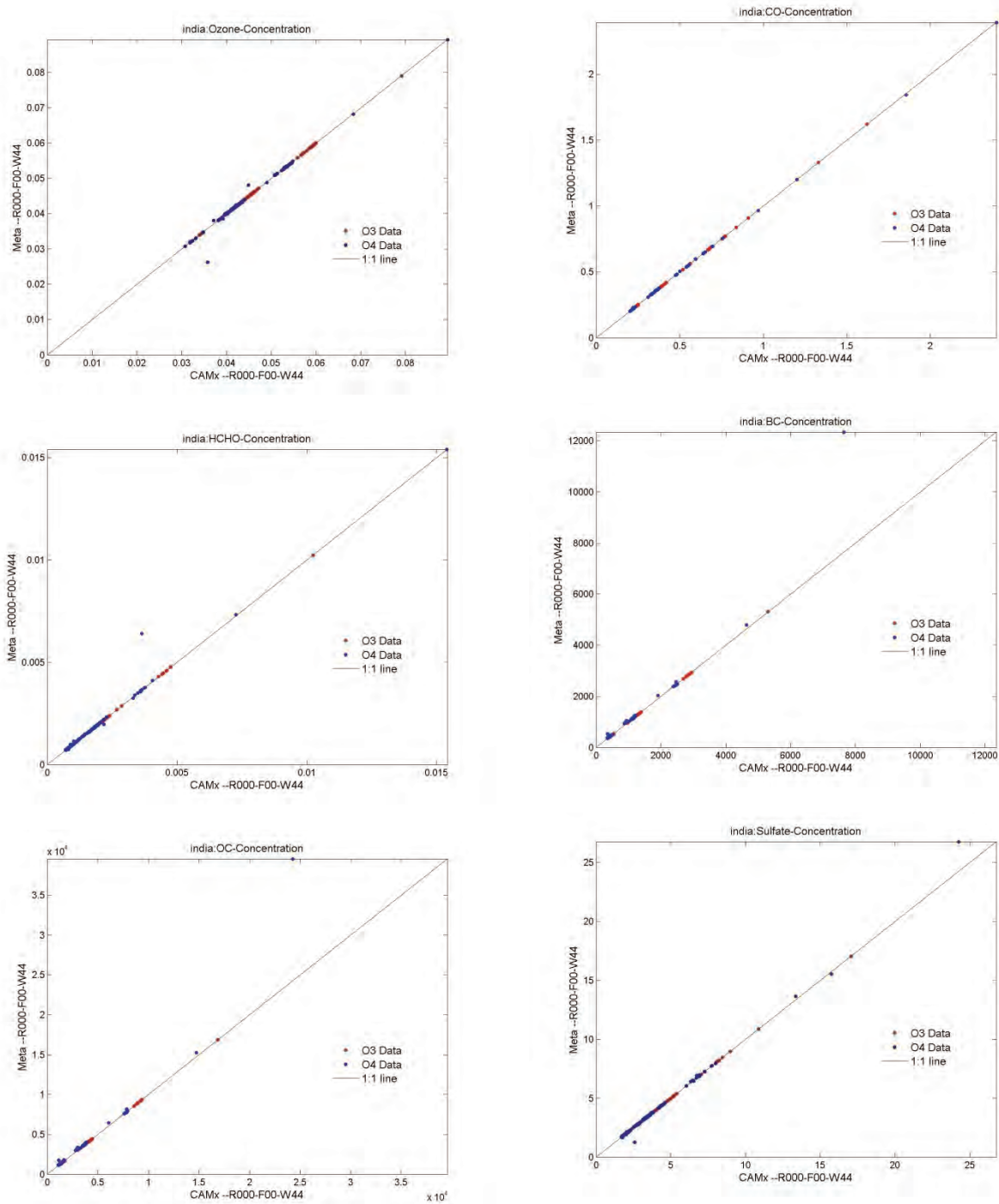


Figure A6. Results obtained for the urban concentrations of ozone, CO, formaldehyde, BC, OC, and sulfate based on runs of CAMx model (X-axis) compared with the India metamodel (Y-axis), for the R000-F00-W44 meteorology scenario.

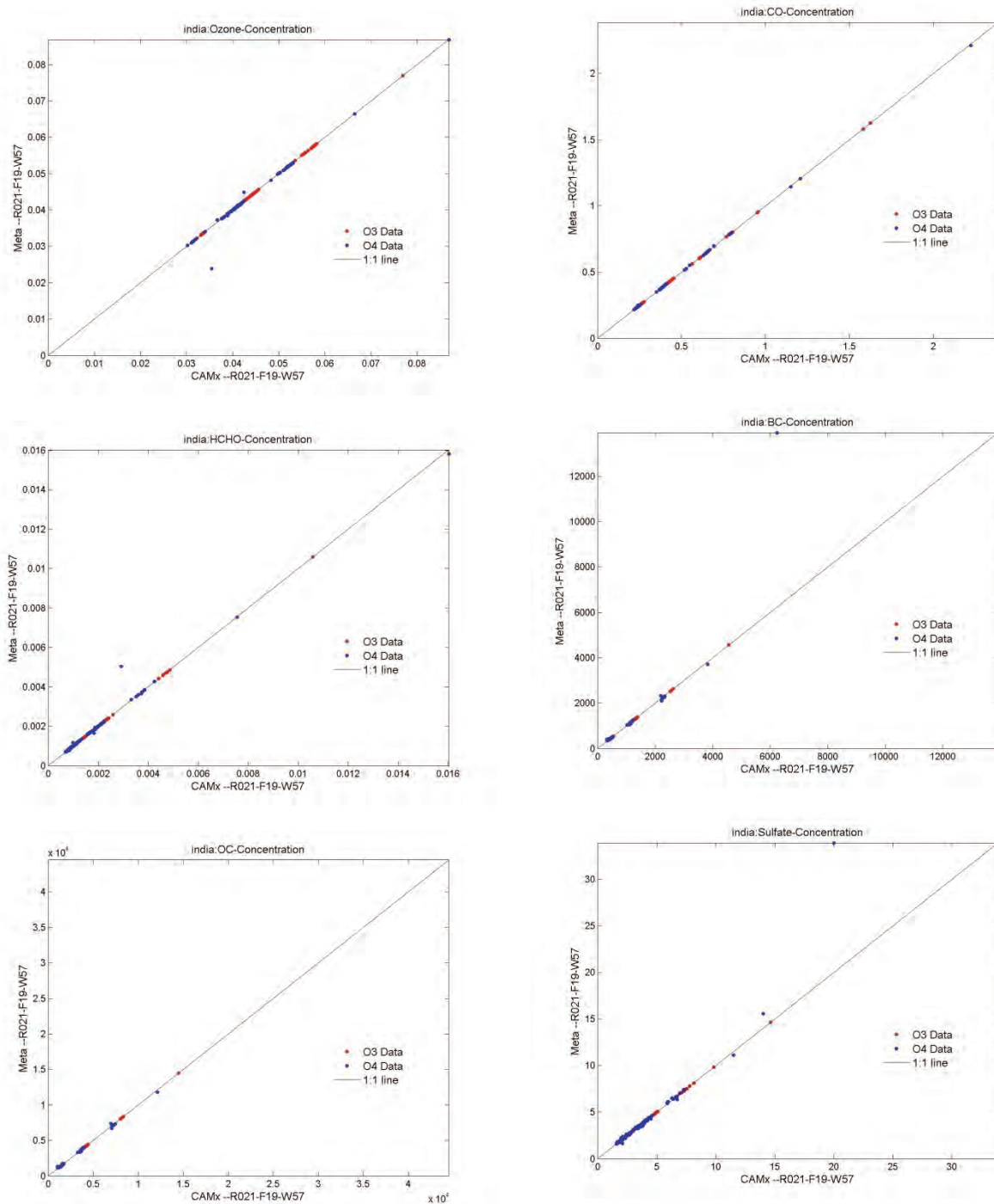


Figure A7. Results obtained for the urban concentrations of ozone, CO, formaldehyde, BC, OC, and sulfate based on runs of CAMx model (X-axis) compared with the India metamodel (Y-axis), for the R002-F02-W16 meteorology scenario.

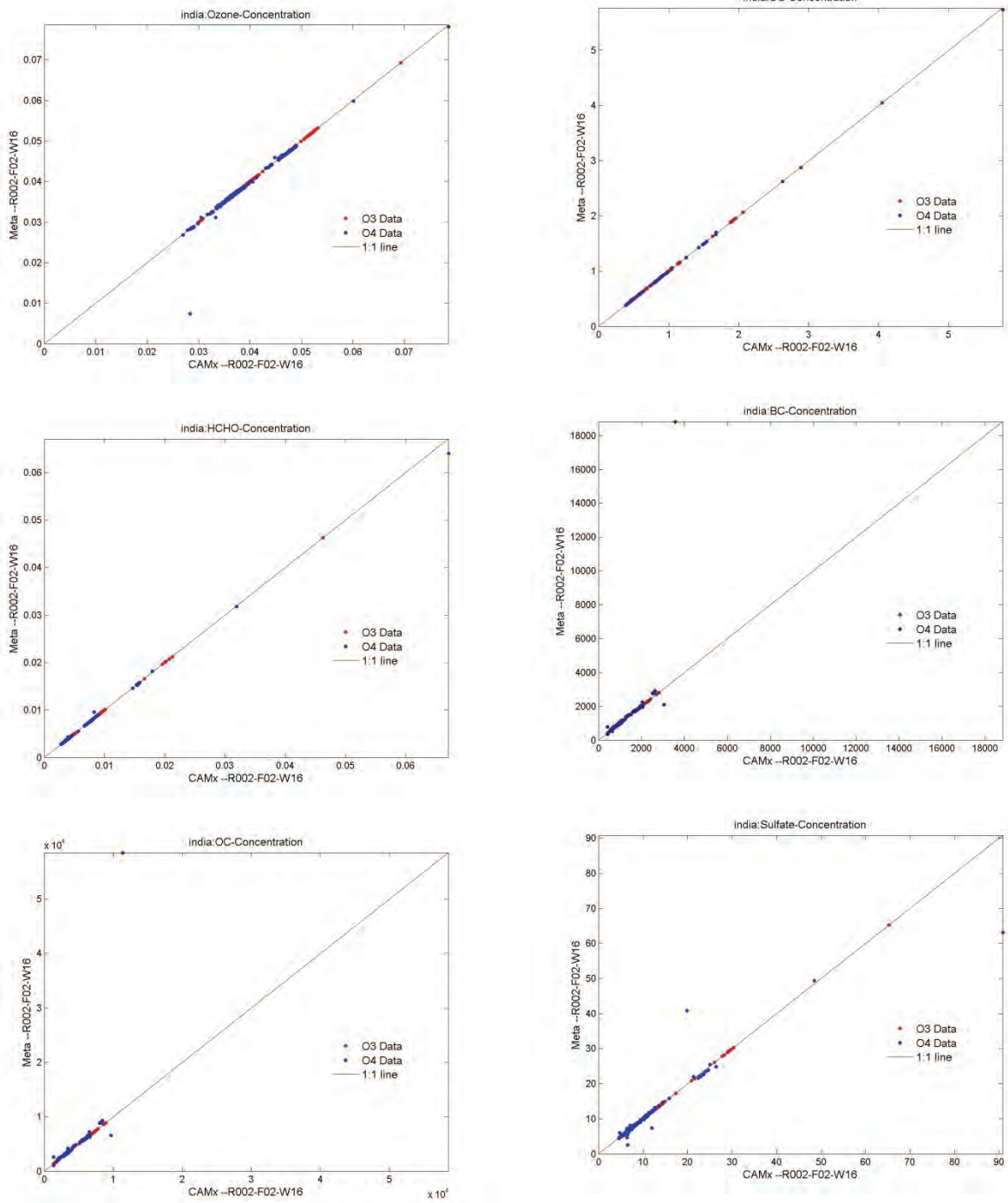


Figure A8. Results obtained for the urban concentrations of ozone, CO, formaldehyde, BC, OC, and sulfate based on runs of CAMx model (X-axis) compared with the India metamodel (Y-axis), for the R021-F19-W57 meteorology scenario.

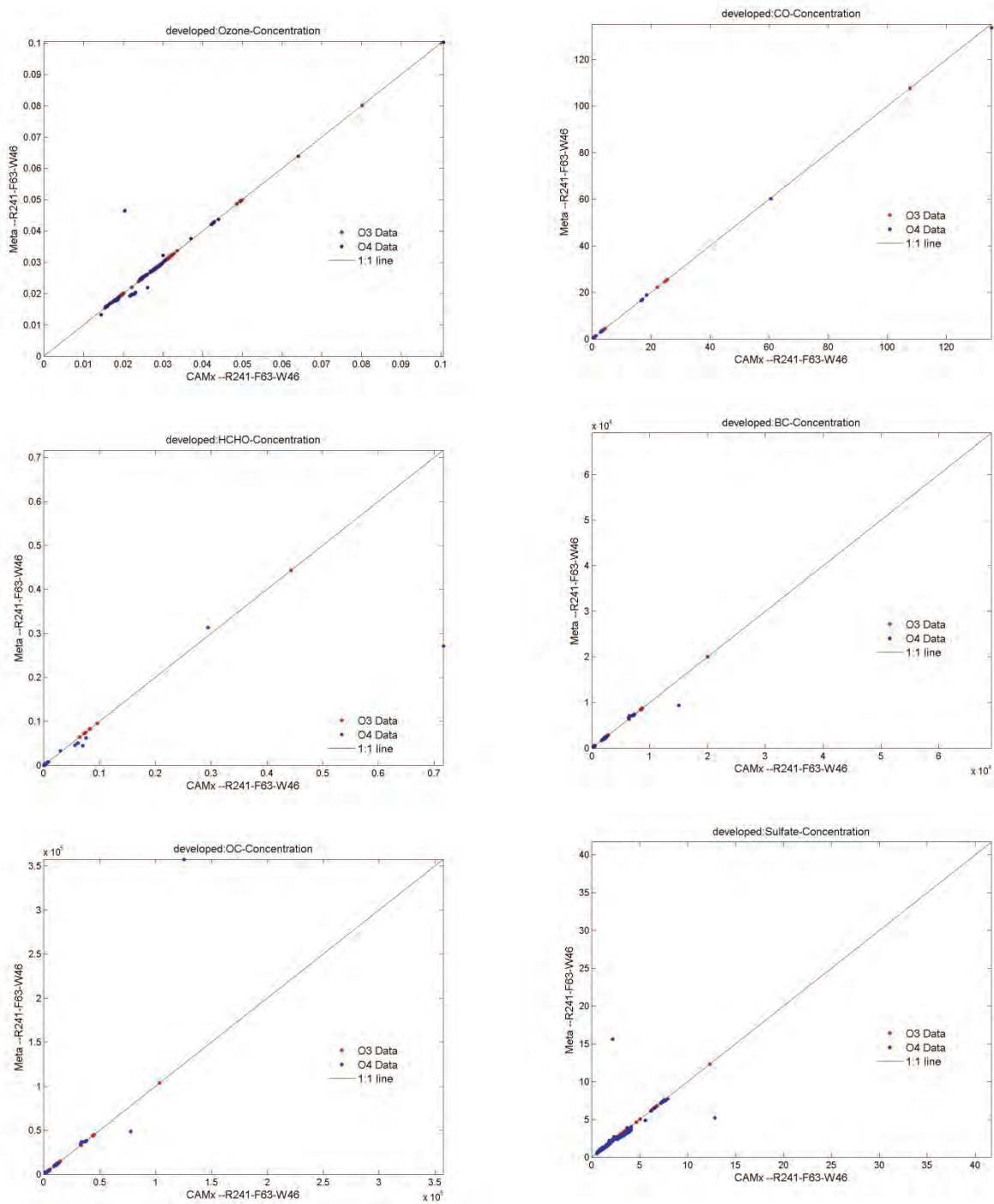


Figure A9. Results obtained for the urban concentrations of ozone, CO, formaldehyde, BC, OC, and sulfate based on runs of CAMx model (X-axis) compared with the Developed metamodel (Y-axis), for the R241-F63-W46 meteorology scenario.

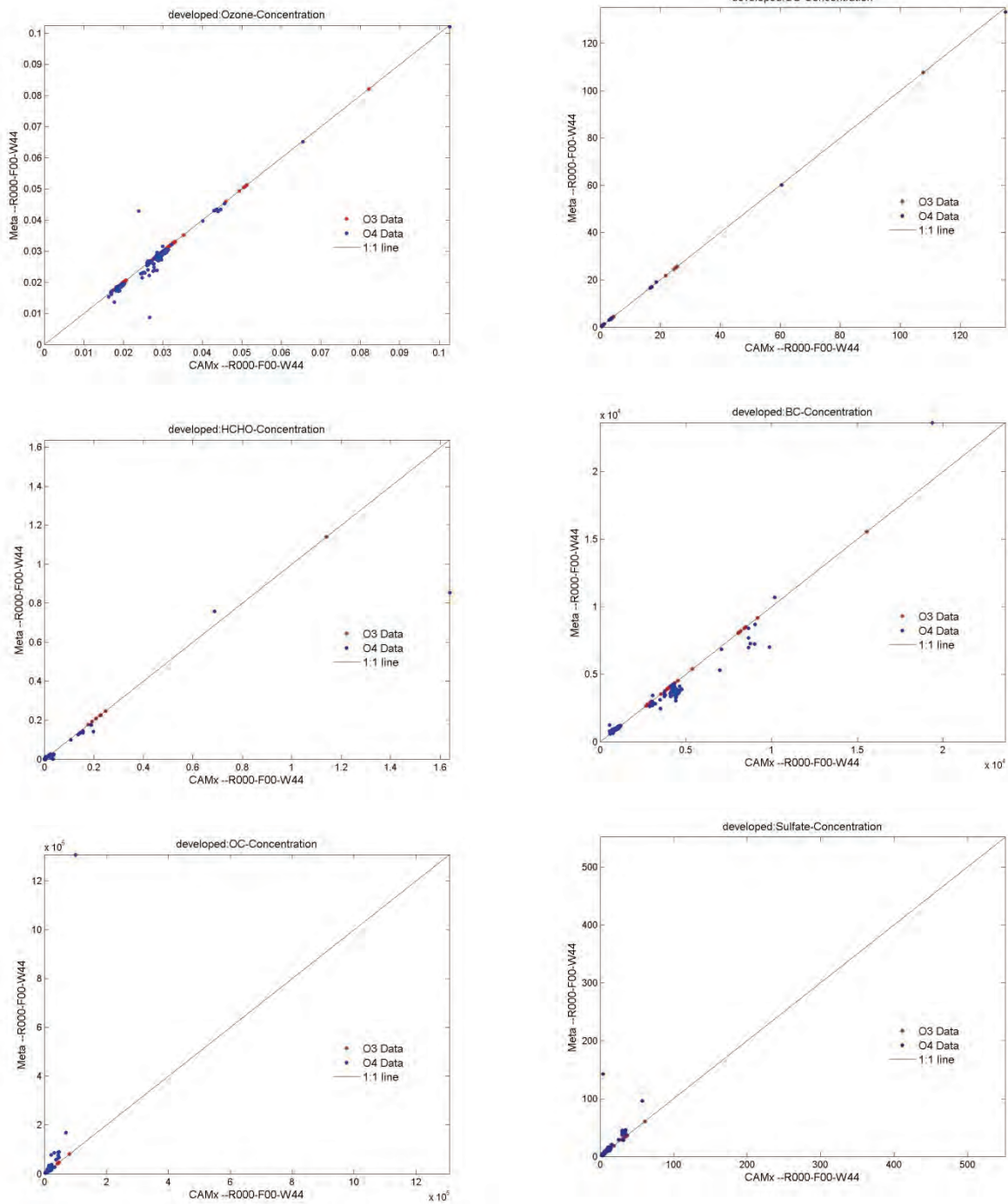


Figure A10. Results obtained for the urban concentrations of ozone, CO, formaldehyde, BC, OC, and sulfate based on runs of CAMx model (X-axis) compared with the Developed metamodel (Y-axis), for the R000-F00-W44 meteorology scenario.

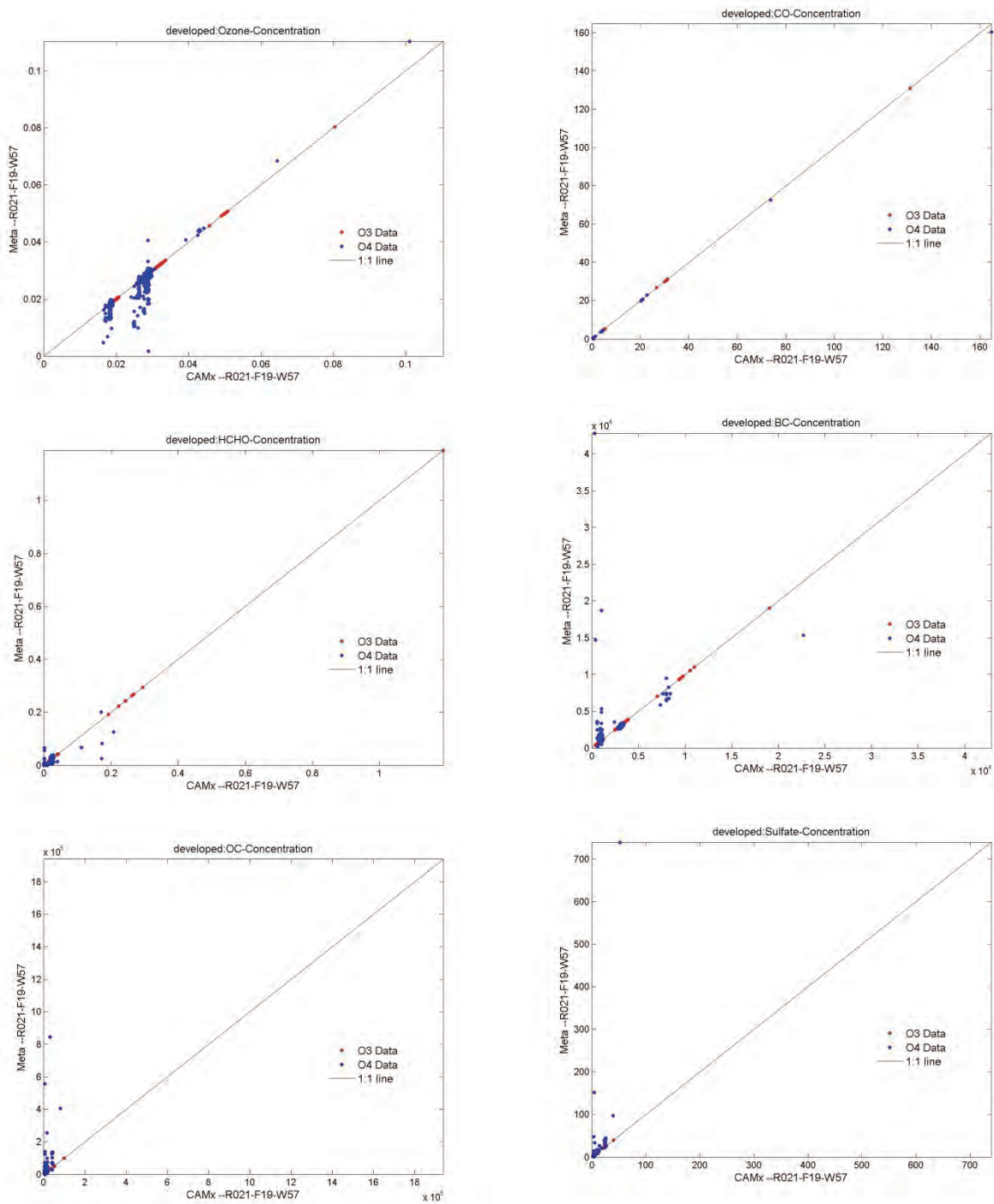


Figure A11. Results obtained for the urban concentrations of ozone, CO, formaldehyde, BC, OC, and sulfate based on runs of CAMx model (X-axis) compared with the Developed metamodel (Y-axis), for the R002-F02-W16 meteorology scenario.

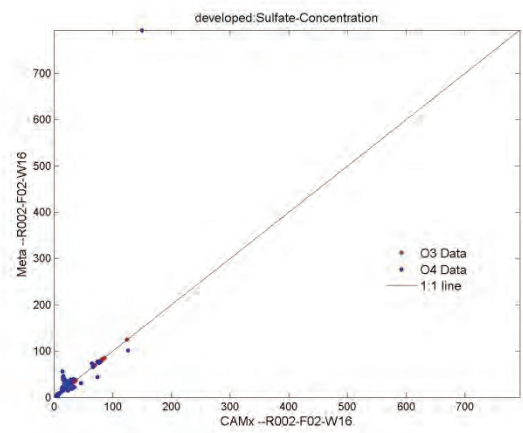
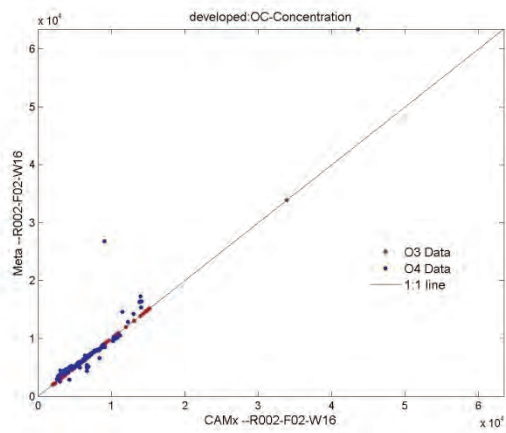
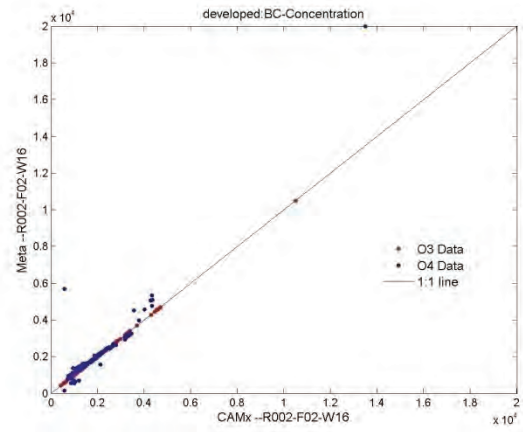
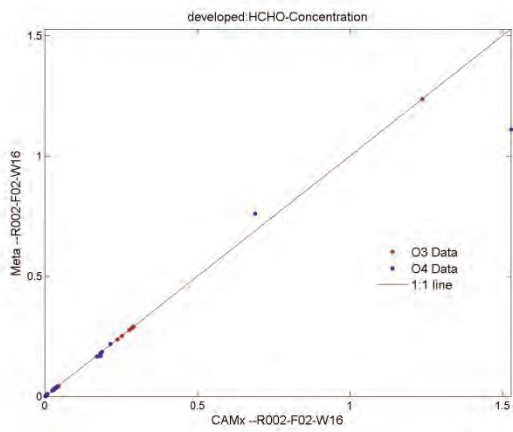
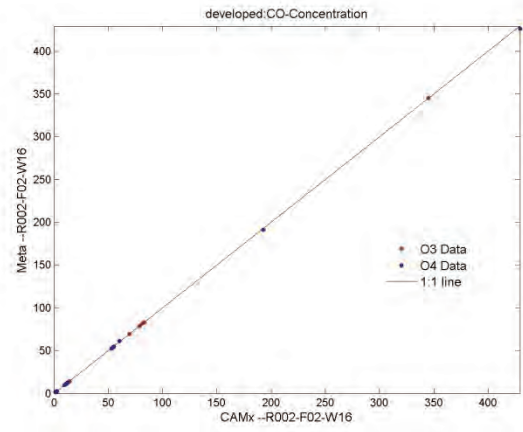
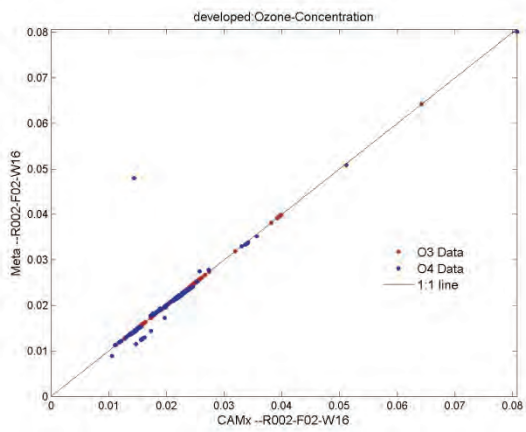


Figure A12. Results obtained for the urban concentrations of ozone, CO, formaldehyde, BC, OC, and sulfate based on runs of CAMx model (X-axis) compared with the Developed metamodel (Y-axis), for the R021-F19-W57 meteorology scenario.

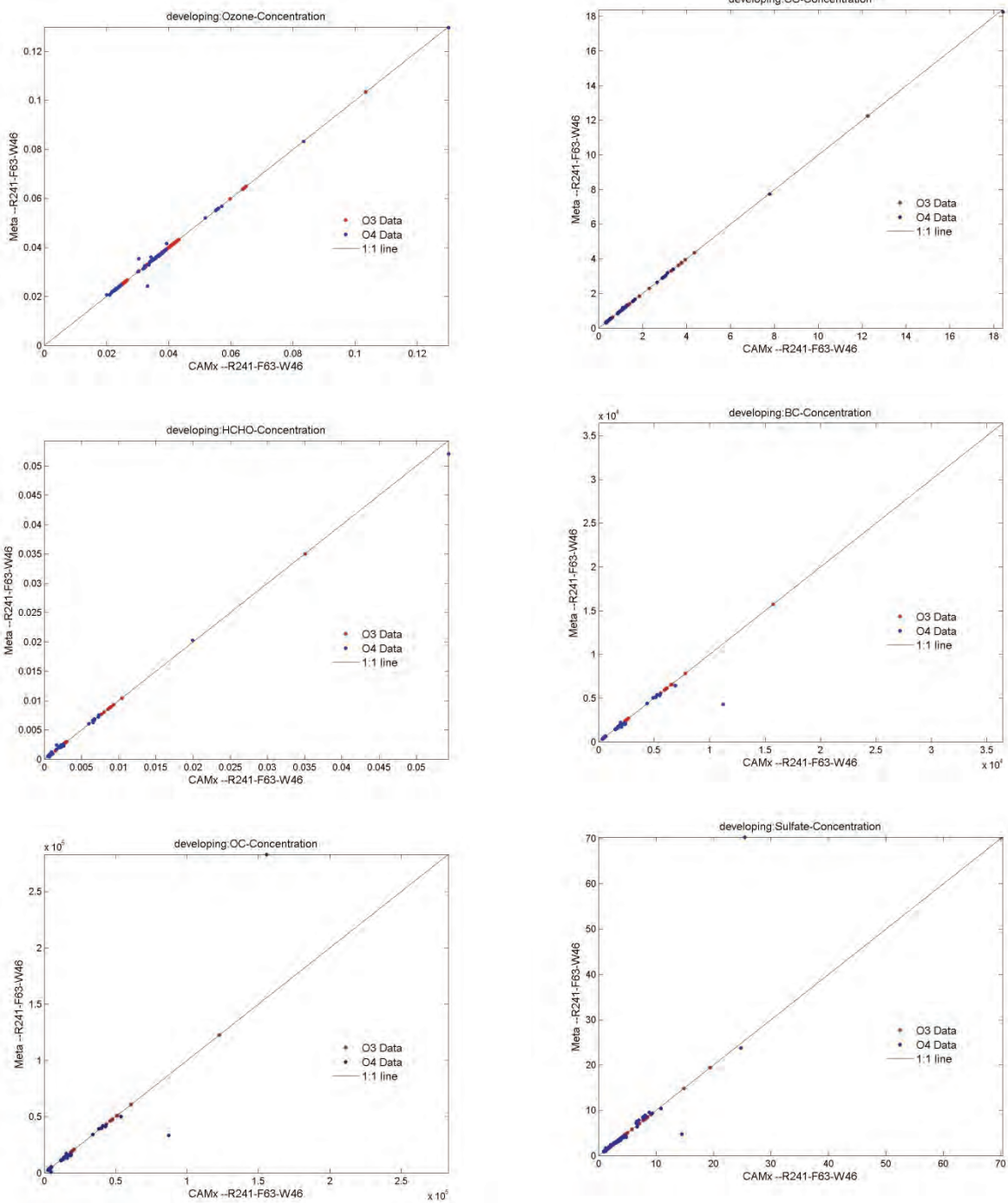


Figure A13. Results obtained for the urban concentrations of ozone, CO, formaldehyde, BC, OC, and sulfate based on runs of CAMx model (X-axis) compared with the Developing metamodel (Y-axis), for the R241-F63-W46 meteorology scenario.

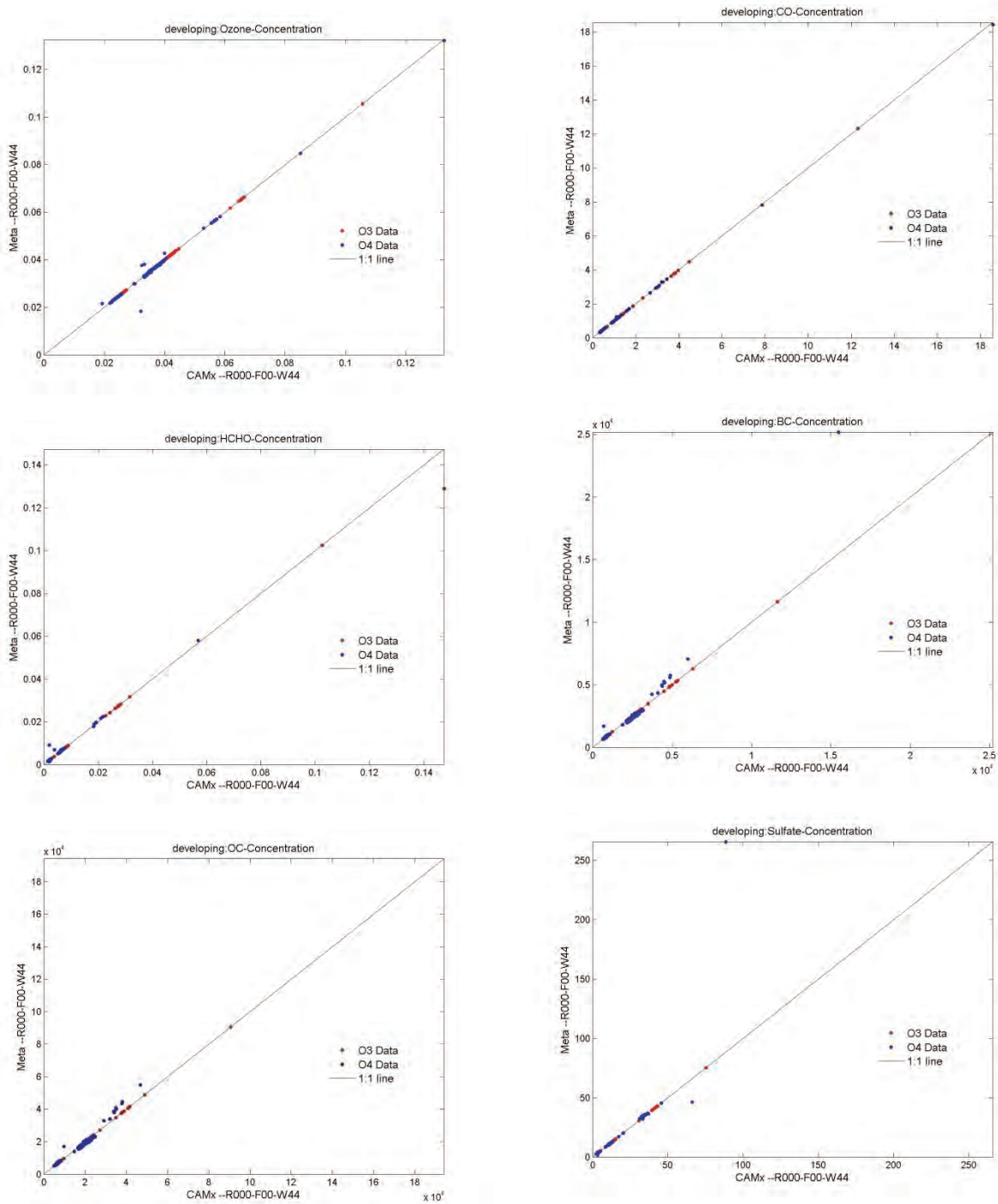


Figure A14. Results obtained for the urban concentrations of ozone, CO, formaldehyde, BC, OC, and sulfate based on runs of CAMx model (X-axis) compared with the Developing metamodel (Y-axis), for the R000-F00-W44 meteorology scenario.

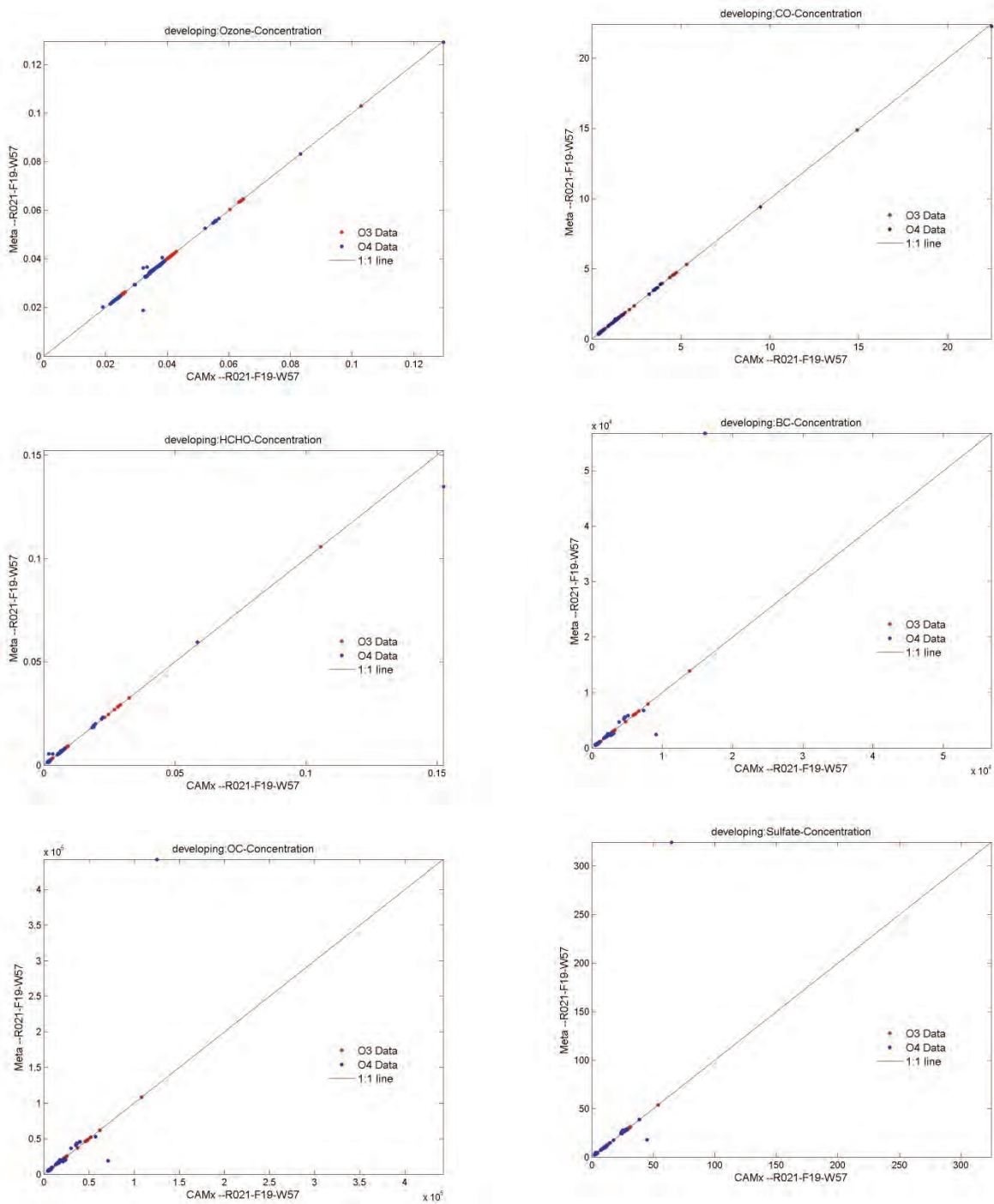


Figure A15. Results obtained for the urban concentrations of ozone, CO, formaldehyde, BC, OC, and sulfate based on runs of CAMx model (X-axis) compared with the Developing metamodel (Y-axis), for the R002-F02-W16 meteorology scenario.

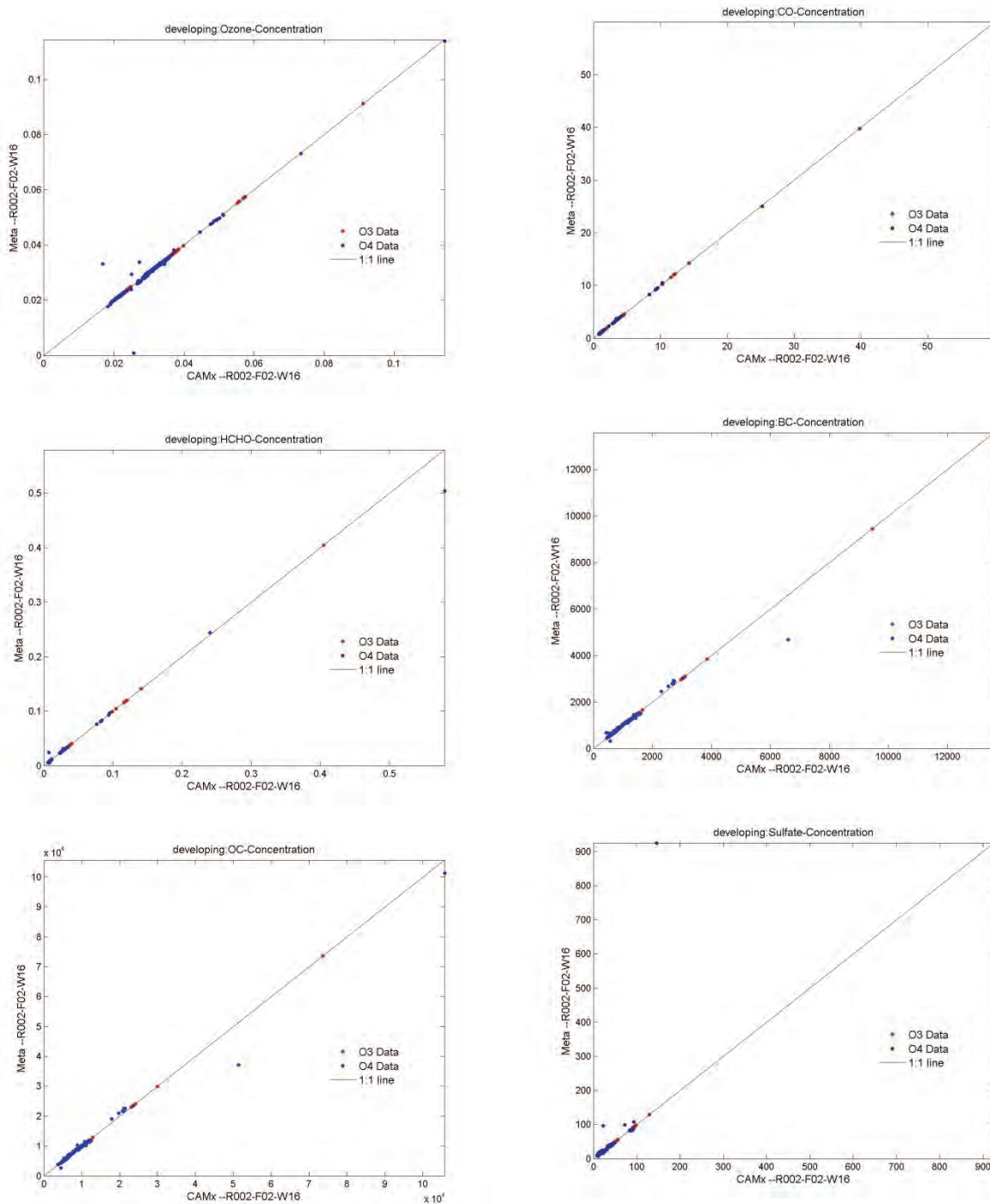


Figure A16. Results obtained for the urban concentrations of ozone, CO, formaldehyde, BC, OC, and sulfate based on runs of CAMx model (X-axis) compared with the Developing metamodel (Y-axis), for the R021-F19-W57 meteorology scenario.

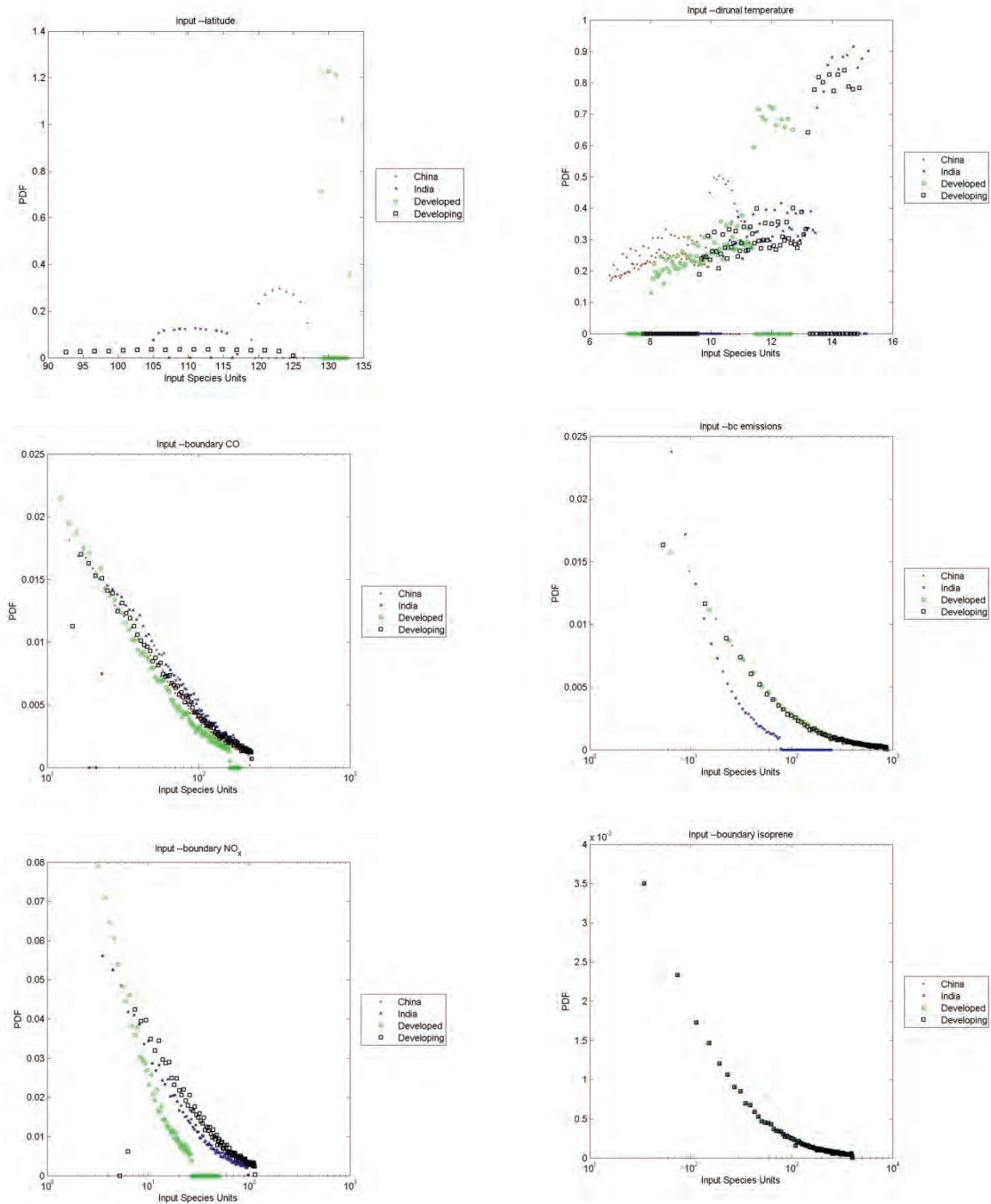


Figure A17a. PDFs of the input variables used for the 50,000 run sensitivity test.

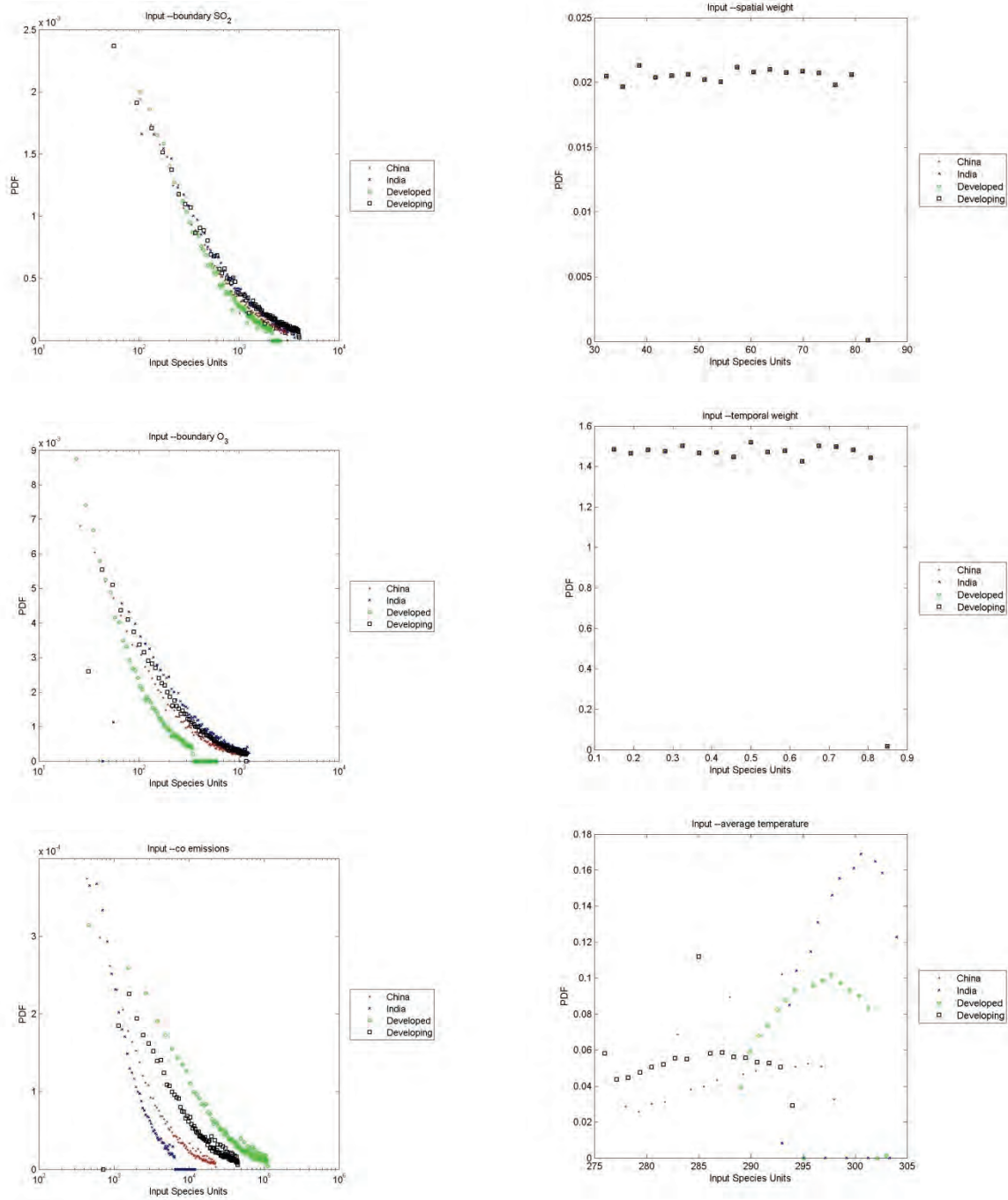


Figure A17b. PDFs of the input variables used for the 50,000 run sensitivity test.

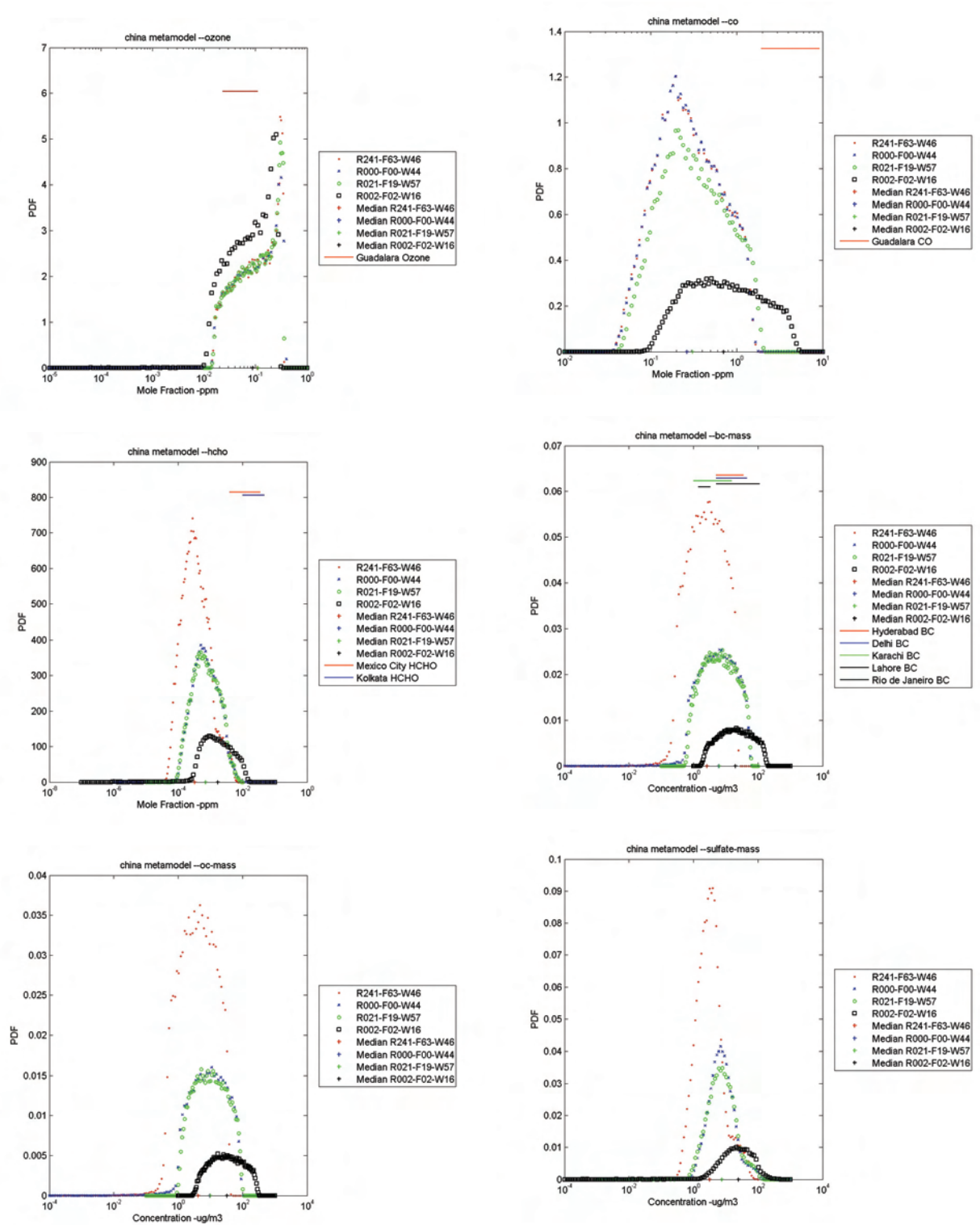


Figure A18. Results of the urban concentrations of ozone, CO, formaldehyde, BC, OC, and sulfate from the China metamodel 50,000 run sensitivity test.

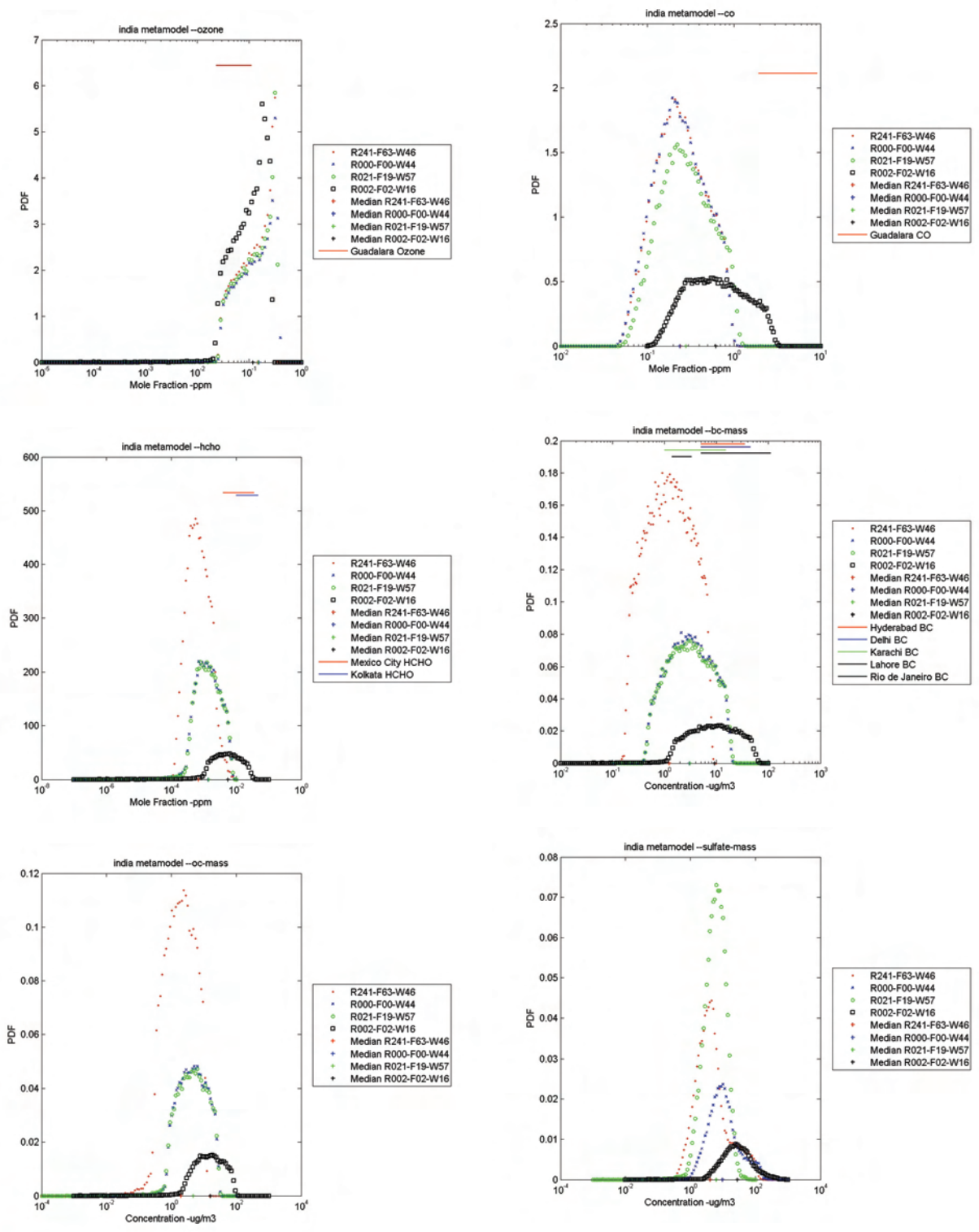


Figure A19. Results of the urban concentrations of ozone, CO, formaldehyde, BC, OC, and sulfate from the India metamodel 50,000 run sensitivity test.

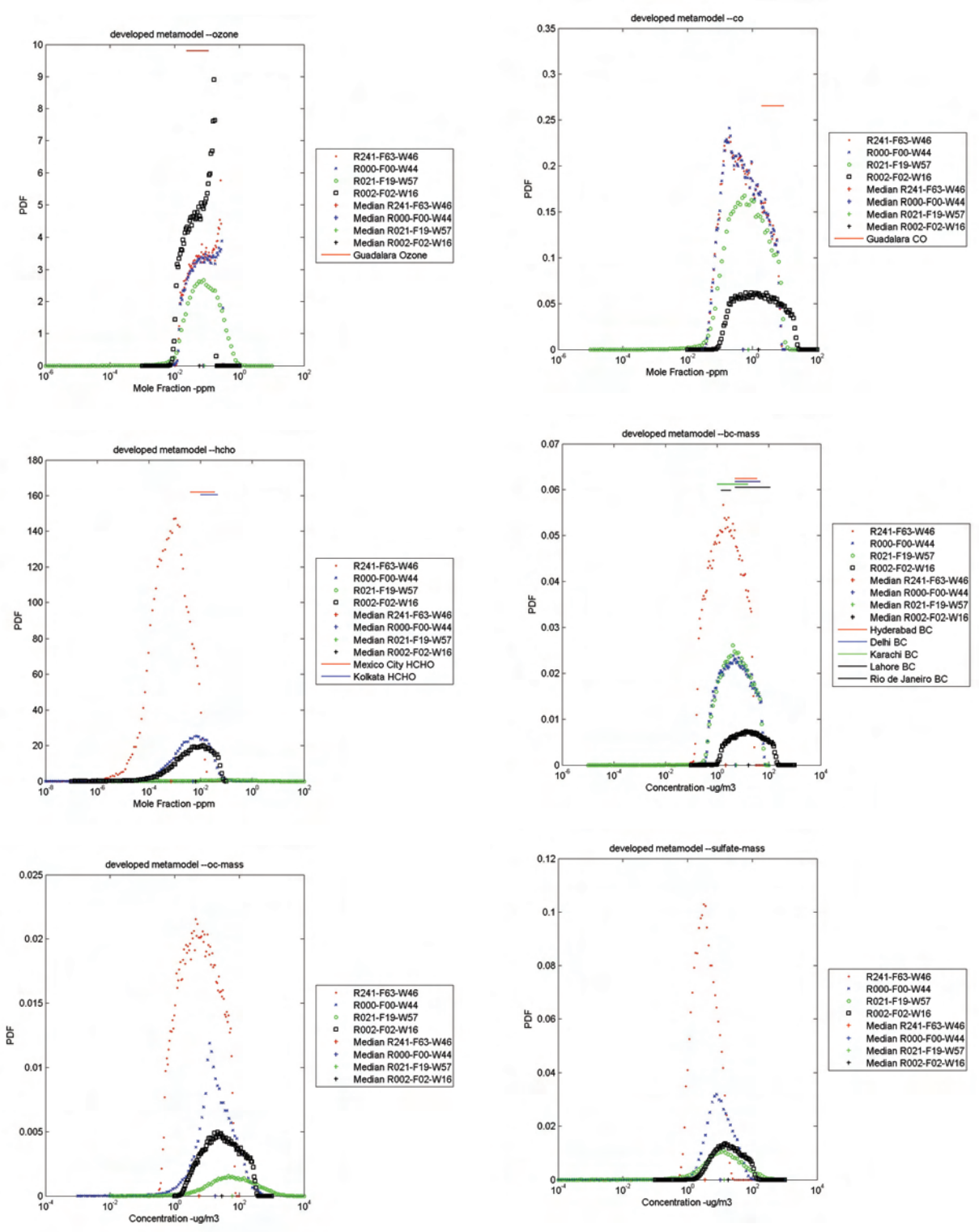


Figure A20. Results of the urban concentrations of ozone, CO, formaldehyde, BC, OC, and sulfate from the Developed metamodel 50,000 run sensitivity test.

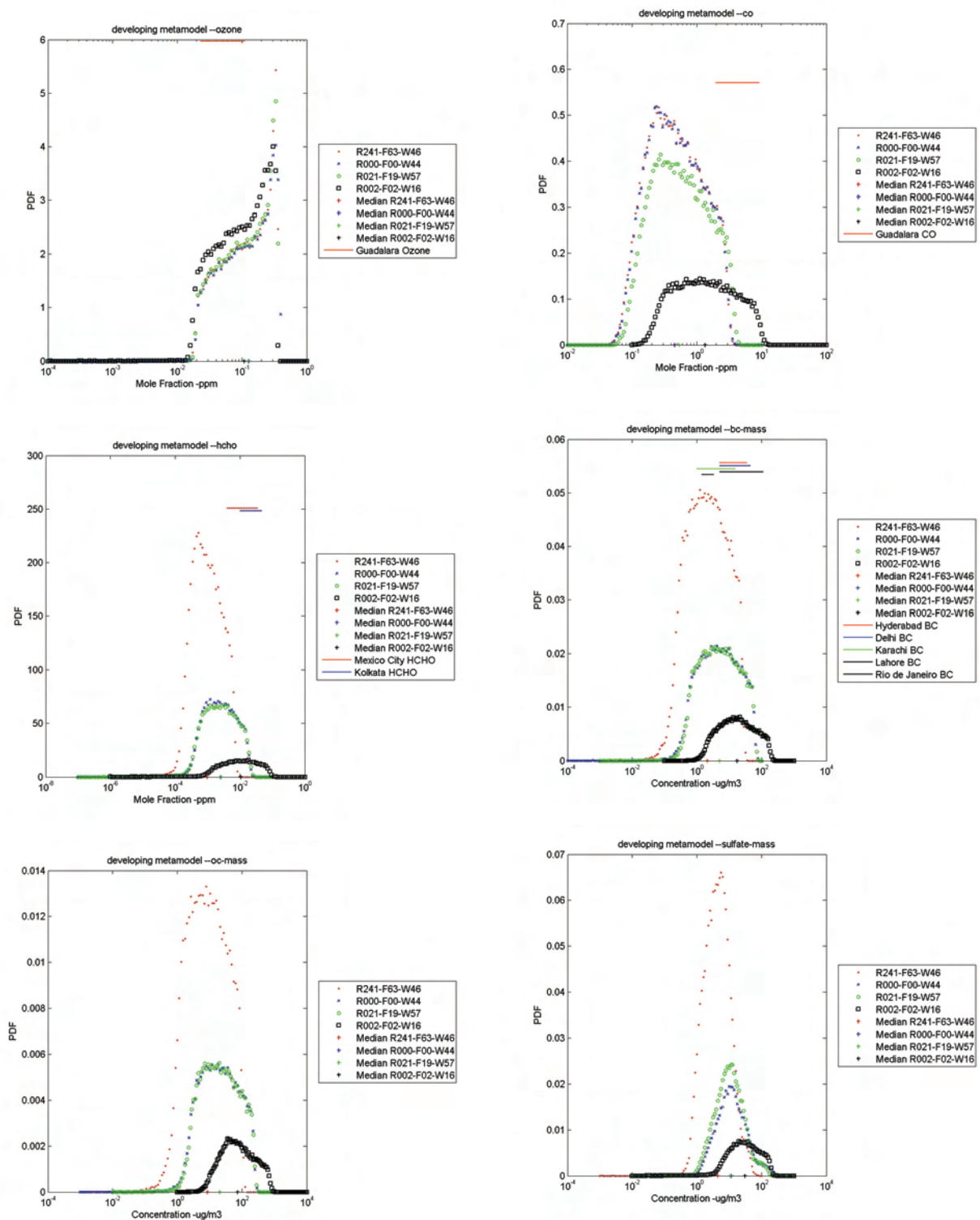


Figure A21. Results of the urban concentrations of ozone, CO, formaldehyde, BC, OC, and sulfate from the Developing metamodel 50,000 run sensitivity test.

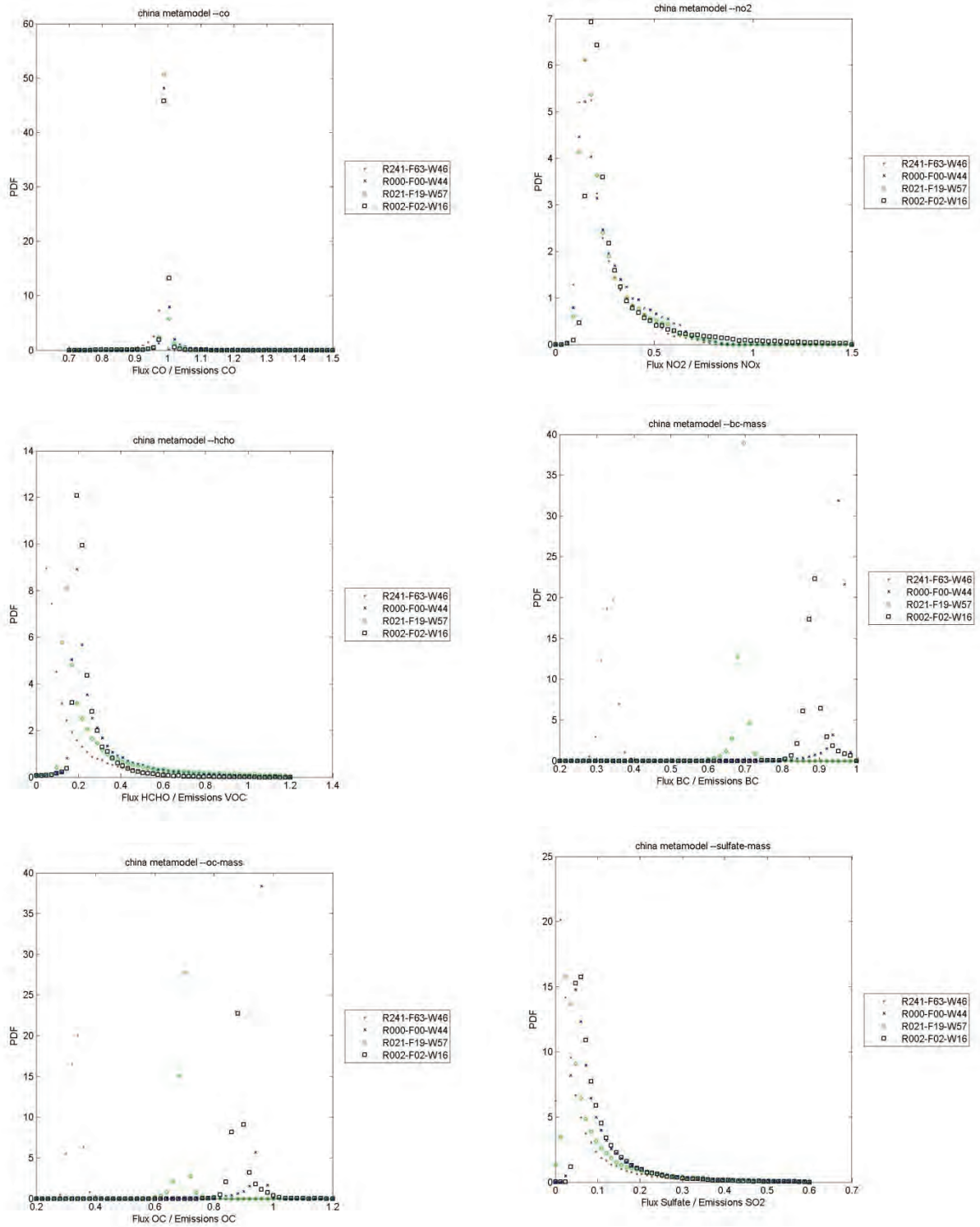


Figure A22. Results for the urban Flux/Emissions ratio of CO, NO₂, formaldehyde, BC, OC, and sulfate from the China metamodel 50,000 run sensitivity test.

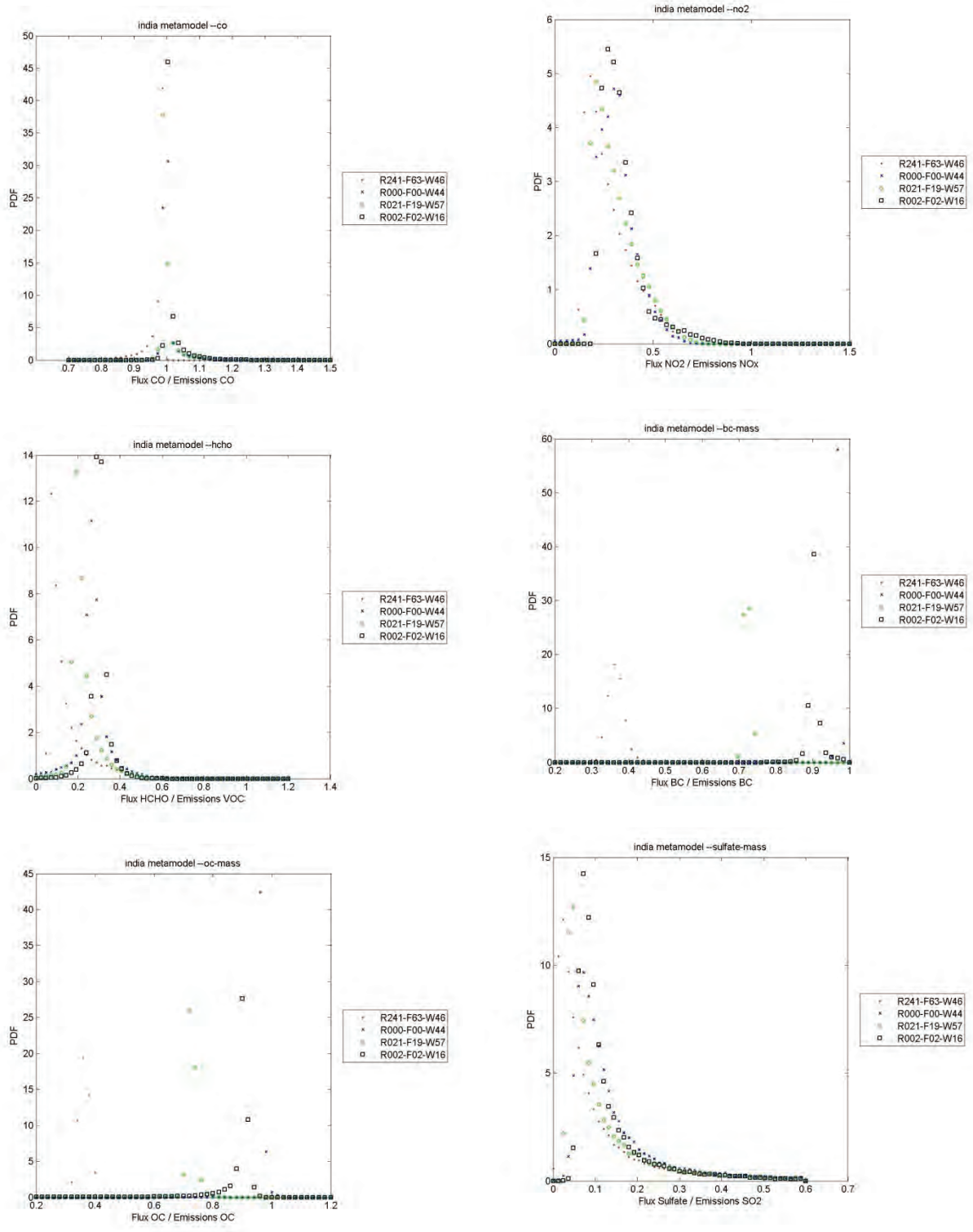


Figure A23. Results for the urban Flux/Emissions ratios of CO, NO₂, formaldehyde, BC, OC, and sulfate from the India metamodel 50,000 run sensitivity test.

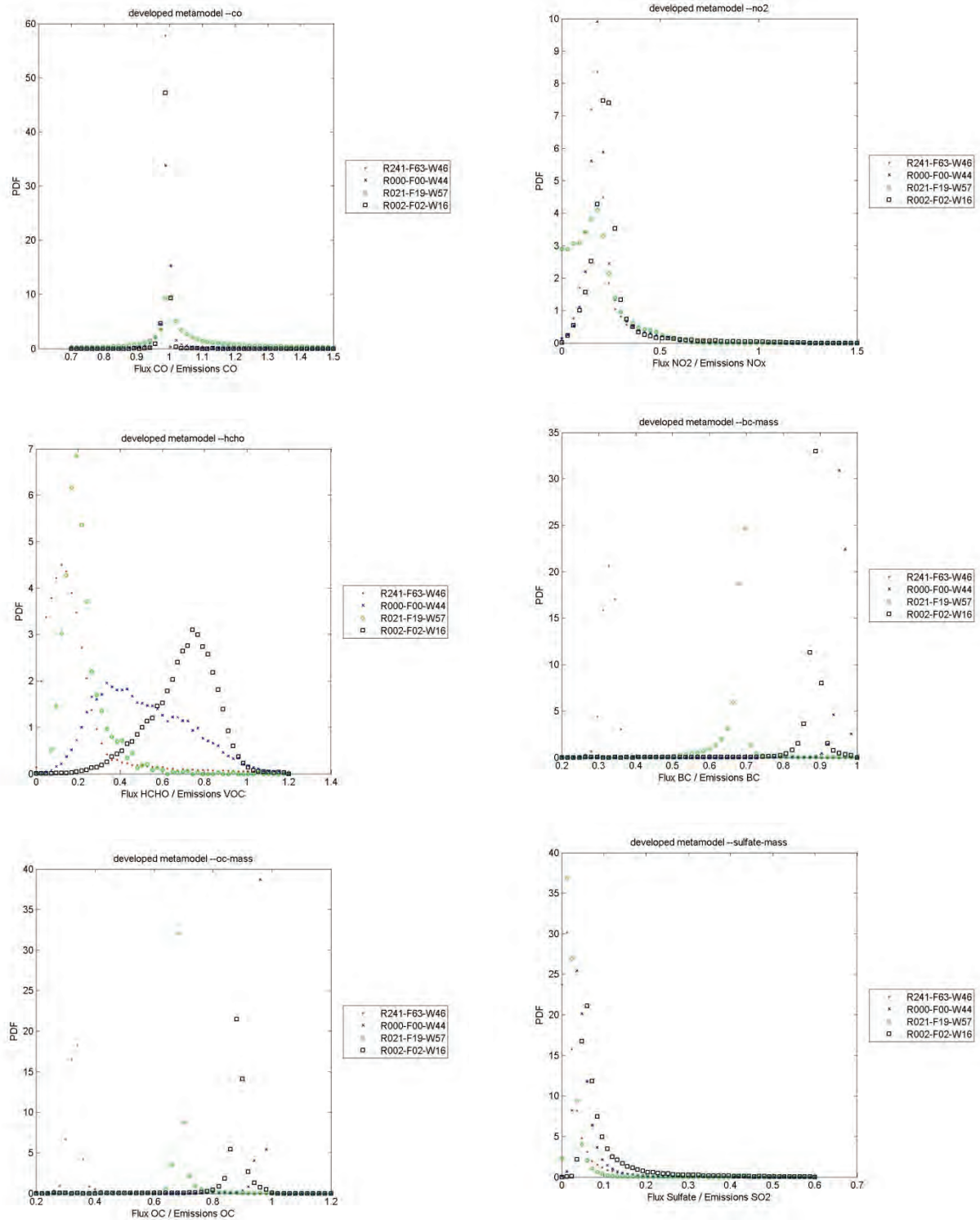


Figure A24. Results for the urban Flux/Emissions ratios of CO, NO₂, formaldehyde, BC, OC, and sulfate from the Developed metamodel 50,000 run sensitivity test.

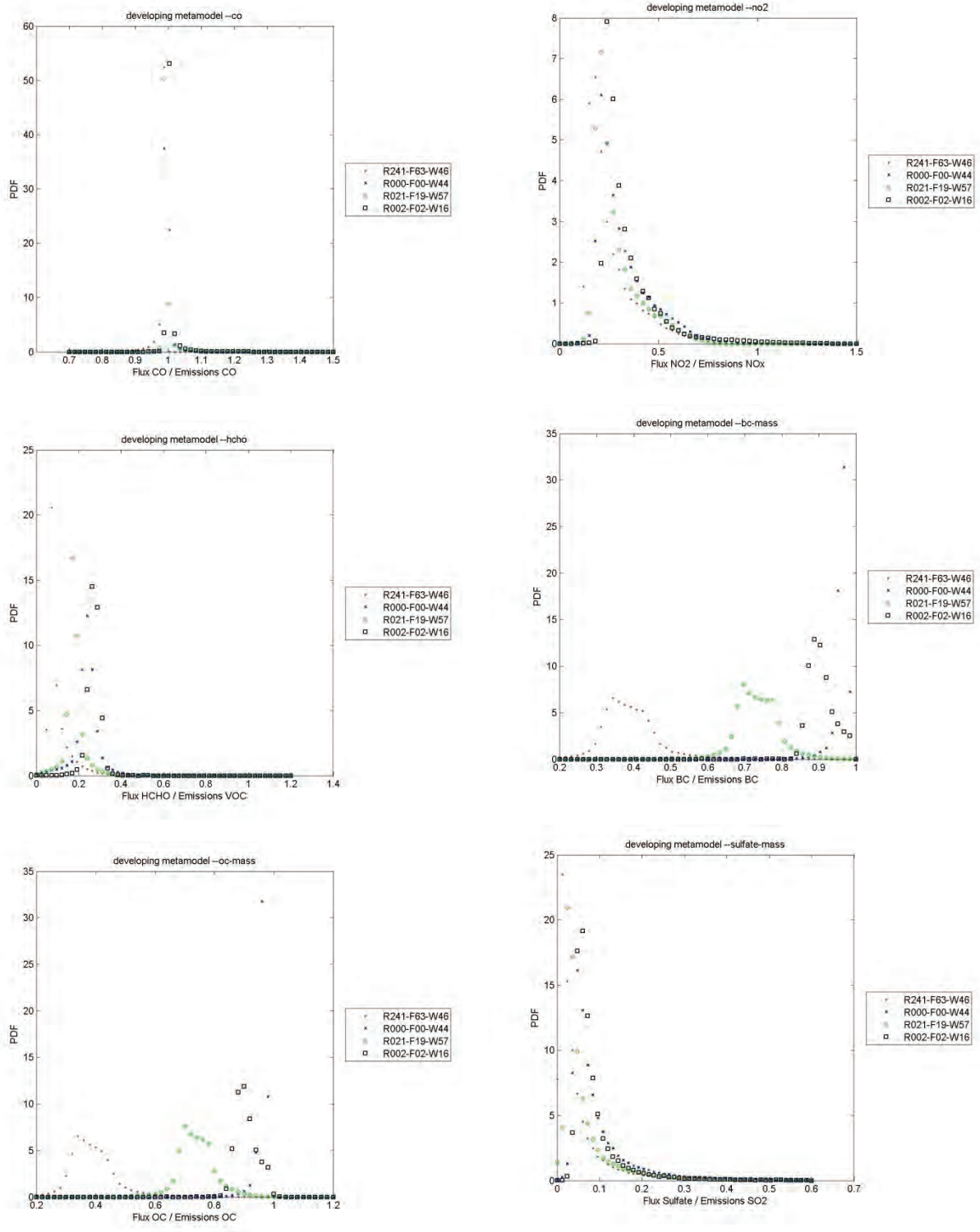


Figure A25. Results for the urban Flux/Emissions ratios of CO, NO2, formaldehyde, BC, OC, and sulfate from the Developing metamodel 50,000 run sensitivity test.

REPORT SERIES of the MIT Joint Program on the Science and Policy of Global Change

1. **Uncertainty in Climate Change Policy Analysis**
Jacoby & Prinn December 1994
2. **Description and Validation of the MIT Version of the GISS 2D Model** *Sokolov & Stone* June 1995
3. **Responses of Primary Production and Carbon Storage to Changes in Climate and Atmospheric CO₂ Concentration** *Xiao et al.* October 1995
4. **Application of the Probabilistic Collocation Method for an Uncertainty Analysis** *Webster et al.* January 1996
5. **World Energy Consumption and CO₂ Emissions: 1950-2050** *Schmalensee et al.* April 1996
6. **The MIT Emission Prediction and Policy Analysis (EPPA) Model** *Yang et al.* May 1996 (*superseded* by No. 125)
7. **Integrated Global System Model for Climate Policy Analysis** *Prinn et al.* June 1996 (*superseded* by No. 124)
8. **Relative Roles of Changes in CO₂ and Climate to Equilibrium Responses of Net Primary Production and Carbon Storage** *Xiao et al.* June 1996
9. **CO₂ Emissions Limits: Economic Adjustments and the Distribution of Burdens** *Jacoby et al.* July 1997
10. **Modeling the Emissions of N₂O and CH₄ from the Terrestrial Biosphere to the Atmosphere** *Liu* Aug. 1996
11. **Global Warming Projections: Sensitivity to Deep Ocean Mixing** *Sokolov & Stone* September 1996
12. **Net Primary Production of Ecosystems in China and its Equilibrium Responses to Climate Changes** *Xiao et al.* November 1996
13. **Greenhouse Policy Architectures and Institutions** *Schmalensee* November 1996
14. **What Does Stabilizing Greenhouse Gas Concentrations Mean?** *Jacoby et al.* November 1996
15. **Economic Assessment of CO₂ Capture and Disposal** *Eckaus et al.* December 1996
16. **What Drives Deforestation in the Brazilian Amazon?** *Pfaff* December 1996
17. **A Flexible Climate Model For Use In Integrated Assessments** *Sokolov & Stone* March 1997
18. **Transient Climate Change and Potential Croplands of the World in the 21st Century** *Xiao et al.* May 1997
19. **Joint Implementation: Lessons from Title IV's Voluntary Compliance Programs** *Atkeson* June 1997
20. **Parameterization of Urban Subgrid Scale Processes in Global Atm. Chemistry Models** *Calbo et al.* July 1997
21. **Needed: A Realistic Strategy for Global Warming** *Jacoby, Prinn & Schmalensee* August 1997
22. **Same Science, Differing Policies; The Saga of Global Climate Change** *Skolnikoff* August 1997
23. **Uncertainty in the Oceanic Heat and Carbon Uptake and their Impact on Climate Projections** *Sokolov et al.* September 1997
24. **A Global Interactive Chemistry and Climate Model** *Wang, Prinn & Sokolov* September 1997
25. **Interactions Among Emissions, Atmospheric Chemistry & Climate Change** *Wang & Prinn* Sept. 1997
26. **Necessary Conditions for Stabilization Agreements** *Yang & Jacoby* October 1997
27. **Annex I Differentiation Proposals: Implications for Welfare, Equity and Policy** *Reiner & Jacoby* Oct. 1997
28. **Transient Climate Change and Net Ecosystem Production of the Terrestrial Biosphere** *Xiao et al.* November 1997
29. **Analysis of CO₂ Emissions from Fossil Fuel in Korea: 1961-1994** *Choi* November 1997
30. **Uncertainty in Future Carbon Emissions: A Preliminary Exploration** *Webster* November 1997
31. **Beyond Emissions Paths: Rethinking the Climate Impacts of Emissions Protocols** *Webster & Reiner* November 1997
32. **Kyoto's Unfinished Business** *Jacoby et al.* June 1998
33. **Economic Development and the Structure of the Demand for Commercial Energy** *Judson et al.* April 1998
34. **Combined Effects of Anthropogenic Emissions and Resultant Climatic Changes on Atmospheric OH** *Wang & Prinn* April 1998
35. **Impact of Emissions, Chemistry, and Climate on Atmospheric Carbon Monoxide** *Wang & Prinn* April 1998
36. **Integrated Global System Model for Climate Policy Assessment: Feedbacks and Sensitivity Studies** *Prinn et al.* June 1998
37. **Quantifying the Uncertainty in Climate Predictions** *Webster & Sokolov* July 1998
38. **Sequential Climate Decisions Under Uncertainty: An Integrated Framework** *Valverde et al.* September 1998
39. **Uncertainty in Atmospheric CO₂ (Ocean Carbon Cycle Model Analysis)** *Holian* Oct. 1998 (*superseded* by No. 80)
40. **Analysis of Post-Kyoto CO₂ Emissions Trading Using Marginal Abatement Curves** *Ellerman & Decaux* Oct. 1998
41. **The Effects on Developing Countries of the Kyoto Protocol and CO₂ Emissions Trading** *Ellerman et al.* November 1998
42. **Obstacles to Global CO₂ Trading: A Familiar Problem** *Ellerman* November 1998
43. **The Uses and Misuses of Technology Development as a Component of Climate Policy** *Jacoby* November 1998
44. **Primary Aluminum Production: Climate Policy, Emissions and Costs** *Harnisch et al.* December 1998
45. **Multi-Gas Assessment of the Kyoto Protocol** *Reilly et al.* January 1999
46. **From Science to Policy: The Science-Related Politics of Climate Change Policy in the U.S.** *Skolnikoff* January 1999
47. **Constraining Uncertainties in Climate Models Using Climate Change Detection Techniques** *Forest et al.* April 1999
48. **Adjusting to Policy Expectations in Climate Change Modeling** *Shackley et al.* May 1999
49. **Toward a Useful Architecture for Climate Change Negotiations** *Jacoby et al.* May 1999
50. **A Study of the Effects of Natural Fertility, Weather and Productive Inputs in Chinese Agriculture** *Eckaus & Tso* July 1999
51. **Japanese Nuclear Power and the Kyoto Agreement** *Babiker, Reilly & Ellerman* August 1999
52. **Interactive Chemistry and Climate Models in Global Change Studies** *Wang & Prinn* September 1999
53. **Developing Country Effects of Kyoto-Type Emissions Restrictions** *Babiker & Jacoby* October 1999

Contact the Joint Program Office to request a copy. The Report Series is distributed at no charge.

REPORT SERIES of the MIT Joint Program on the Science and Policy of Global Change

54. **Model Estimates of the Mass Balance of the Greenland and Antarctic Ice Sheets** *Bugnion* Oct 1999
55. **Changes in Sea-Level Associated with Modifications of Ice Sheets over 21st Century** *Bugnion* October 1999
56. **The Kyoto Protocol and Developing Countries** *Babiker et al.* October 1999
57. **Can EPA Regulate Greenhouse Gases Before the Senate Ratifies the Kyoto Protocol?** *Bugnion & Reiner* November 1999
58. **Multiple Gas Control Under the Kyoto Agreement** *Reilly, Mayer & Harnisch* March 2000
59. **Supplementarity: An Invitation for Monopsony?** *Ellerman & Sue Wing* April 2000
60. **A Coupled Atmosphere-Ocean Model of Intermediate Complexity** *Kamenkovich et al.* May 2000
61. **Effects of Differentiating Climate Policy by Sector: A U.S. Example** *Babiker et al.* May 2000
62. **Constraining Climate Model Properties Using Optimal Fingerprint Detection Methods** *Forest et al.* May 2000
63. **Linking Local Air Pollution to Global Chemistry and Climate** *Mayer et al.* June 2000
64. **The Effects of Changing Consumption Patterns on the Costs of Emission Restrictions** *Lahiri et al.* Aug 2000
65. **Rethinking the Kyoto Emissions Targets** *Babiker & Eckaus* August 2000
66. **Fair Trade and Harmonization of Climate Change Policies in Europe** *Viguié* September 2000
67. **The Curious Role of "Learning" in Climate Policy: Should We Wait for More Data?** *Webster* October 2000
68. **How to Think About Human Influence on Climate** *Forest, Stone & Jacoby* October 2000
69. **Tradable Permits for Greenhouse Gas Emissions: A primer with reference to Europe** *Ellerman* Nov 2000
70. **Carbon Emissions and The Kyoto Commitment in the European Union** *Viguié et al.* February 2001
71. **The MIT Emissions Prediction and Policy Analysis Model: Revisions, Sensitivities and Results** *Babiker et al.* February 2001 (*superseded* by No. 125)
72. **Cap and Trade Policies in the Presence of Monopoly and Distortionary Taxation** *Fullerton & Metcalf* March '01
73. **Uncertainty Analysis of Global Climate Change Projections** *Webster et al.* Mar. '01 (*superseded* by No. 95)
74. **The Welfare Costs of Hybrid Carbon Policies in the European Union** *Babiker et al.* June 2001
75. **Feedbacks Affecting the Response of the Thermohaline Circulation to Increasing CO₂** *Kamenkovich et al.* July 2001
76. **CO₂ Abatement by Multi-fueled Electric Utilities: An Analysis Based on Japanese Data** *Ellerman & Tsukada* July 2001
77. **Comparing Greenhouse Gases** *Reilly et al.* July 2001
78. **Quantifying Uncertainties in Climate System Properties using Recent Climate Observations** *Forest et al.* July 2001
79. **Uncertainty in Emissions Projections for Climate Models** *Webster et al.* August 2001
80. **Uncertainty in Atmospheric CO₂ Predictions from a Global Ocean Carbon Cycle Model** *Holian et al.* September 2001
81. **A Comparison of the Behavior of AO GCMs in Transient Climate Change Experiments** *Sokolov et al.* December 2001
82. **The Evolution of a Climate Regime: Kyoto to Marrakech** *Babiker, Jacoby & Reiner* February 2002
83. **The "Safety Valve" and Climate Policy** *Jacoby & Ellerman* February 2002
84. **A Modeling Study on the Climate Impacts of Black Carbon Aerosols** *Wang* March 2002
85. **Tax Distortions and Global Climate Policy** *Babiker et al.* May 2002
86. **Incentive-based Approaches for Mitigating Greenhouse Gas Emissions: Issues and Prospects for India** *Gupta* June 2002
87. **Deep-Ocean Heat Uptake in an Ocean GCM with Idealized Geometry** *Huang, Stone & Hill* September 2002
88. **The Deep-Ocean Heat Uptake in Transient Climate Change** *Huang et al.* September 2002
89. **Representing Energy Technologies in Top-down Economic Models using Bottom-up Information** *McFarland et al.* October 2002
90. **Ozone Effects on Net Primary Production and Carbon Sequestration in the U.S. Using a Biogeochemistry Model** *Felzer et al.* November 2002
91. **Exclusionary Manipulation of Carbon Permit Markets: A Laboratory Test** *Carlén* November 2002
92. **An Issue of Permanence: Assessing the Effectiveness of Temporary Carbon Storage** *Herzog et al.* December 2002
93. **Is International Emissions Trading Always Beneficial?** *Babiker et al.* December 2002
94. **Modeling Non-CO₂ Greenhouse Gas Abatement** *Hyman et al.* December 2002
95. **Uncertainty Analysis of Climate Change and Policy Response** *Webster et al.* December 2002
96. **Market Power in International Carbon Emissions Trading: A Laboratory Test** *Carlén* January 2003
97. **Emissions Trading to Reduce Greenhouse Gas Emissions in the United States: The McCain-Lieberman Proposal** *Paltsev et al.* June 2003
98. **Russia's Role in the Kyoto Protocol** *Bernard et al.* Jun '03
99. **Thermohaline Circulation Stability: A Box Model Study** *Lucarini & Stone* June 2003
100. **Absolute vs. Intensity-Based Emissions Caps** *Ellerman & Sue Wing* July 2003
101. **Technology Detail in a Multi-Sector CGE Model: Transport Under Climate Policy** *Schafer & Jacoby* July 2003
102. **Induced Technical Change and the Cost of Climate Policy** *Sue Wing* September 2003
103. **Past and Future Effects of Ozone on Net Primary Production and Carbon Sequestration Using a Global Biogeochemical Model** *Felzer et al.* (revised) January 2004
104. **A Modeling Analysis of Methane Exchanges Between Alaskan Ecosystems and the Atmosphere** *Zhuang et al.* November 2003

Contact the Joint Program Office to request a copy. The Report Series is distributed at no charge.

REPORT SERIES of the MIT Joint Program on the Science and Policy of Global Change

105. **Analysis of Strategies of Companies under Carbon Constraint** Hashimoto January 2004
106. **Climate Prediction: The Limits of Ocean Models** Stone February 2004
107. **Informing Climate Policy Given Incommensurable Benefits Estimates** Jacoby February 2004
108. **Methane Fluxes Between Terrestrial Ecosystems and the Atmosphere at High Latitudes During the Past Century** Zhuang et al. March 2004
109. **Sensitivity of Climate to Diapycnal Diffusivity in the Ocean** Dalan et al. May 2004
110. **Stabilization and Global Climate Policy** Sarofim et al. July 2004
111. **Technology and Technical Change in the MIT EPPA Model** Jacoby et al. July 2004
112. **The Cost of Kyoto Protocol Targets: The Case of Japan** Paltsev et al. July 2004
113. **Economic Benefits of Air Pollution Regulation in the USA: An Integrated Approach** Yang et al. (revised) Jan. 2005
114. **The Role of Non-CO₂ Greenhouse Gases in Climate Policy: Analysis Using the MIT IGSM** Reilly et al. Aug. '04
115. **Future U.S. Energy Security Concerns** Deutch Sep. '04
116. **Explaining Long-Run Changes in the Energy Intensity of the U.S. Economy** Sue Wing Sept. 2004
117. **Modeling the Transport Sector: The Role of Existing Fuel Taxes in Climate Policy** Paltsev et al. November 2004
118. **Effects of Air Pollution Control on Climate** Prinn et al. January 2005
119. **Does Model Sensitivity to Changes in CO₂ Provide a Measure of Sensitivity to the Forcing of Different Nature?** Sokolov March 2005
120. **What Should the Government Do To Encourage Technical Change in the Energy Sector?** Deutch May '05
121. **Climate Change Taxes and Energy Efficiency in Japan** Kasahara et al. May 2005
122. **A 3D Ocean-Seaice-Carbon Cycle Model and its Coupling to a 2D Atmospheric Model: Uses in Climate Change Studies** Dutkiewicz et al. (revised) November 2005
123. **Simulating the Spatial Distribution of Population and Emissions to 2100** Asadoorian May 2005
124. **MIT Integrated Global System Model (IGSM) Version 2: Model Description and Baseline Evaluation** Sokolov et al. July 2005
125. **The MIT Emissions Prediction and Policy Analysis (EPPA) Model: Version 4** Paltsev et al. August 2005
126. **Estimated PDFs of Climate System Properties Including Natural and Anthropogenic Forcings** Forest et al. September 2005
127. **An Analysis of the European Emission Trading Scheme** Reilly & Paltsev October 2005
128. **Evaluating the Use of Ocean Models of Different Complexity in Climate Change Studies** Sokolov et al. November 2005
129. **Future Carbon Regulations and Current Investments in Alternative Coal-Fired Power Plant Designs** Sekar et al. December 2005
130. **Absolute vs. Intensity Limits for CO₂ Emission Control: Performance Under Uncertainty** Sue Wing et al. January 2006
131. **The Economic Impacts of Climate Change: Evidence from Agricultural Profits and Random Fluctuations in Weather** Deschenes & Greenstone January 2006
132. **The Value of Emissions Trading** Webster et al. Feb. 2006
133. **Estimating Probability Distributions from Complex Models with Bifurcations: The Case of Ocean Circulation Collapse** Webster et al. March 2006
134. **Directed Technical Change and Climate Policy** Otto et al. April 2006
135. **Modeling Climate Feedbacks to Energy Demand: The Case of China** Asadoorian et al. June 2006
136. **Bringing Transportation into a Cap-and-Trade Regime** Ellerman, Jacoby & Zimmerman June 2006
137. **Unemployment Effects of Climate Policy** Babiker & Eckaus July 2006
138. **Energy Conservation in the United States: Understanding its Role in Climate Policy** Metcalf Aug. '06
139. **Directed Technical Change and the Adoption of CO₂ Abatement Technology: The Case of CO₂ Capture and Storage** Otto & Reilly August 2006
140. **The Allocation of European Union Allowances: Lessons, Unifying Themes and General Principles** Buchner et al. October 2006
141. **Over-Allocation or Abatement? A preliminary analysis of the EU ETS based on the 2006 emissions data** Ellerman & Buchner December 2006
142. **Federal Tax Policy Towards Energy** Metcalf Jan. 2007
143. **Technical Change, Investment and Energy Intensity** Kratena March 2007
144. **Heavier Crude, Changing Demand for Petroleum Fuels, Regional Climate Policy, and the Location of Upgrading Capacity** Reilly et al. April 2007
145. **Biomass Energy and Competition for Land** Reilly & Paltsev April 2007
146. **Assessment of U.S. Cap-and-Trade Proposals** Paltsev et al. April 2007
147. **A Global Land System Framework for Integrated Climate-Change Assessments** Schlosser et al. May 2007
148. **Relative Roles of Climate Sensitivity and Forcing in Defining the Ocean Circulation Response to Climate Change** Scott et al. May 2007
149. **Global Economic Effects of Changes in Crops, Pasture, and Forests due to Changing Climate, CO₂ and Ozone** Reilly et al. May 2007
150. **U.S. GHG Cap-and-Trade Proposals: Application of a Forward-Looking Computable General Equilibrium Model** Gurgel et al. June 2007
151. **Consequences of Considering Carbon/Nitrogen Interactions on the Feedbacks between Climate and the Terrestrial Carbon Cycle** Sokolov et al. June 2007
152. **Energy Scenarios for East Asia: 2005-2025** Paltsev & Reilly July 2007
153. **Climate Change, Mortality, and Adaptation: Evidence from Annual Fluctuations in Weather in the U.S.** Deschênes & Greenstone August 2007

REPORT SERIES of the MIT *Joint Program on the Science and Policy of Global Change*

- 154. Modeling the Prospects for Hydrogen Powered Transportation Through 2100** *Sandoval et al.*
February 2008
- 155. Potential Land Use Implications of a Global Biofuels Industry** *Gurgel et al.* March 2008
- 156. Estimating the Economic Cost of Sea-Level Rise** *Sugiyama et al.* April 2008
- 157. Constraining Climate Model Parameters from Observed 20th Century Changes** *Forest et al.* April 2008
- 158. Analysis of the Coal Sector under Carbon Constraints** *McFarland et al.* April 2008
- 159. Impact of Sulfur and Carbonaceous Emissions from International Shipping on Aerosol Distributions and Direct Radiative Forcing** *Wang & Kim* April 2008
- 160. Analysis of U.S. Greenhouse Gas Tax Proposals** *Metcalf et al.* April 2008
- 161. A Forward Looking Version of the MIT Emissions Prediction and Policy Analysis (EPPA) Model** *Babiker et al.* May 2008
- 162. The European Carbon Market in Action: Lessons from the first trading period** Interim Report
Convery, Ellerman, & de Perthuis June 2008
- 163. The Influence on Climate Change of Differing Scenarios for Future Development Analyzed Using the MIT Integrated Global System Model** *Prinn et al.*
September 2008
- 164. Marginal Abatement Costs and Marginal Welfare Costs for Greenhouse Gas Emissions Reductions: Results from the EPPA Model** *Holak et al.* November 2008
- 165. Uncertainty in Greenhouse Emissions and Costs of Atmospheric Stabilization** *Webster et al.* November 2008
- 166. Sensitivity of Climate Change Projections to Uncertainties in the Estimates of Observed Changes in Deep-Ocean Heat Content** *Sokolov et al.* November 2008
- 167. Sharing the Burden of GHG Reductions** *Jacoby et al.*
November 2008
- 168. Unintended Environmental Consequences of a Global Biofuels Program** *Melillo et al.* January 2009
- 169. Probabilistic Forecast for 21st Century Climate Based on Uncertainties in Emissions (without Policy) and Climate Parameters** *Sokolov et al.* January 2009
- 170. The EU's Emissions Trading Scheme: A Proto-type Global System?** *Ellerman* February 2009
- 171. Designing a U.S. Market for CO₂** *Parsons et al.*
February 2009
- 172. Prospects for Plug-in Hybrid Electric Vehicles in the United States & Japan: A General Equilibrium Analysis** *Karplus et al.* April 2009
- 173. The Cost of Climate Policy in the United States** *Paltsev et al.* April 2009
- 174. A Semi-Empirical Representation of the Temporal Variation of Total Greenhouse Gas Levels Expressed as Equivalent Levels of Carbon Dioxide** *Huang et al.*
June 2009
- 175. Potential Climatic Impacts and Reliability of Very Large Scale Wind Farms** *Wang & Prinn* June 2009
- 176. Biofuels, Climate Policy and the European Vehicle Fleet** *Gittiaux et al.* August 2009
- 177. Global Health and Economic Impacts of Future Ozone Pollution** *Selin et al.* August 2009
- 178. Measuring Welfare Loss Caused by Air Pollution in Europe: A CGE Analysis** *Nam et al.* August 2009
- 179. Assessing Evapotranspiration Estimates from the Global Soil Wetness Project Phase 2 (GSWP-2) Simulations** *Schlosser and Gao* September 2009
- 180. Analysis of Climate Policy Targets under Uncertainty** *Webster et al.* September 2009
- 181. Development of a Fast and Detailed Model of Urban-Scale Chemical and Physical Processing** *Cohen & Prinn* October 2009